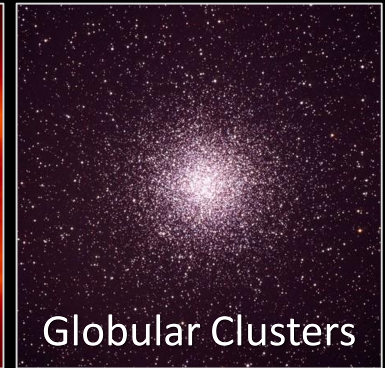

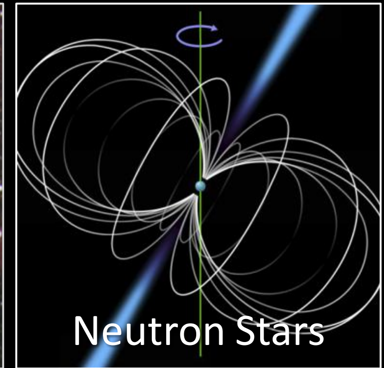

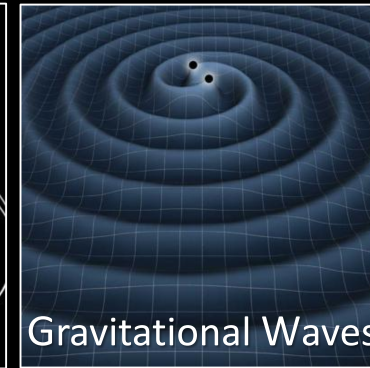

Looking at Stars
Aiming for Axions

20th Patras Workshop on Axions, WIMPs and WISPs
La Laguna, Tenerife, 22 September 2025

ORIGINS Excellence Cluster

COSMIC WISPERS CA21106

MAX-PLANCK-INSTITUT FÜR PHYSIK

SFB 1258 | Neutrinos Dark Matter Messengers

Georg G. Raffelt, Max-Planck-Institut für Physik, Garching

Particles and Stars

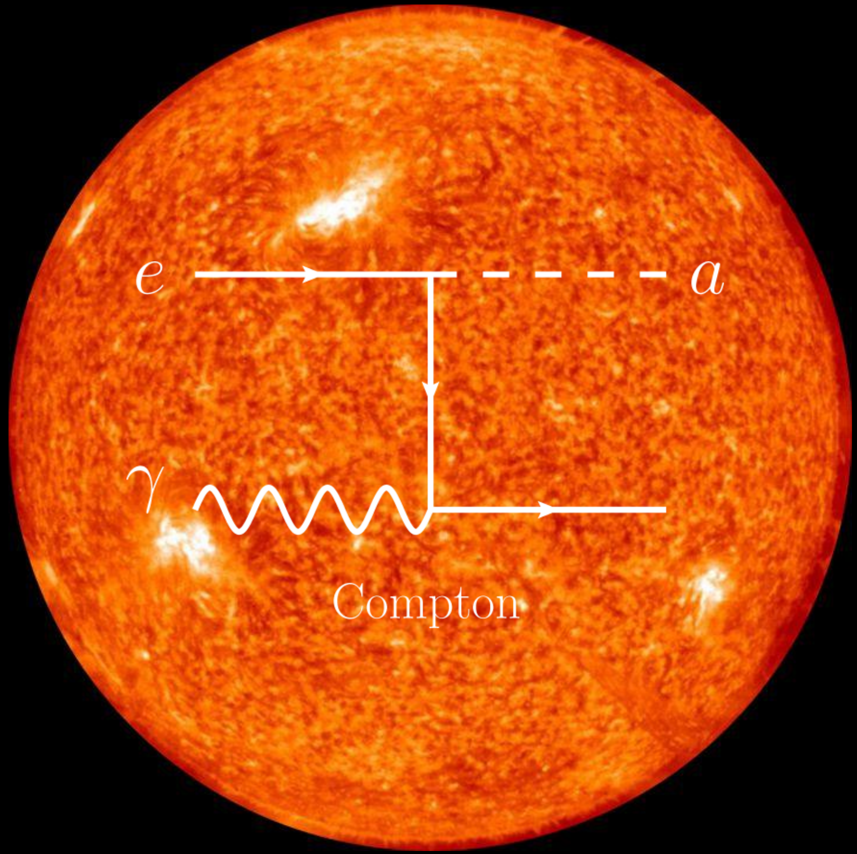

Low-mass particles are produced in stellar interiors

- **Detection opportunity (Sun or Supernovae)**
- **Backreaction on stellar properties**

→ Neutrinos

→ Axions & friends

MARCH 1, 1939 PHYSICAL REVIEW VOLUME 55

Energy Production in Stars*

H. A. BETHE
Cornell University, Ithaca, New York

(Received September 7, 1938)

The combination of four protons and two electrons can occur essentially only in two ways. The first mechanism starts with the combination of two protons to form a deuteron with positron emission, *viz.*

$$H+H=D+\epsilon^{+}. \quad (1)$$

The deuteron is then transformed into He^4 by further capture of protons; these captures occur very rapidly compared with process (1). The second mechanism uses carbon and nitrogen as catalysts, according to the chain reaction

$$\begin{aligned} &C^{12}+H=N^{13}+\gamma, && N^{13}=C^{13}+\epsilon^{+} \\ &C^{13}+H=N^{14}+\gamma, && \\ &N^{14}+H=O^{15}+\gamma, && O^{15}=N^{15}+\epsilon^{+} \\ &N^{15}+H=C^{12}+He^{4}. && \end{aligned} \quad (2)$$

Hans Bethe
1906–2005

- First mention of neutrino emission from stars
- Neutrino losses discussed, although overestimated

Some Early Papers on Stellar Particle Physics

Neutrinos (since 1960s)

- Bernstein, Ruderman & Feinberg:
  Electromagnetic properties of the neutrino, Phys. Rev. 132 (1963) 1227
- Gribov & Pontecorvo:
  Neutrino astronomy and lepton charge, PLB 28 (1969) 493

Flavor oscillations!

- Cowsik:
  Limits on the radiative decay of neutrinos, PRL 39 (1978) 511
- Falk & Schramm:
  Limits from supernovae on neutrino radiative lifetimes, PLB 79 (1978) 511

Axions & light Higgs (ca 1978)

- Vysotsky, Zeldovich, Khlopov & Chechetkin:
  Some astrophysical limitations on the axion mass,
  Pisma Zh. Eksp. Teor. Fiz. 27 (1978) 533 [JETP Lett. 27 (1978) 502]
- Dicus, Kolb, Teplitz & Wagoner:
  Astrophysical bounds on the masses of axions and Higgs particles, PRD 18 (1978) 1829
- K. O. Mikaelian: Astrophysical implications of new light Higgs bosons, PRD 18 (1978) 3605
- K. Sato: Astrophysical constraints on the axion mass and the number of quark flavors,
  Prog. Theor. Phys. 60 (1978) 1942

Particles from the Sun

2002 Solar Neutrinos (R.Davis, M.Koshiba)

2015 Solar Nu Oscillations (A.McDonald)

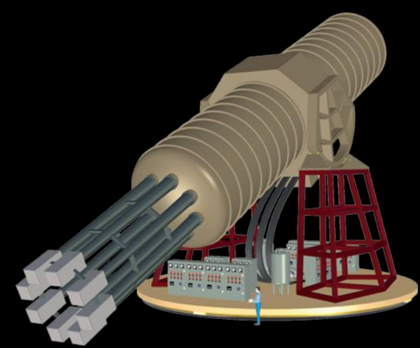

Search for solar axions
with CAST and future IAXO

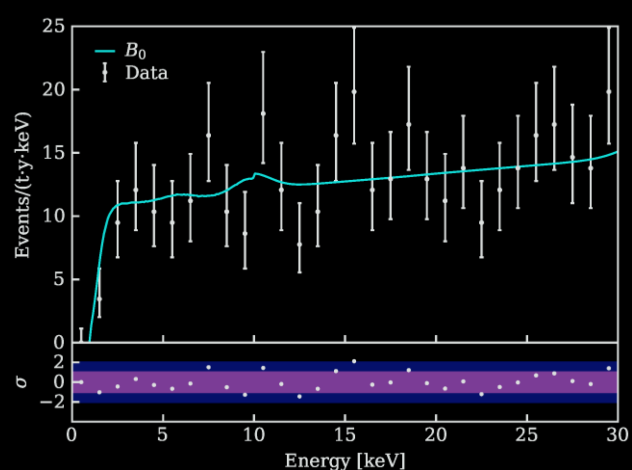

No excess in XENONnT
arXiv:2207.11330
Bounds on axions,
dark photons, neutrino
dipole moments

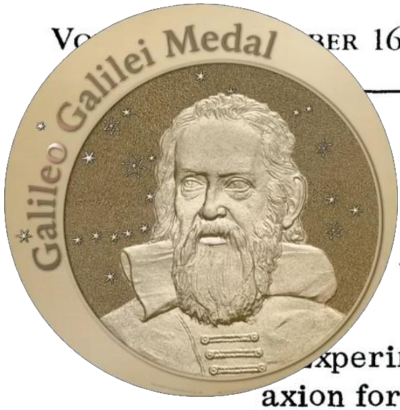

VO… BER 16 PHYSICAL REVIEW LETTERS 17 OCTOBER 1983

Experimental Tests of the "Invisible" Axion

P. Sikivie
Physics Department, University of Florida, Gainesville, Florida 32611
(Received 13 July 1983)

…xperiments are proposed which address the question of the existence of the "invisible" axion for the whole allowed range of the axion decay constant. These experiments exploit the coupling of the axion to the electromagnetic field, axion emission by the sun, and/or the cosmological abundance and presumed clustering of axions in the halo of our galaxy.

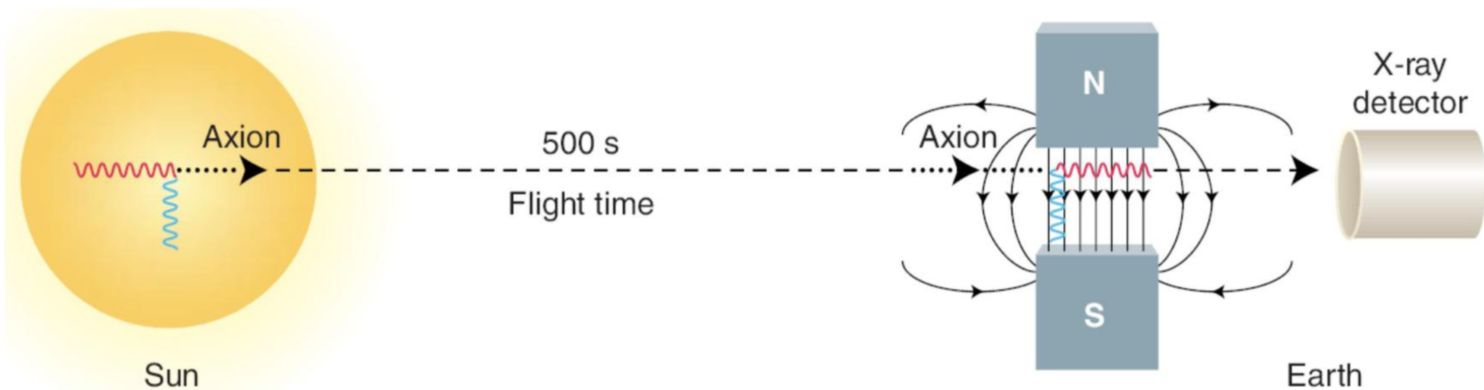

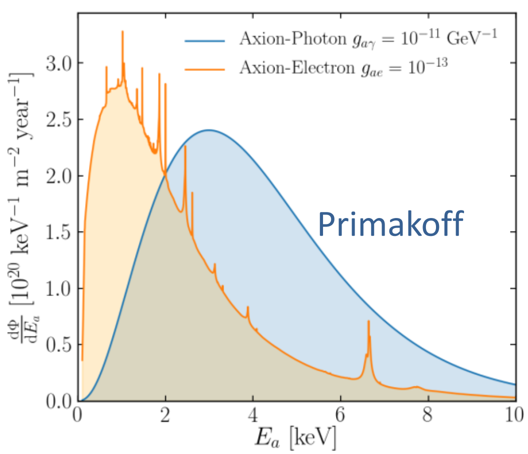

- Large coherence length overcomes small coupling
- Axion-photon conversion in B-field similar to neutrino flavor oscillation, PRD 37 (1988) 1237
- Can be enhanced with gas filling van Bibber+ PRD 39 (1989) 2089

https://cajohare.github.io/IAXOmass/

Let's point a magnet at the sun…

© Sebastian Baum

…and look for X-Rays!

Rochester-Brookhaven-FermiLab

Lazarus+ PRL 69 (1992) 2333

Few hours of data, fixed magnet

$G_{a\gamma\gamma} < 0.77 \times 10^{-8}\ \mathrm{GeV}^{-1}$

Tokyo Helioscope (Sumico)

Fully stearable, 2.3 m long, 4 Tesla

Moriyama+ [hep-ex/9805026]

$G_{a\gamma\gamma} < 0.60 \times 10^{-9}\ \mathrm{GeV}^{-1}$

See also Ohta+ [1201.4622]

Konstantin Zioutas

CAST (1998–2021)

Stearable, 9.26 m long, 9 Tesla

CAST Collaboration [2406.16840]

$G_{a\gamma\gamma} < 0.58 \times 10^{-10}\ \mathrm{GeV}^{-1}$

CAST Movie on YouTube

https://youtu.be/XY2lFDXz8aQ

Parameter Space for Axion-Like Particles (ALPs)

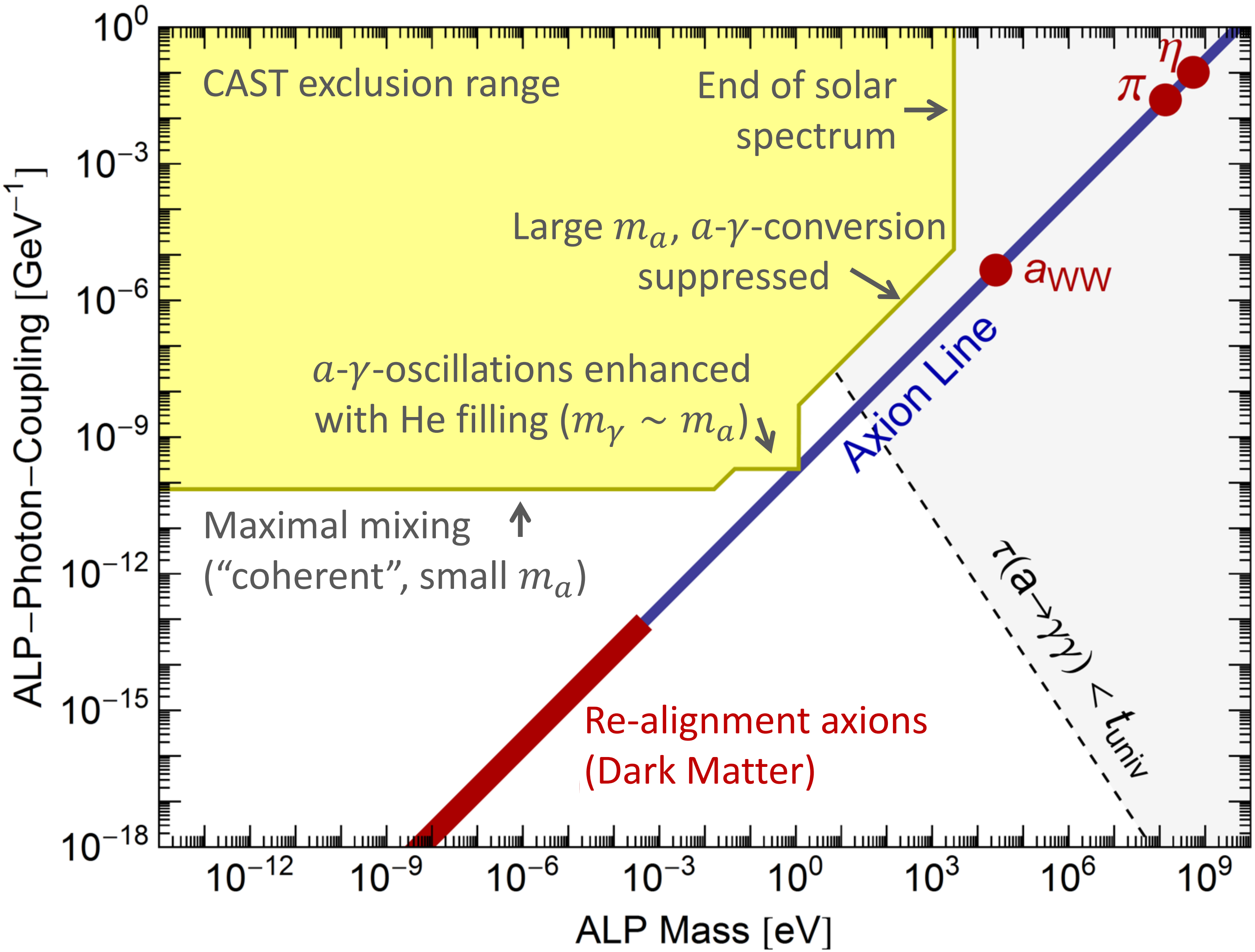

(Baby) IAXO Sensitivity Forecast

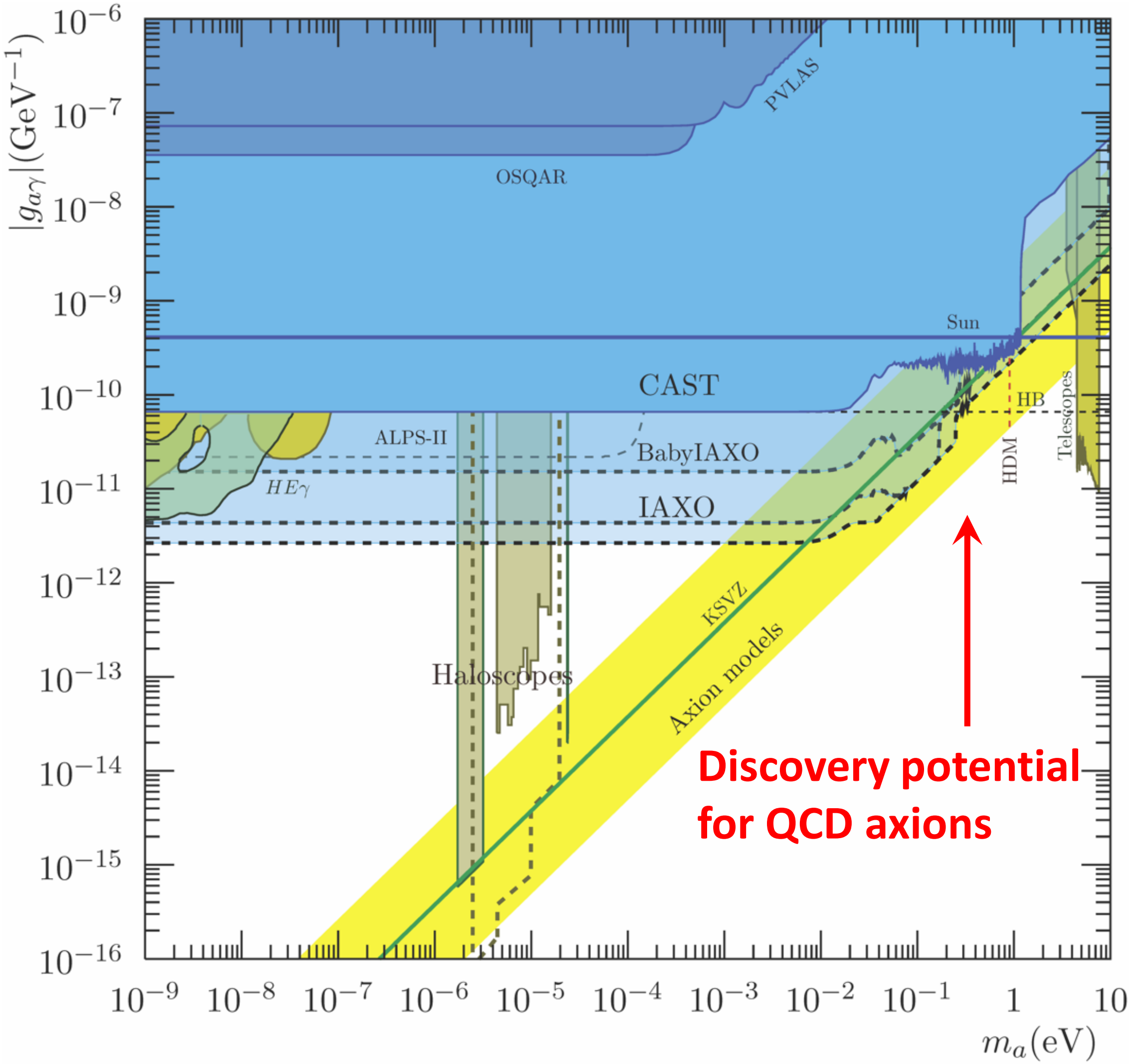

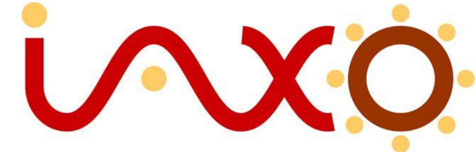

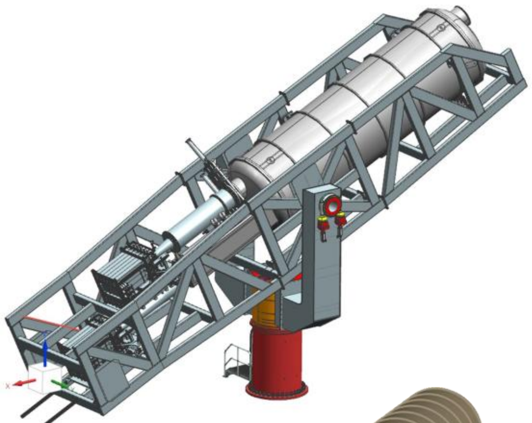

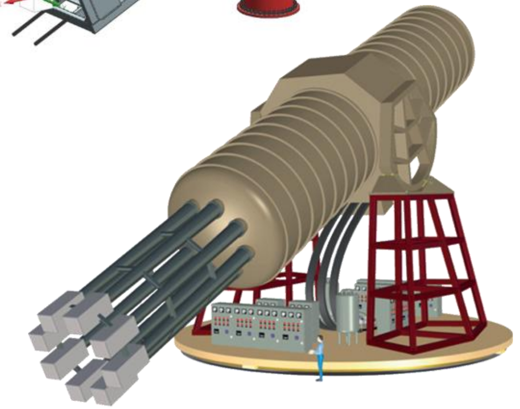

Physics potential of the International Axion Observatory (IAXO)

JCAP 1906 (2019) 047, arXiv:1904.09155

Grand Unified ALP Scape

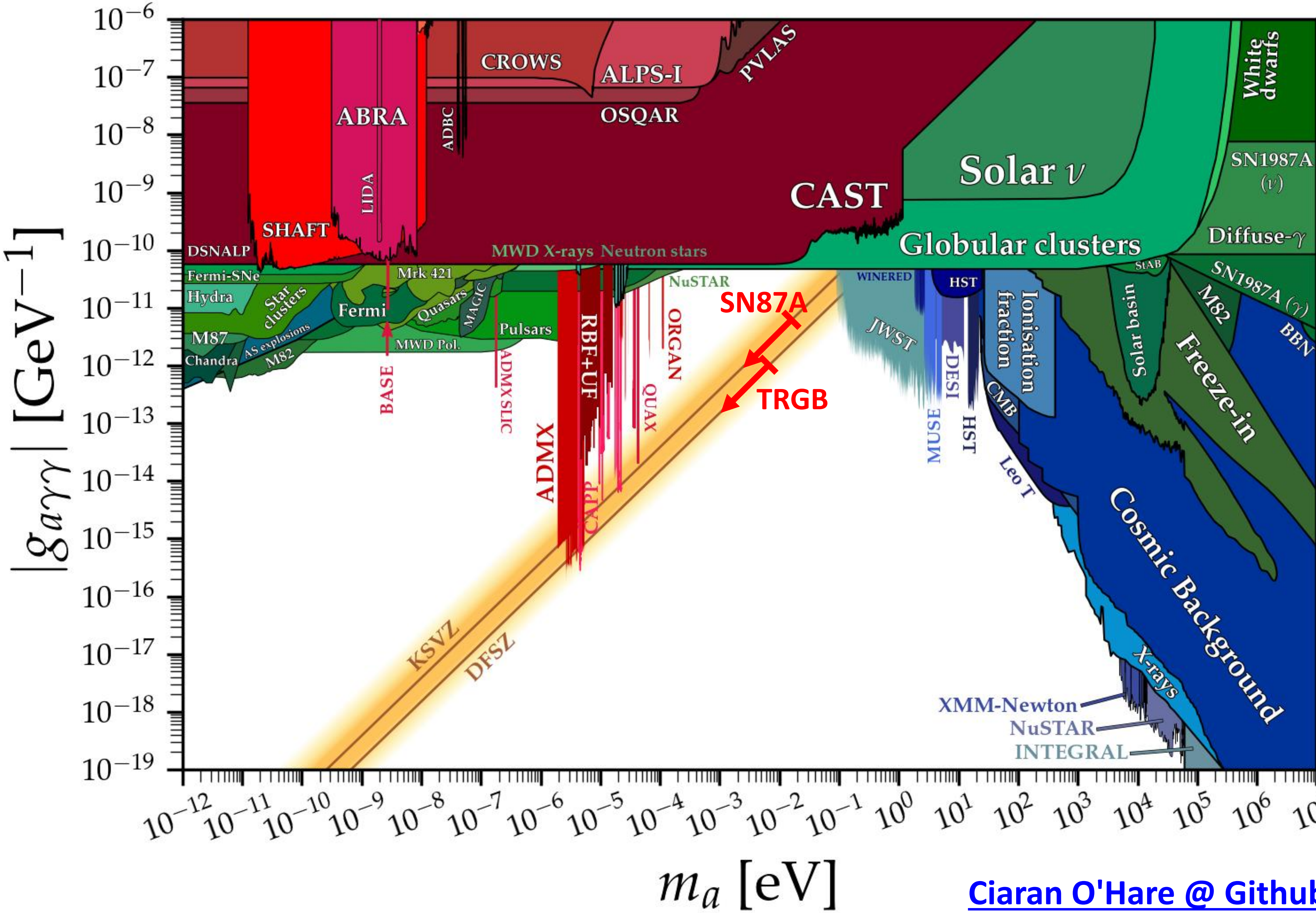

Ciaran O'Hare @ Github

Hillas Plot

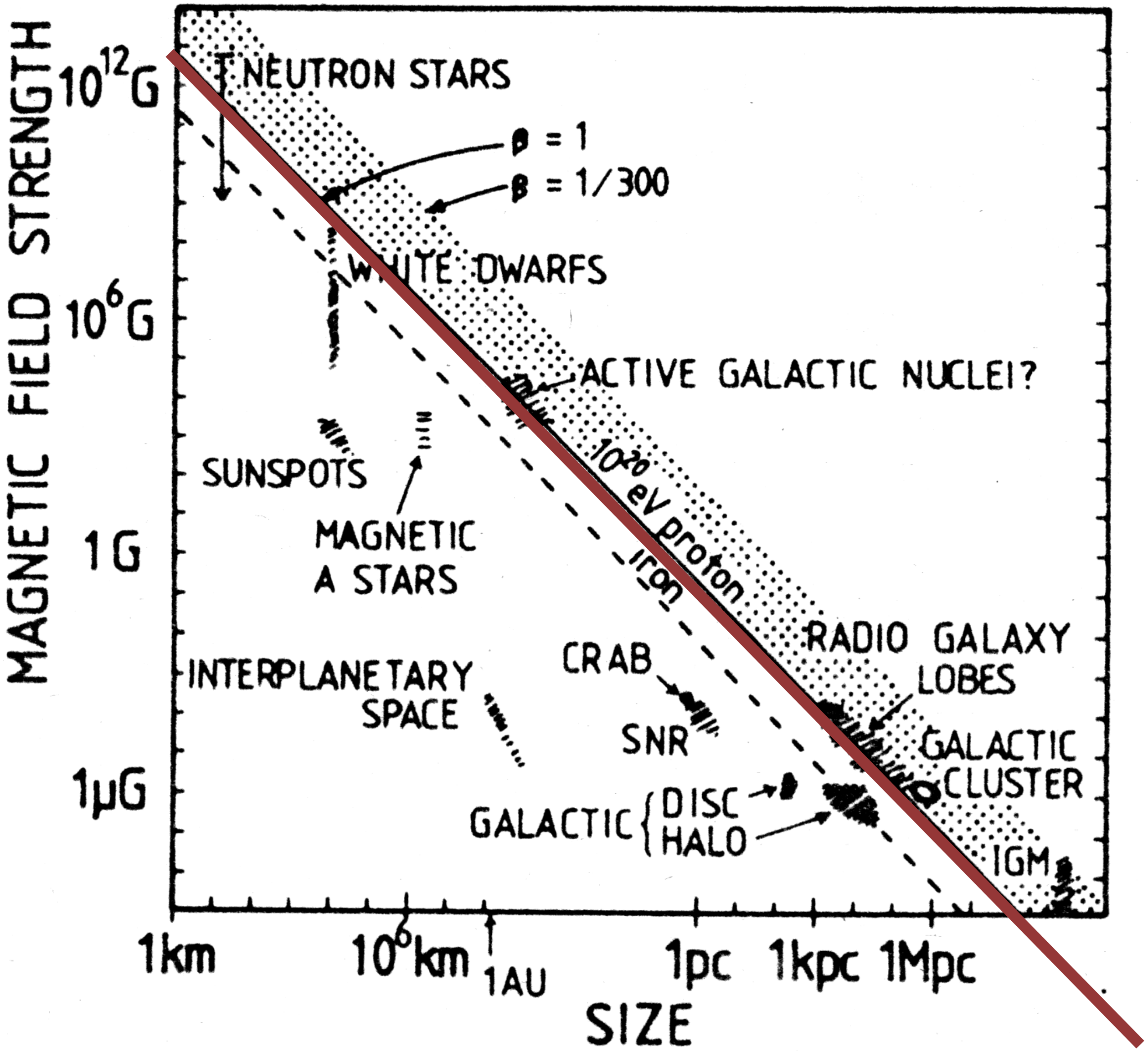

A. M. Hillas
Ann. Rev. Astron. Astrophys.
22, 425 (1984)

Size and B field strength of possible sites for particle acceleration. Objects below the line cannot accelerate protons to 10^{20} eV

ALP-γ conversion

$$\frac{g_{a\gamma}}{10^{12}\mathrm{GeV}} BL \sim 1$$

EVOLUTION OF STARS

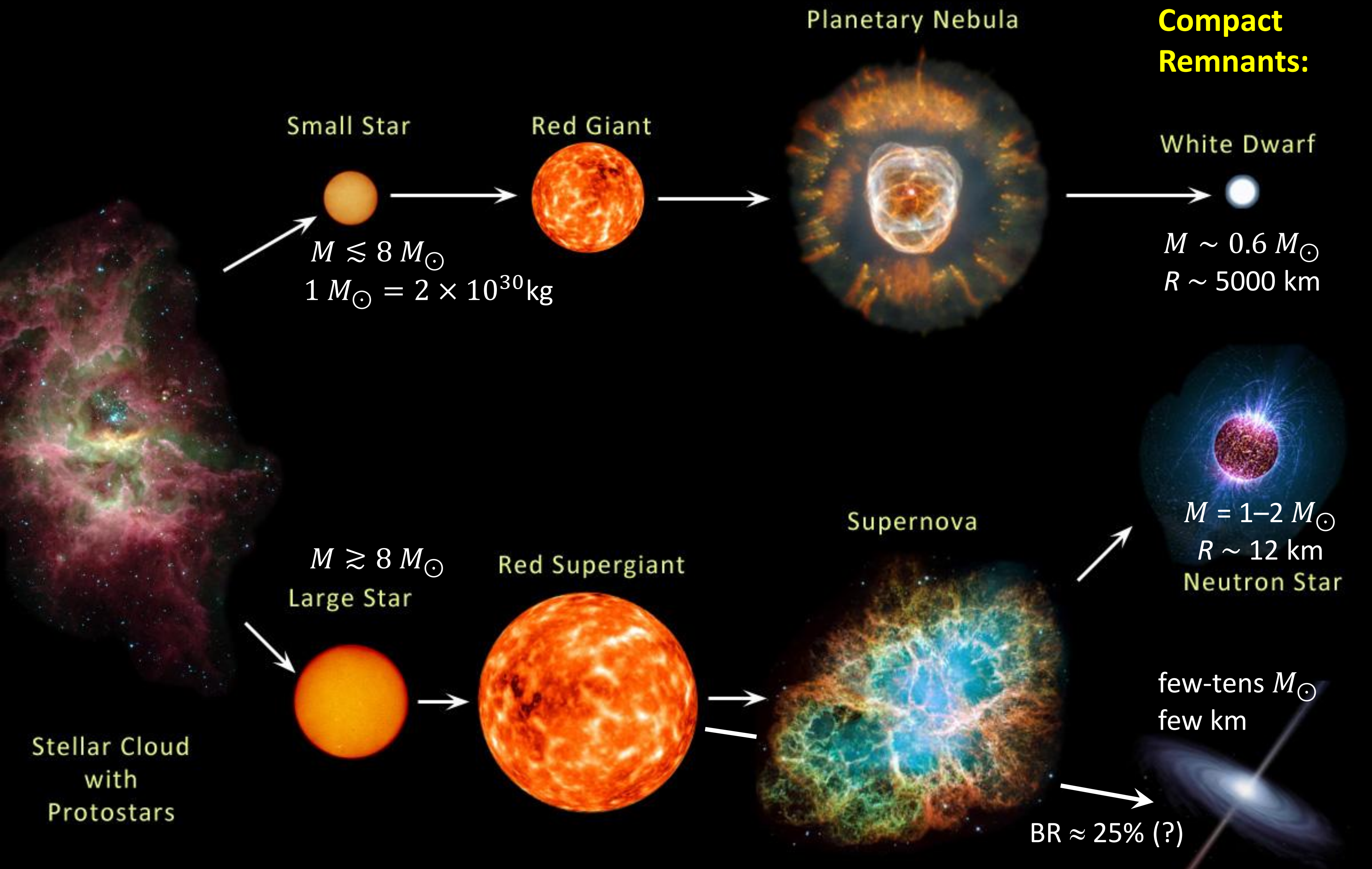

http://earthspacecircle.blogspot.com/2013/07/stellar-evolution.html

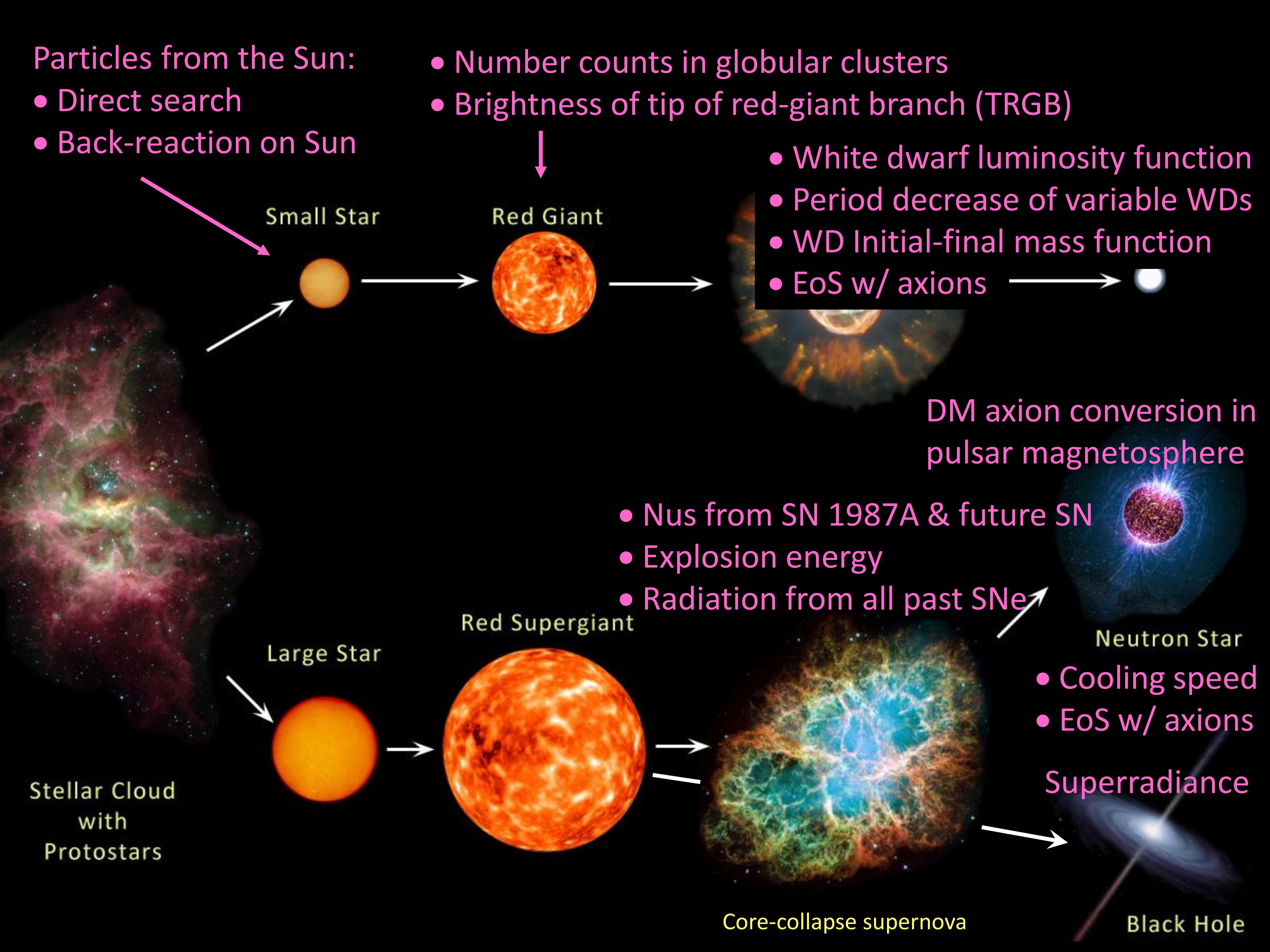
Particles from the Sun:
• Direct search
• Back-reaction on Sun
• Number counts in globular clusters
• Brightness of tip of red-giant branch (TRGB)
• White dwarf luminosity function
• Period decrease of variable WDs
• WD Initial-final mass function
• EoS w/ axions
Small Star
Red Giant
DM axion conversion in pulsar magnetosphere
• Nus from SN 1987A & future SN
• Explosion energy
• Radiation from all past SNe
Red Supergiant
Large Star
Neutron Star
• Cooling speed
• EoS w/ axions
Superradiance
Stellar Cloud with Protostars
Core-collapse supernova
Black Hole

Galactic Globular Cluster M55

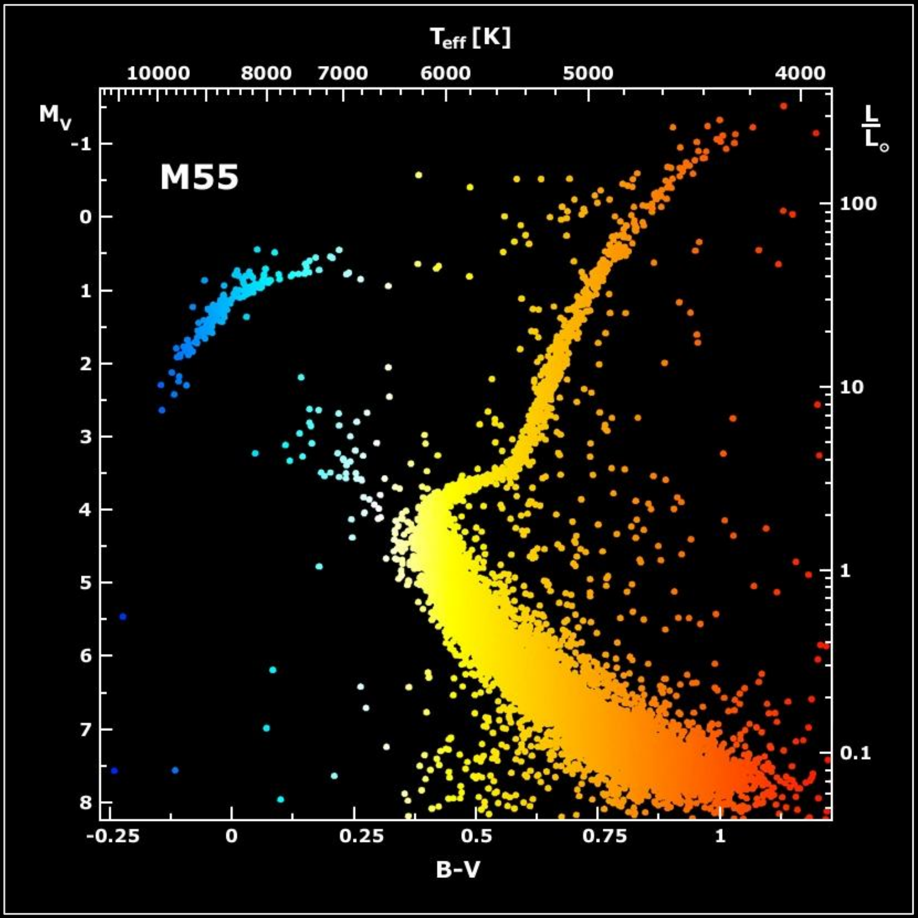

TRGB in 46 Globular Clusters [Cerny+ 2012.09701]

Color-Magnitude Diagram for Globular Clusters

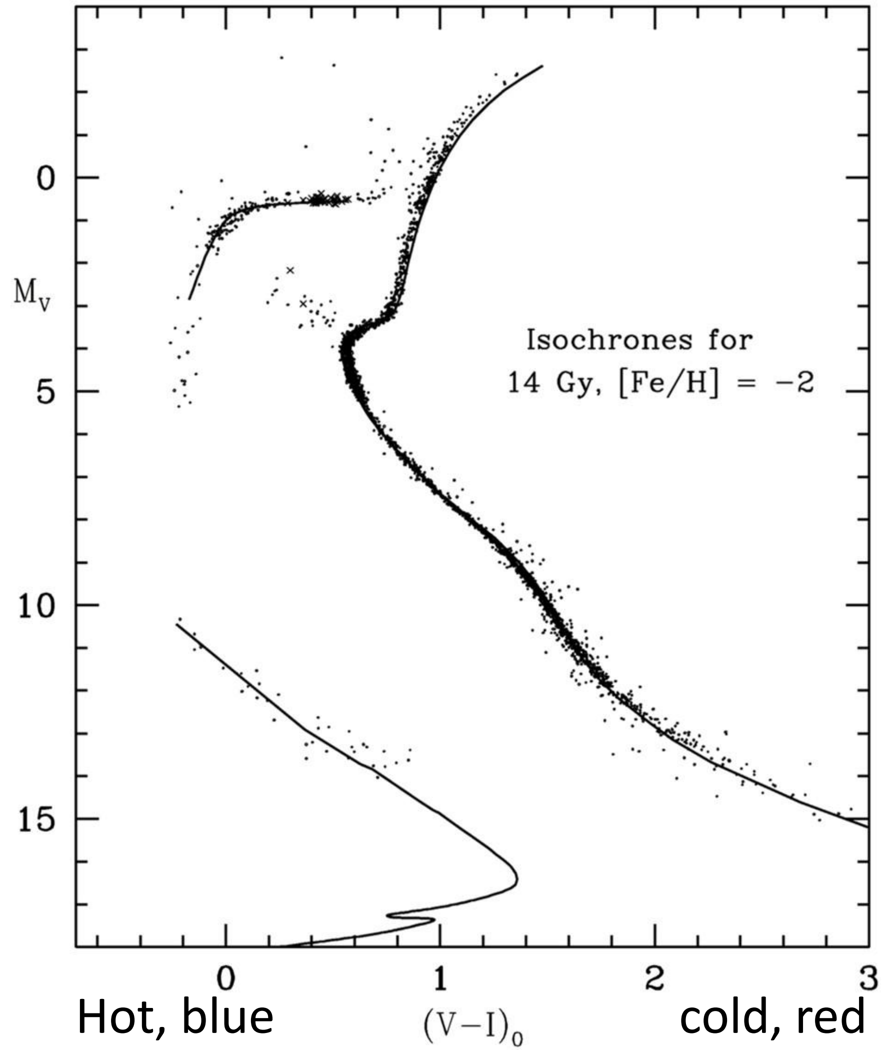

Color-magnitude diagram synthesized from several low-metallicity globular clusters and compared with theoretical isochrones (W.Harris, 2000)

Color-Magnitude Diagram for Globular Clusters

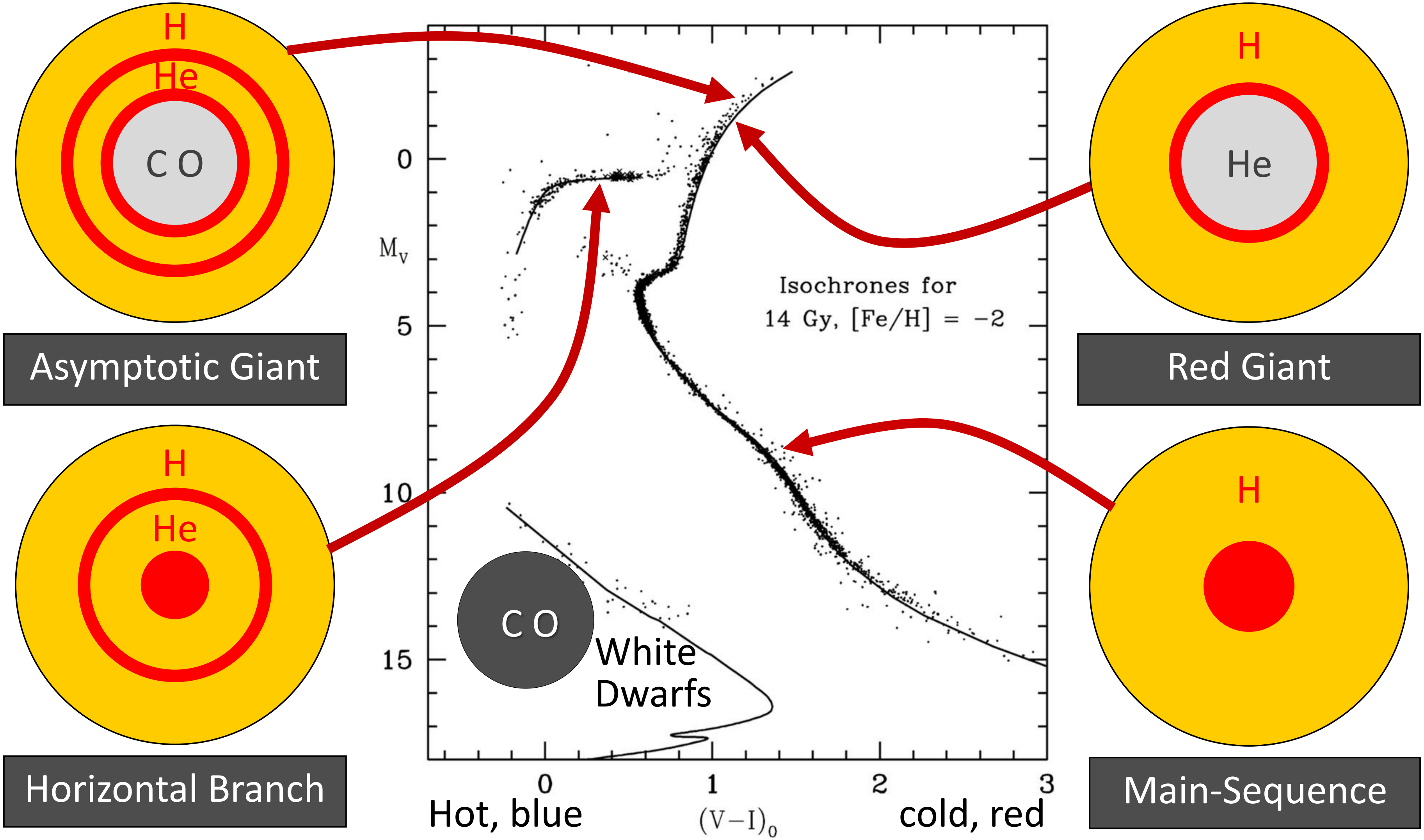

Color-magnitude diagram synthesized from several low-metallicity globular clusters and compared with theoretical isochrones (W.Harris, 2000)

Color-Magnitude Diagram for Globular Clusters

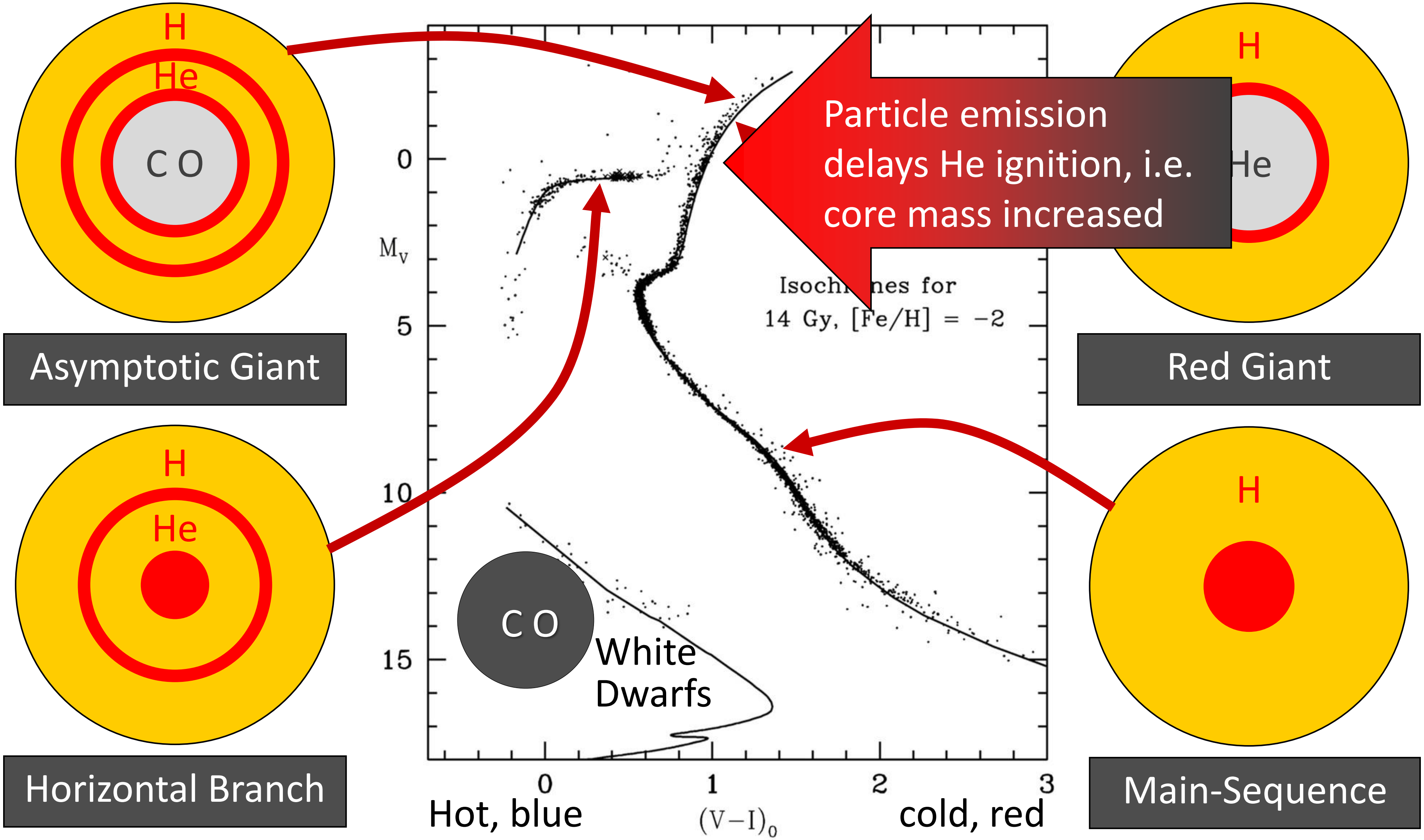

Color-magnitude diagram synthesized from several low-metallicity globular clusters and compared with theoretical isochrones (W.Harris, 2000)

New TRGB Calibration from 21 Globular Clusters

Straniero+ arXiv:2010.03833 and https://www.ggi.infn.it/talkfiles/slides/slides6554.pdf

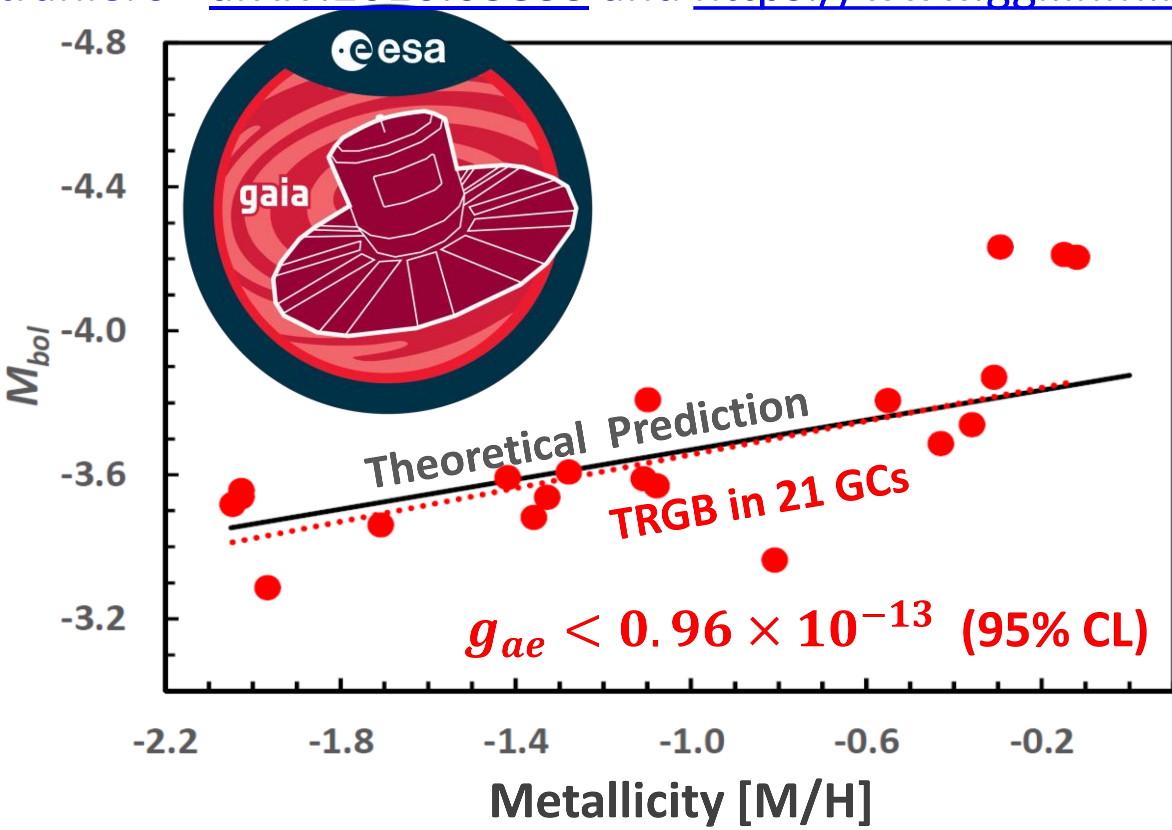

Emission of axions & friends with direct electron coupling

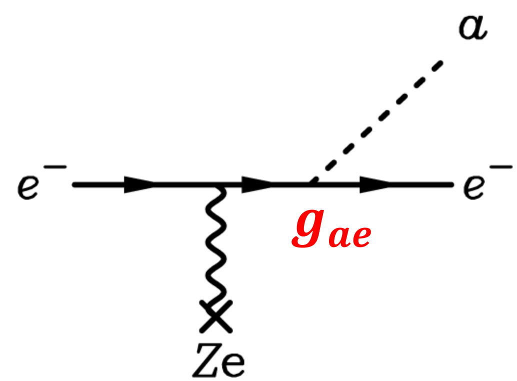

Bremsstrahlung emission by degenerate electrons

Bound for neutrino dipole moments

$$\sqrt{\sum_i |\mu_i|^2} < 0.92 \times 10^{-12} \mu_B \text{ (95\% CL)}$$

Plasmon decay

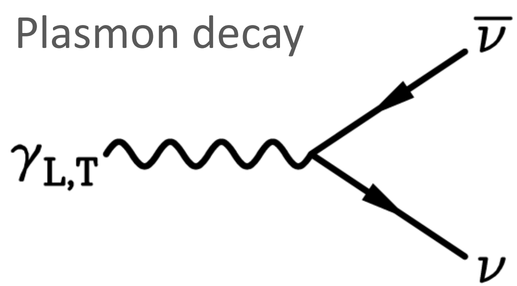

Supernova 1987A

23 February 1987

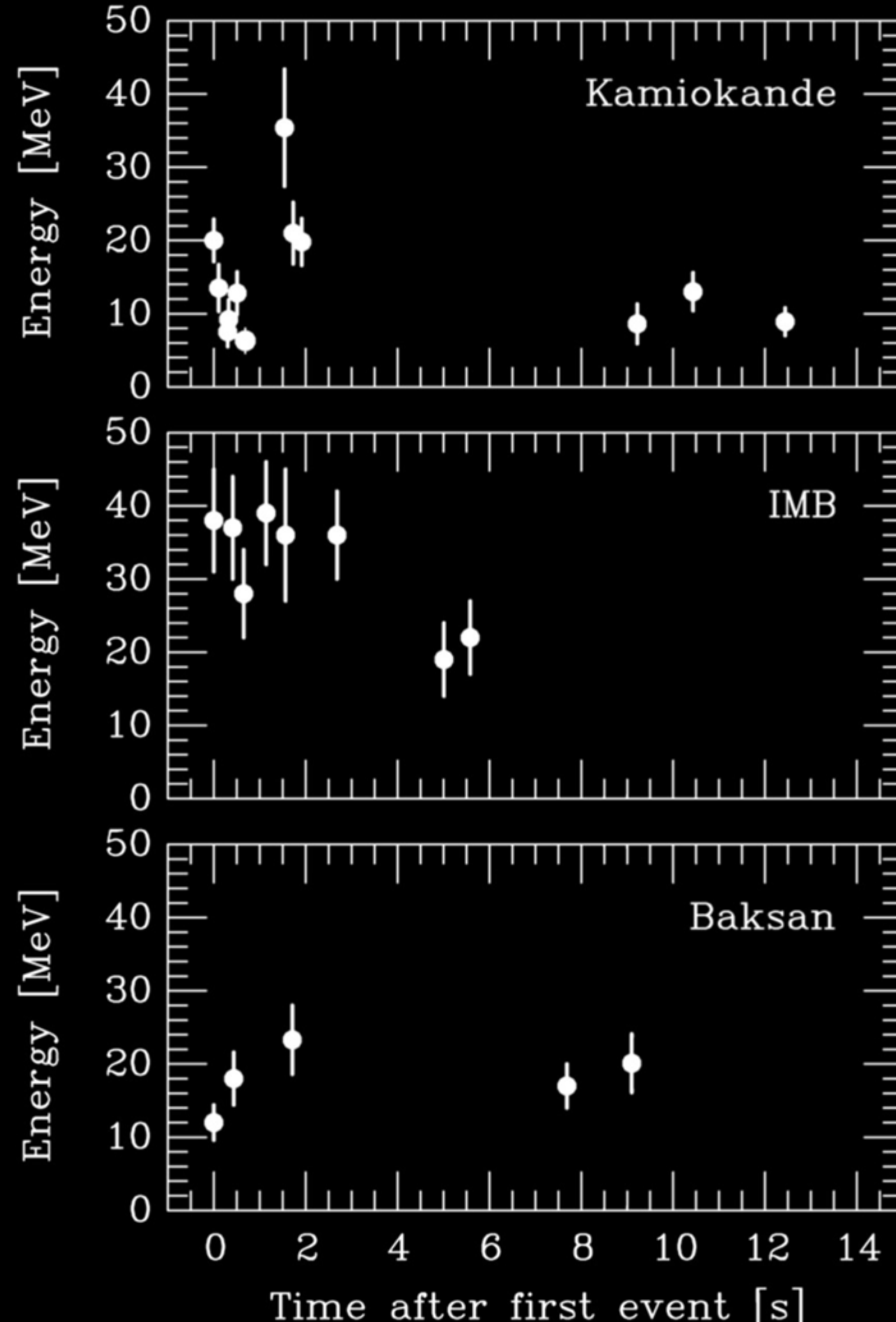

Stellar Collapse and Explosion

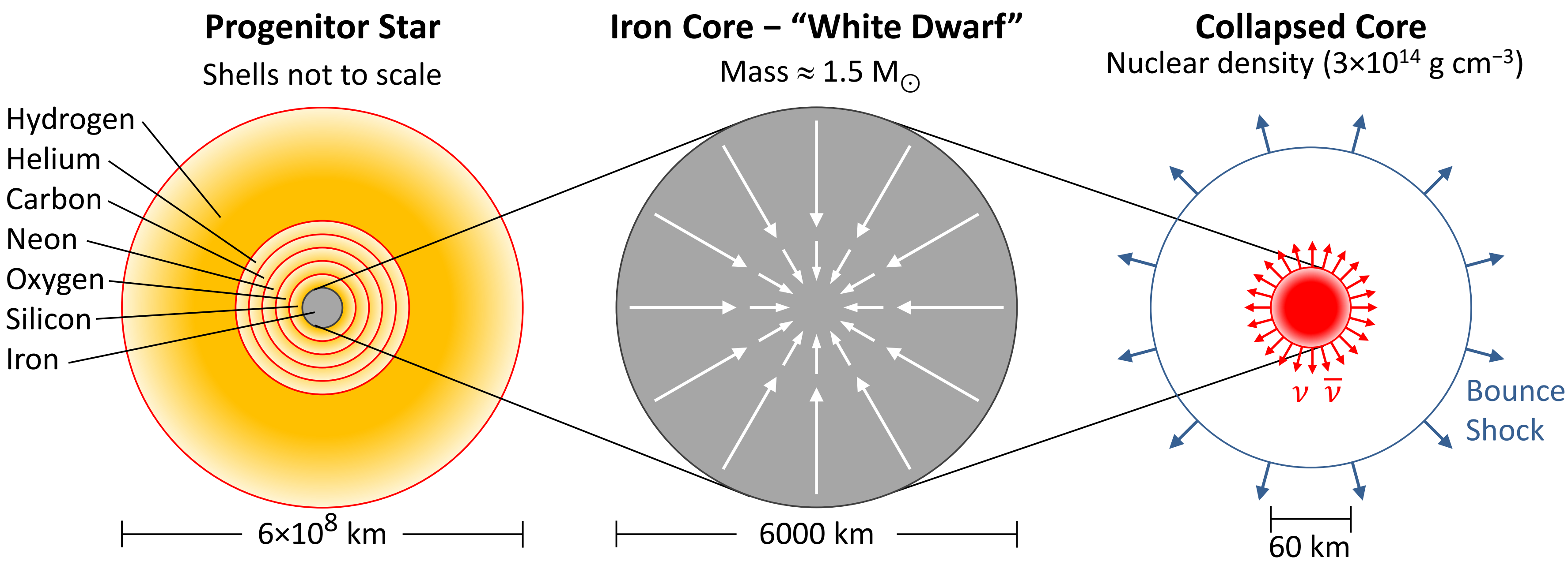

Gravitational binding energy

$$E_b \approx 3 \times 10^{53}\,\text{erg} \approx 15\%\, M_{SUN}\, c^2$$

This shows up as

99% Neutrinos

1% Kinetic energy of explosion

0.01% Photons, outshine host galaxy

Supernova 1987A Energy-Loss Argument

SN 1987A neutrino signal

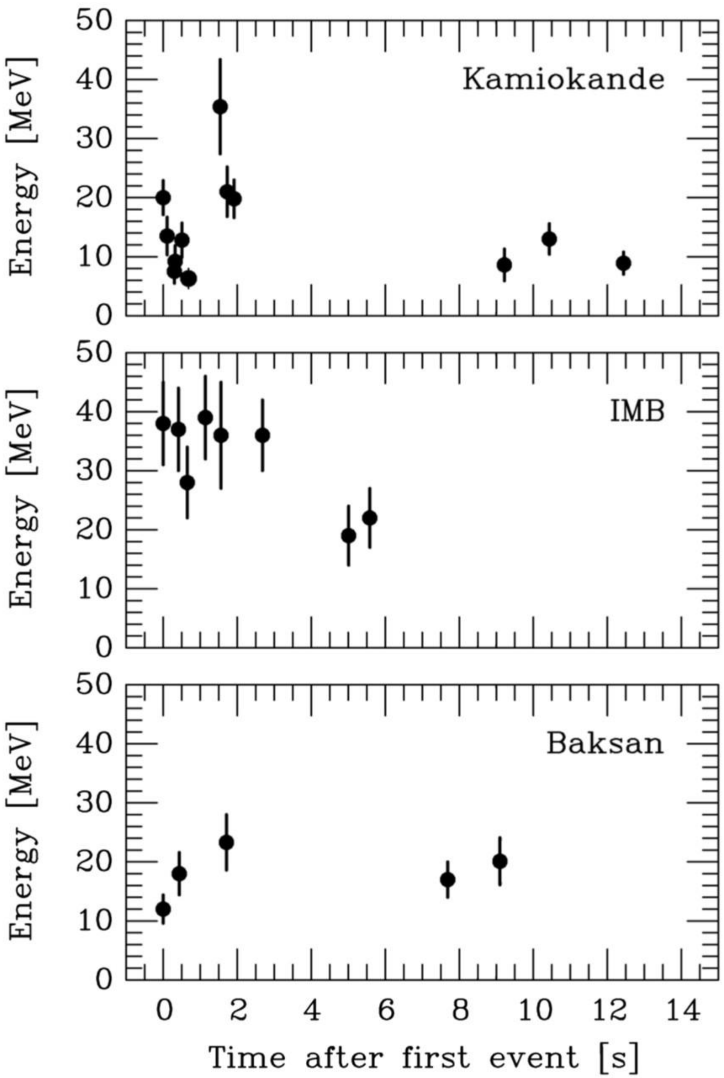

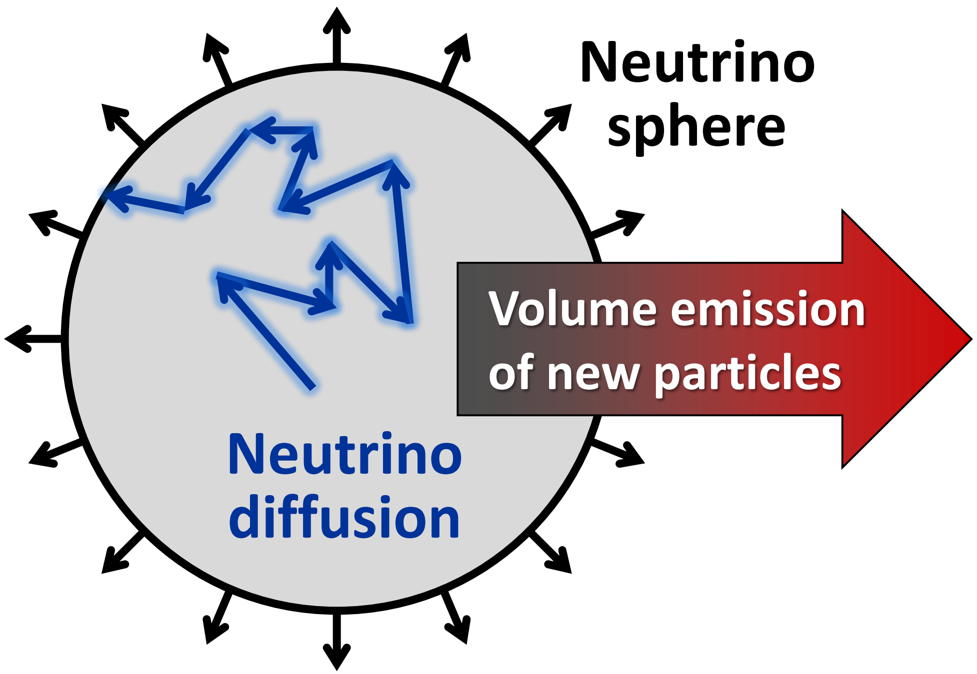

Emission of very weakly interacting particles would "steal" energy from the neutrino burst and shorten it.
(Early neutrino burst powered by accretion, not sensitive to volume energy loss.)

Late-time signal most sensitive observable

Axion Emission from a Nuclear Medium

Axion-nucleon interaction: $\mathcal{L}_{\rm int} = \frac{C_N}{2f_a}\,\overline{\Psi}_N\gamma_\mu\gamma_5\Psi_N\partial^\mu a = \frac{C_N}{2f_a}J^A_\mu\partial^\mu_a$

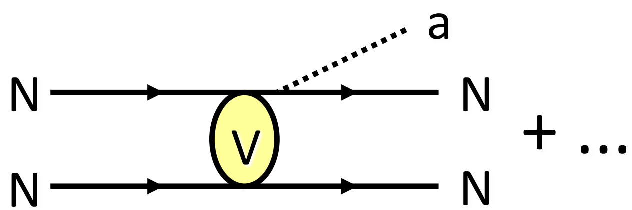

Nucleon-Nucleon Bremsstrahlung

Axial-vector interaction implies dominance of spin-dependent process

- Interaction potential (one-pion exchange OPE was often used, but too simplistic) → **Carenza+** arXiv:1906.11844
- In-medium coupling constants → **Springmann+** arXiv:2410.10945
- In-medium effective nucleon properties
- Correlation effects (static and dynamical spin-spin correlations)
- Thermal π^- contribute significantly (dominantly?) → **Carenza+** arXiv:2010.02943

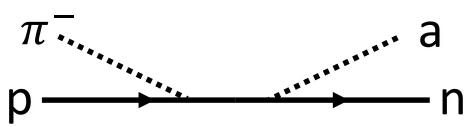

Axion emission is a complicated nuclear physics problem, for several issues see Fiorillo, Gil Muyor, Janka, Raffelt & Vitagliano, arXiv:2509.13322

SN 1987A Axion Limits from Burst Duration

- Raffelt, Lect. Notes Phys. 741 (2008) 51 hep-ph/0611350
  Burst duration calibrated by early numerical studies
  "Generic" emission rates inspired by OPE rates
  $f_a \gtrsim 4 \times 10^8$ GeV and $\boldsymbol{m_a \lesssim 16}$ **meV** (KSVZ, based on proton coupling)
- Chang, Essig & McDermott, JHEP 1809 (2018) 051 1803.00993
  Various correction factors to emission rates, specific SN core models
  $f_a \gtrsim 1 \times 10^8$ GeV and $\boldsymbol{m_a \lesssim 60}$ **meV** (KSVZ, based on proton coupling)
- Carenza, Fischer, Giannotti, Guo, Martínez-Pinedo & Mirizzi, JCAP 10 (2019) 016 & Erratum 1906.11844
  Beyond OPE emission rates, specific SN core models: similar to Chang et al.
  $f_a \gtrsim 4 \times 10^8$ GeV and $\boldsymbol{m_a \lesssim 15}$ **meV** (KSVZ, based on proton coupling)
- Carenza, Fore, Giannotti, Mirizzi & Reddy 2010.02943
  Including thermal pions $\pi^- + p \to n + a$ (factor 3 larger emission)
  $f_a \gtrsim 5 \times 10^8$ GeV and $\boldsymbol{m_a \lesssim 11}$ **meV** (KSVZ, based on proton coupling)
- Bar, Blum & D'Amico, **Is there a supernova bound on axions?** 1907.05020
  Alternative picture of SN explosion (thermonuclear event)
  Observed signal not PNS cooling. SN1987A neutron star (or pulsar) not yet found.
  (but see "NS 1987A in SN 1987A", Page et al. arXiv:2004.06078)

Where is the Neutron Star of SN 1987A?

No pulsar or neutron star has been seen until now (38 years later)

- Infra-red excess observed by ALMA: In "the blob" strong indication for NS Expected position, remnant hidden by dust [Cigan+ arXiv:1910.02960]
- Most plausible model: Thermally cooling non-pulsar NS [Page+ arXiv:2004.06078]

https://www.bbc.com/news/science-environment-50473482

Atacama Large Millimeter/Submillimeter Array (ALMA) at ESO in Chile

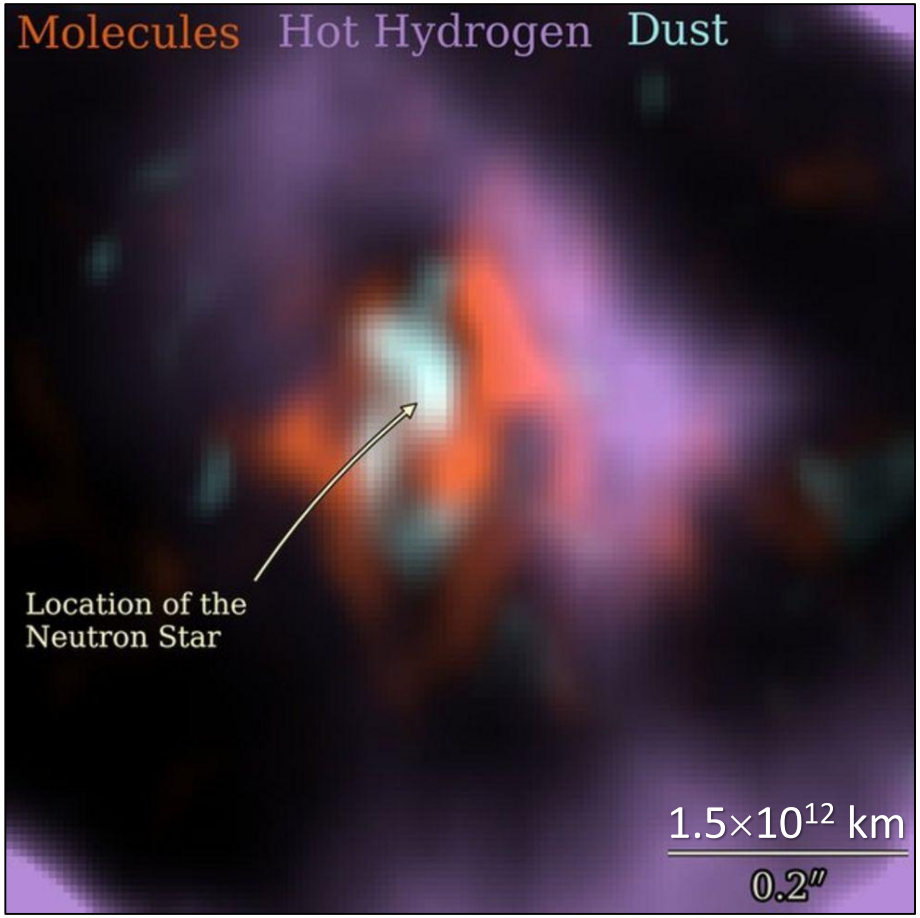

SN 1987A Signal Duration Too Long?

Fiorillo+ arXiv:2308.01403

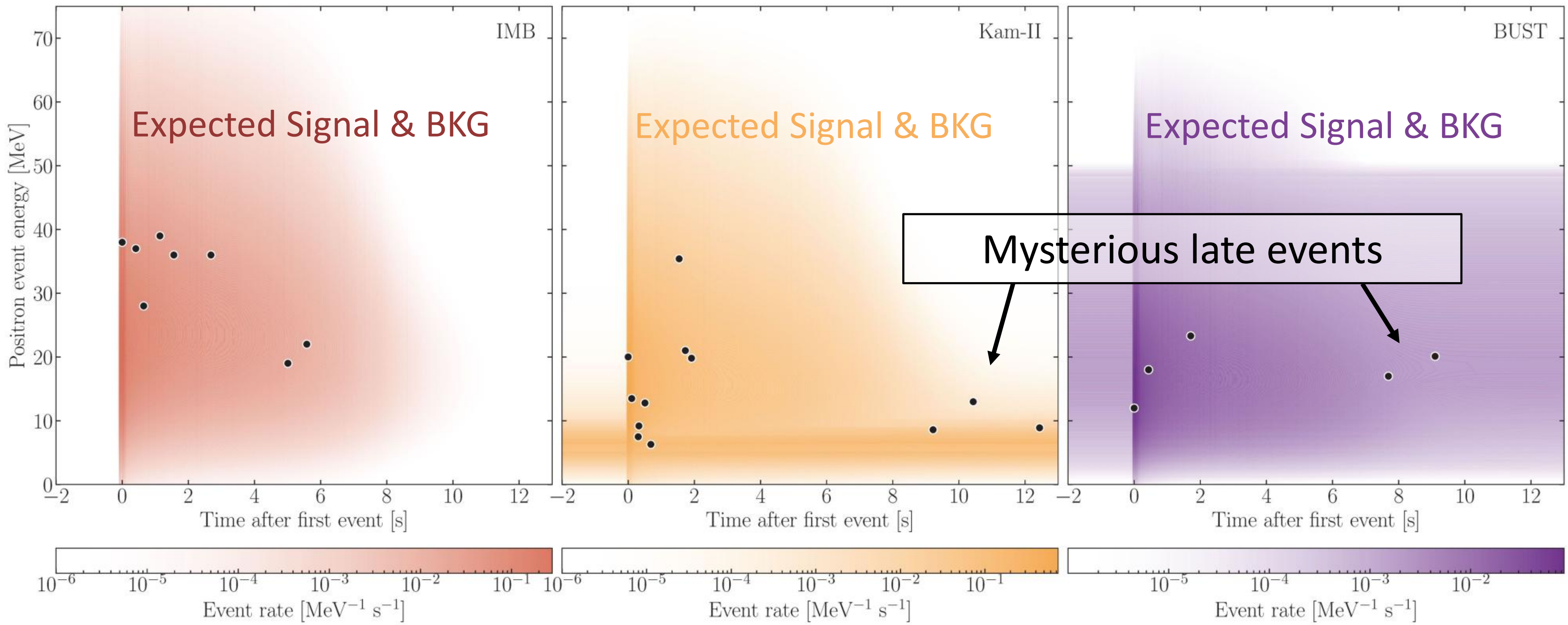

FIG. 17. Differential event distribution (signal and background) at each experiment, compared with the observations. Results are shown for model 1.44-SFHo without flavor swap; the offset time for each experiment is chosen as the best-fit value reported in Table VII.

- **In a suite of Garching models (no axions), expected signal always too short (PNS convection and reduced opacities by correlations!)**
- **Deserves dedicated study**

Detecting Axions with Next Galactic Supernova?

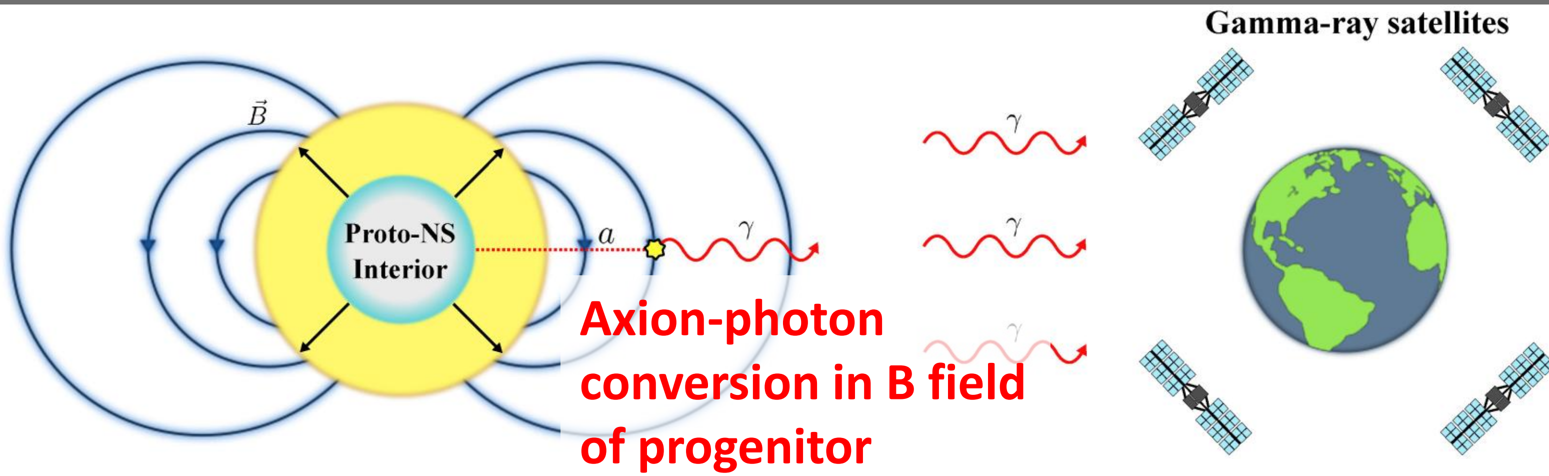

Axion-photon conversion in B field of progenitor

4 Fermi-LAT like satellites (proposed GALAXIS)

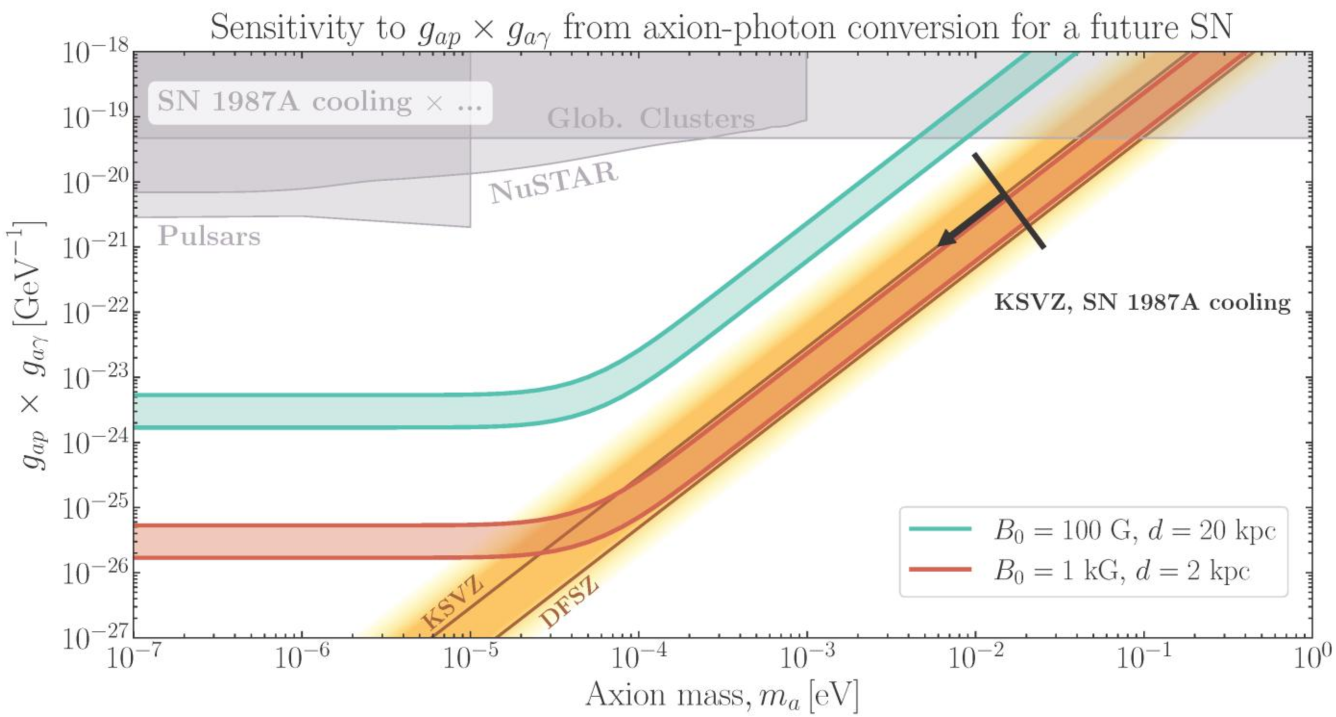

Manzari+
arXiv:2405.19393

This figure:
Fiorillo, Gil Muyor, Janka, Raffelt & Vitagliano
arXiv:2509.13322

For optimistic SN assumptions (distance, B field) QCD axion parameters reachable

Astrophysical Axion Bounds

The 2024 Edition, Caputo & Raffelt, arXiv:2401.13728, 24 Jan 2024

See also Carenza, Giannotti, Isern, Mirizzi & Straniero, arXiv:2411.02492

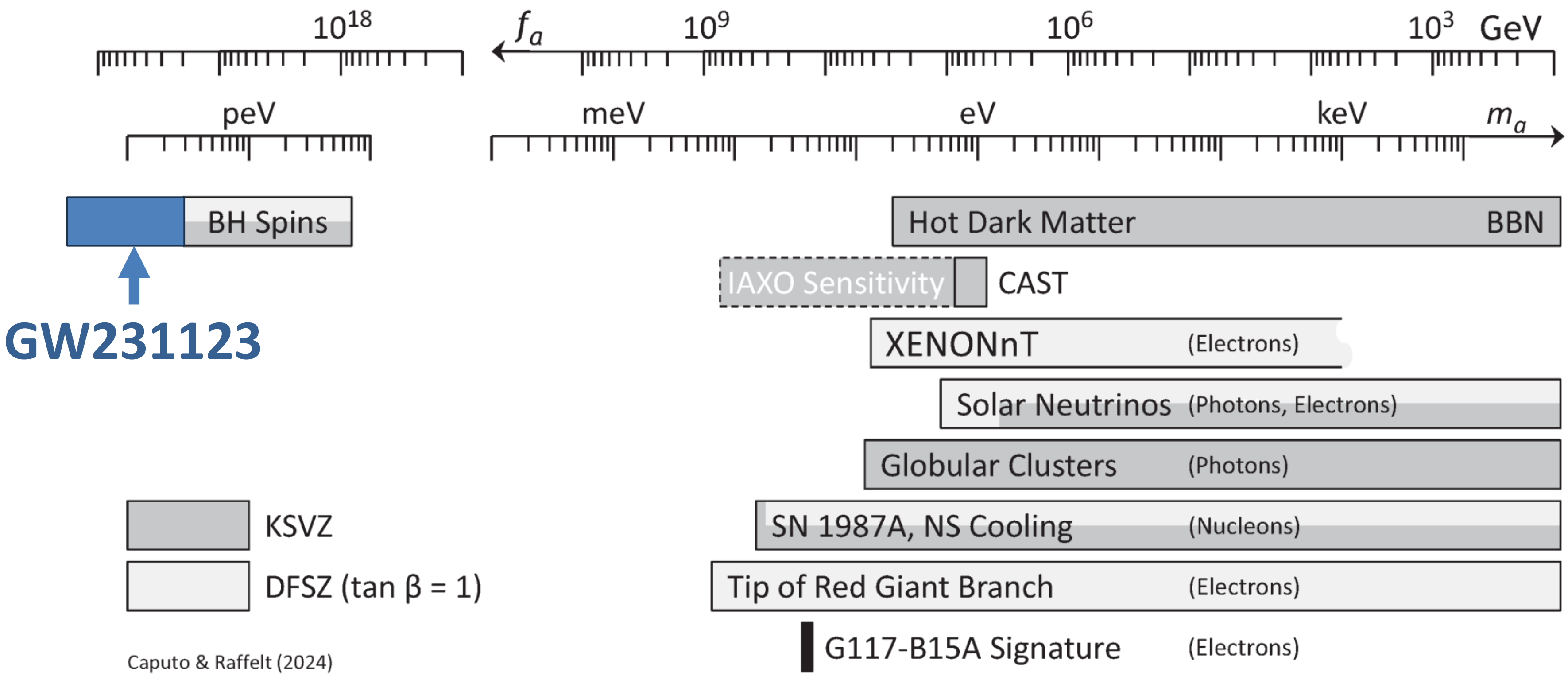

- Many improvements over the years, but overall picture the same
- Specific QCD axion signatures cannot come from cooling effects
- Best stellar detection opportunity probably (Baby)IAXO

Superradiance

Extraction of rotational energy from spinning object by low-frequency modes $\omega < \Omega$ of an external bosonic field

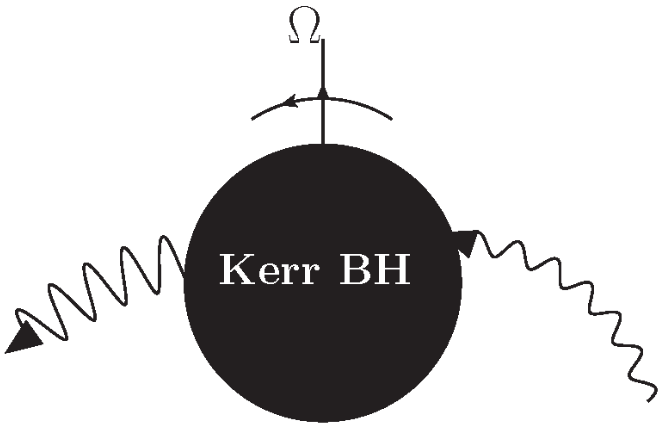

$m\Omega > \omega$

- **Bosons with mass get gravitationally bound**
- **Superradiant run-away mode** $\phi = Y_{lm}(\theta,\phi)\psi_{lmn}(r)e^{\Gamma t}$
- **"Bosonic atom"**
- **Transitions → Gravitational waves**

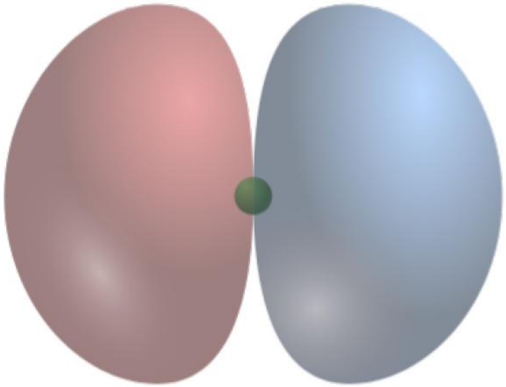

Superradiance: New Frontiers in Black Hole Physics (2020 edition)

R. Brito, V. Cardoso & P. Pani, 1501.06570v8 (8 Jan 2021)

BH Spins from Binary Merger GW231123

LIGO-Virgo-KAGRA observed GWs from BH-BH merger GW231123
$137^{+22}_{-17} M_\odot$ and $103^{+20}_{-52} M_\odot$ with large spins

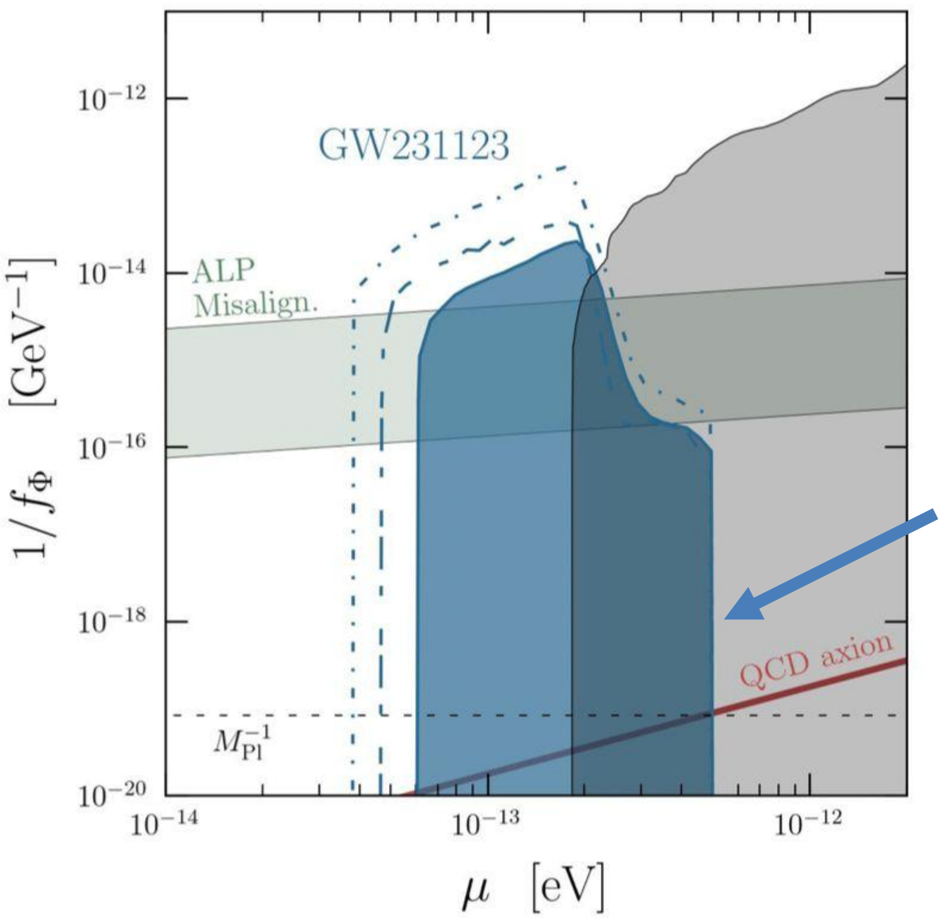

New superradiance bounds on scalar boson masses

Caputo, Franciolini & Witte
arXiv:2507.21788 (29 July 2025)

Aswathi, East, Siemonsen, Sun & Jones
arXiv:2507.20979 (28 July 2025)

Dark Matter Axion-Photon Conversion in Neutron Star Magnetospheres

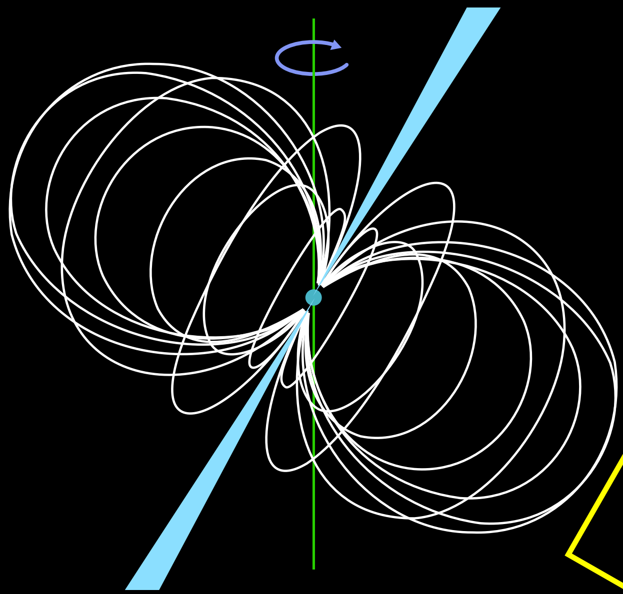

Dark matter axions
$m_a \sim \mu\text{eV},\ v_a \sim 10^{-3}c$

Very narrow radio line

Pshirkov & Popov 2007
arXiv:0711.1264
Many papers recently

Axion mass and plasma frequency
Degenerate near NS surface
→ Resonant conversion

Searching for Axions with Radio Telescopes

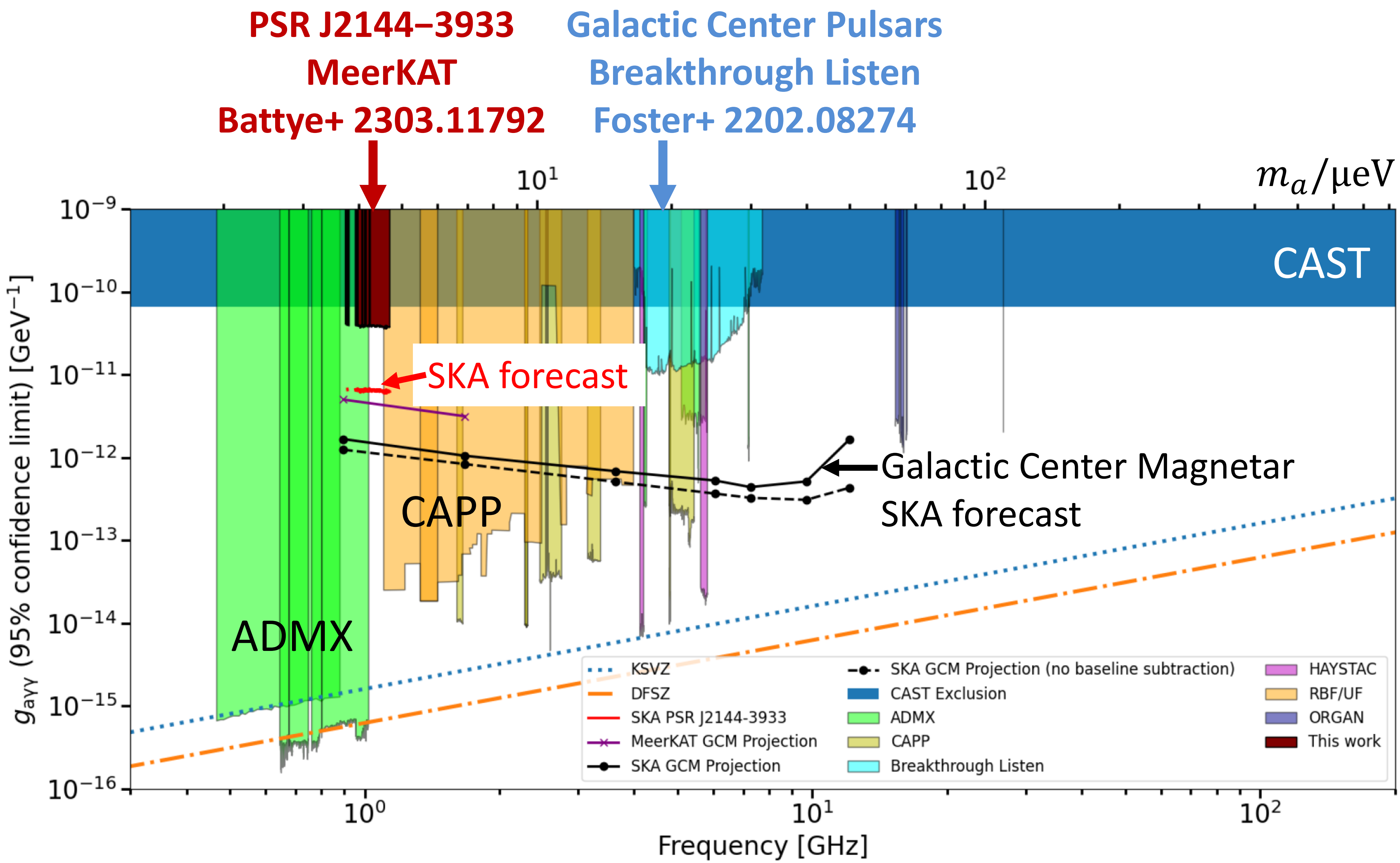

Axion Clouds around Neutron Stars

Polar cap cascades

D.Noordhuis, A.Prabhu, S.J.Witte, A.Y.Chen, F.Cruz & C.Weniger, arXiv:2209.09917

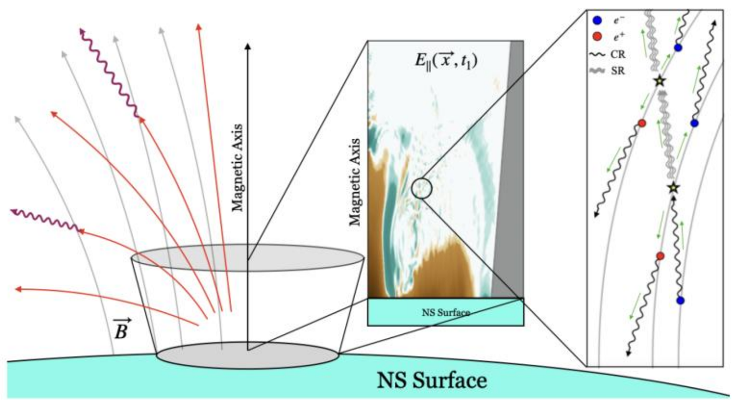

FIG. 1. Schematic figure showing axion production in neutron star vacuum gaps. The vacuum gap is depicted by a trunca cone on the neutron star surface. The left inset shows a time snapshot of $E_{\parallel}$ (as computed in the simulations of [67]), with brown/green coloring reflecting negative/positive values of $E_{\parallel}$. The right inset depicts the microphysical processes respons for the pair cascade, with green arrows indicating the direction the cascade flows with time. Axions (red) are emitted from gap and periodically convert to photons (purple) in the presence of the neutron star's magnetic field, $\vec{B}$ (grey).

- E-field extracts charges
- QED cascade
- Shuts off E-field
- Cascade stops

…

- Periodic E modulation
- Periodic **E.B**
- Sources ALPs

D.Noordhuis, A.Prabhu, C.Weniger & S.J.Witte, arXiv:2307.11811

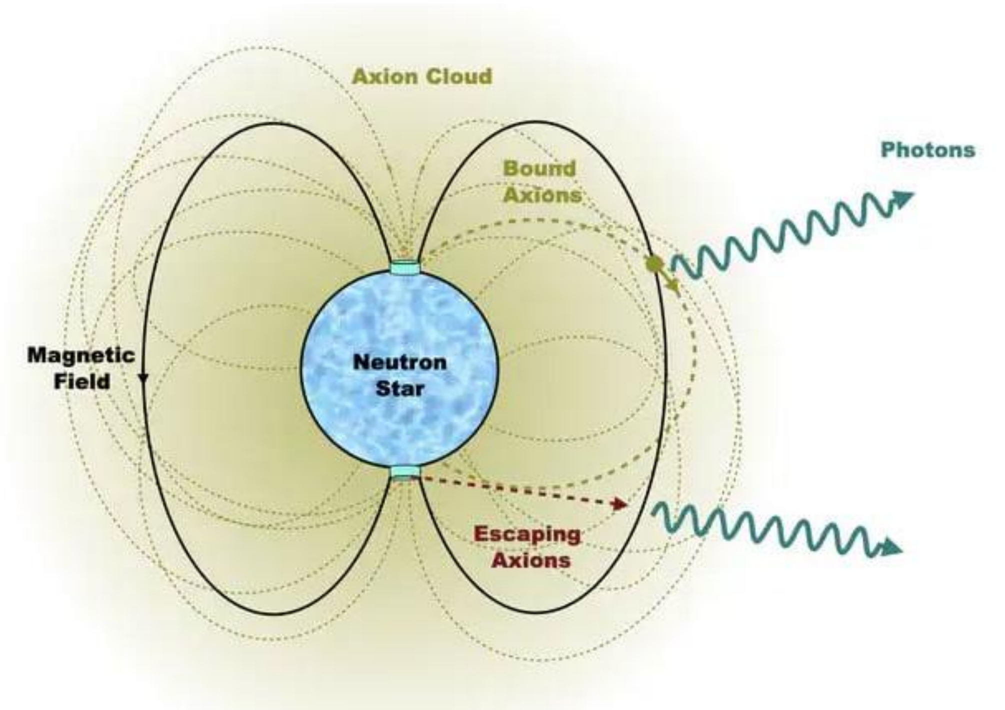

IOP Publishing physicsworld

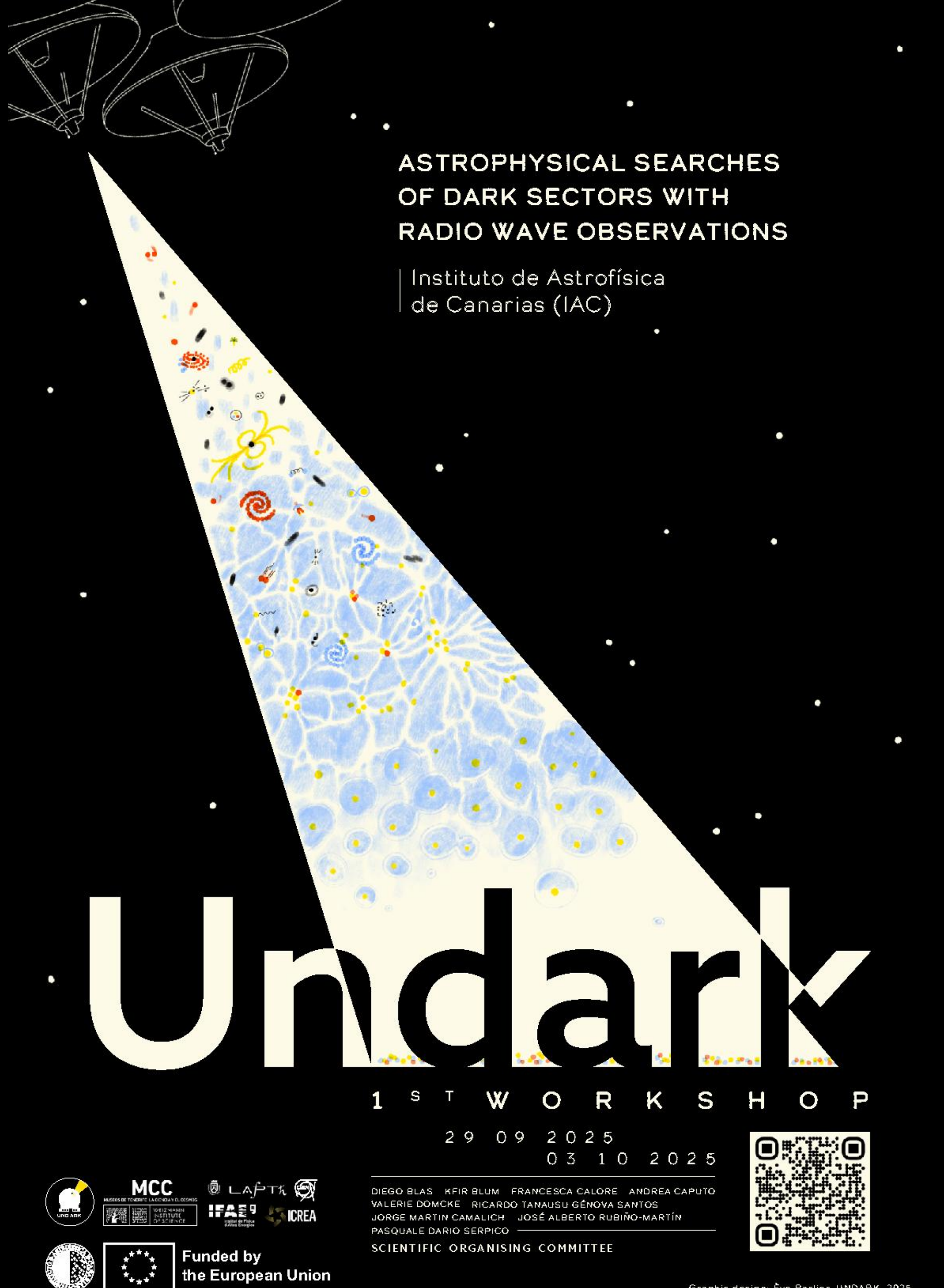
ASTROPHYSICAL SEARCHES
OF DARK SECTORS WITH
RADIO WAVE OBSERVATIONS
Instituto de Astrofísica
de Canarias (IAC)
Undark
1ST WORKSHOP
29 09 2025
03 10 2025
DIEGO BLAS KFIR BLUM FRANCESCA CALORE ANDREA CAPUTO
VALERIE DOMCKE RICARDO TANAUSU GÉNOVA SANTOS
JORGE MARTIN CAMALICH JOSÉ ALBERTO RUBIÑO-MARTÍN
PASQUALE DARIO SERPICO
SCIENTIFIC ORGANISING COMMITTEE
MCC
ICREA
Funded by
the European Union
Graphic design: Ève Barlier, UNDARK, 2025

Astrophysical Axion Bounds and Opportunities

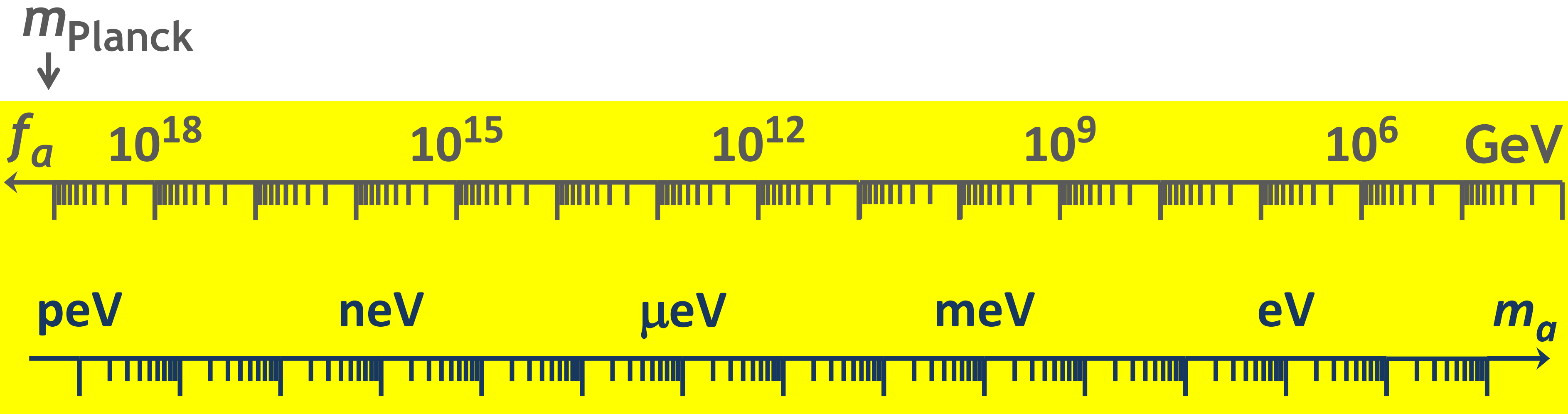

Super Radiance

Opportunities for detection

Astrophysical Bounds (Energy loss of stars)

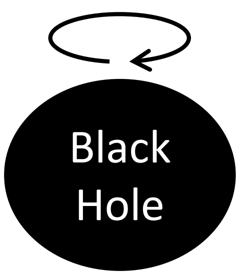

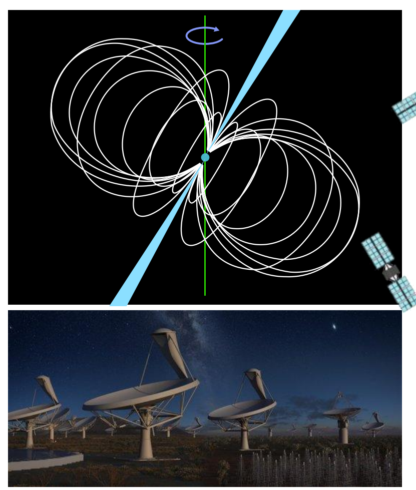

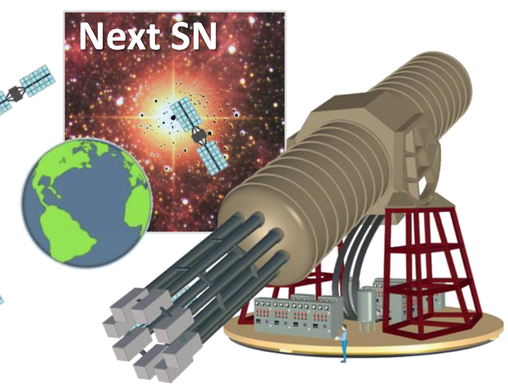

IAXO Solar Axion Telescope

Axion conversion in neutron star magnetospheres

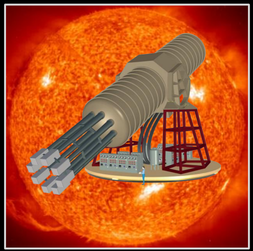

- Best bet for systematic axion search with stars

Globular clusters should be more systematically studied

- Best bounds on electron and photon coupling
- Cooling hints inconsistent

- SN1987A bounds unchanged, many refinements
- Next SN: Putting these on firm basis
- GALAXIS or IAXO detection opportunity

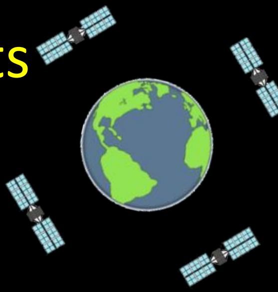

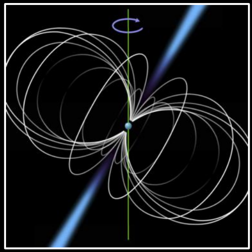

- Radio detection from pulsars
  (DM conversion, polar-cap production)

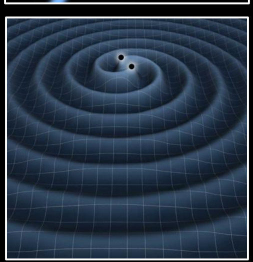

- Superradiance limits from BH spins (very small masses)
- GW signals can still show up


Solar Axions

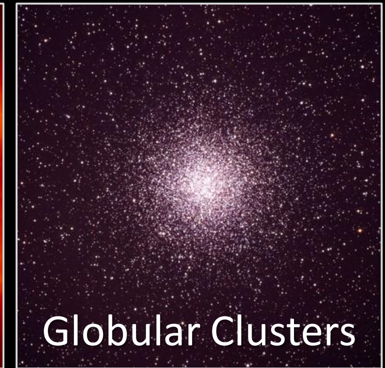
Globular Clusters


Supernova 1987A

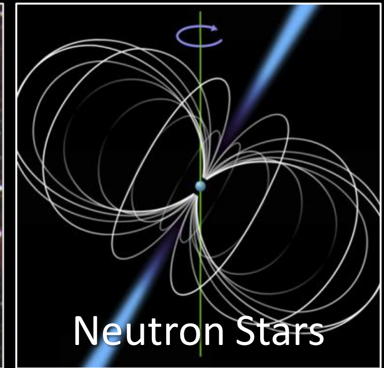
Neutron Stars

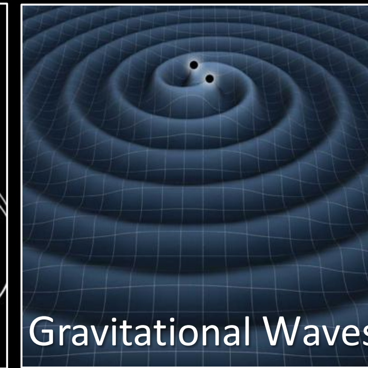
Gravitational Waves

Thanks!

Bonus Topics

Globular Cluster Stars

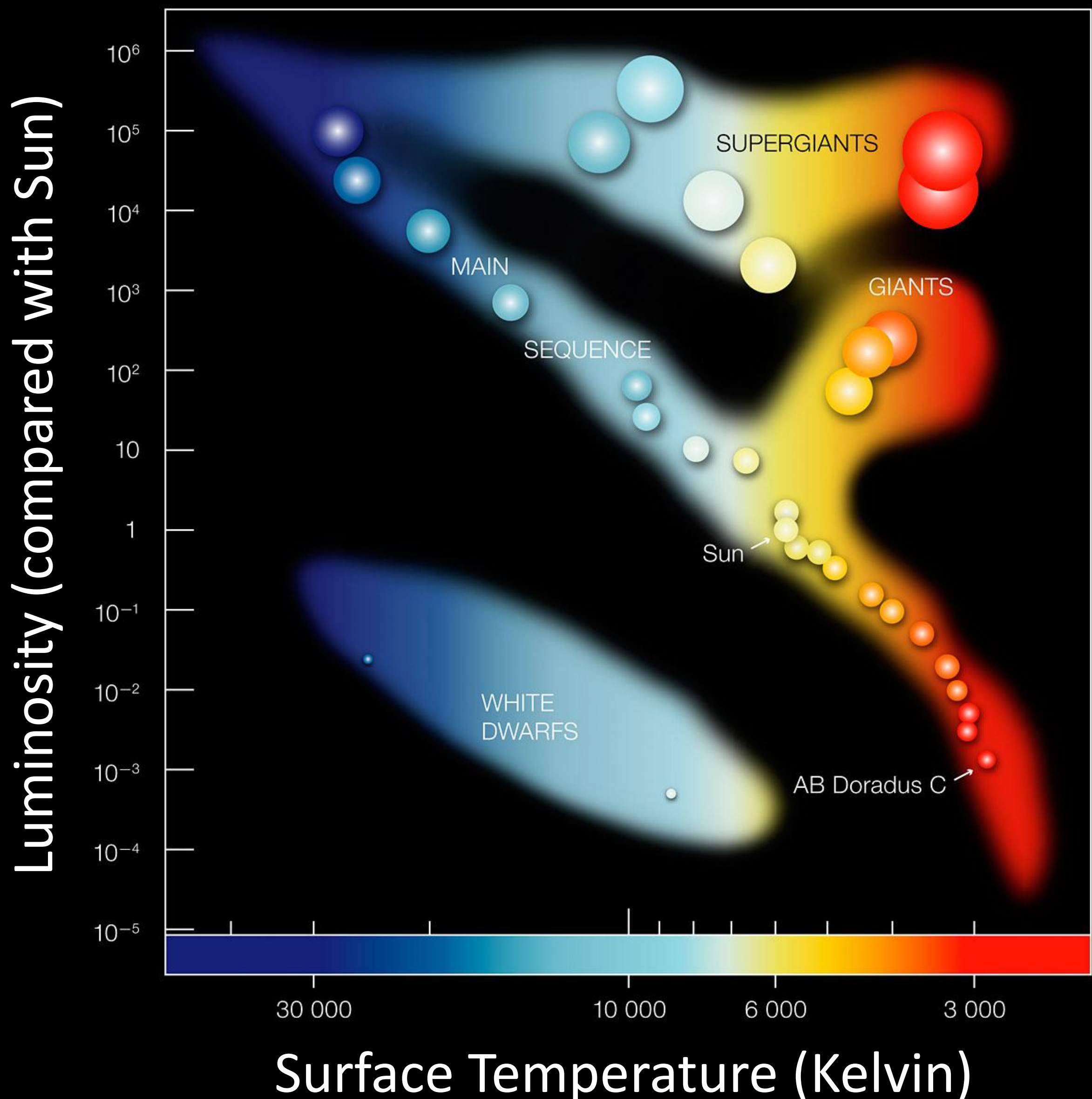

https://www.eso.org/public/images/eso0728c/

Hubble Tension

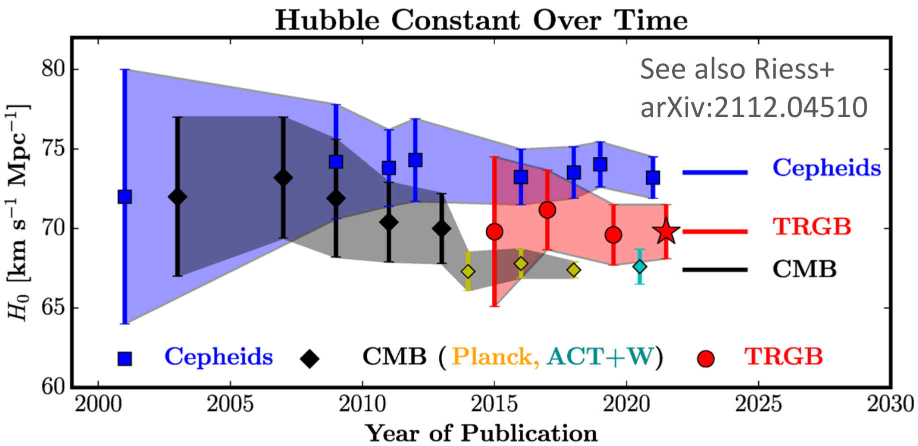

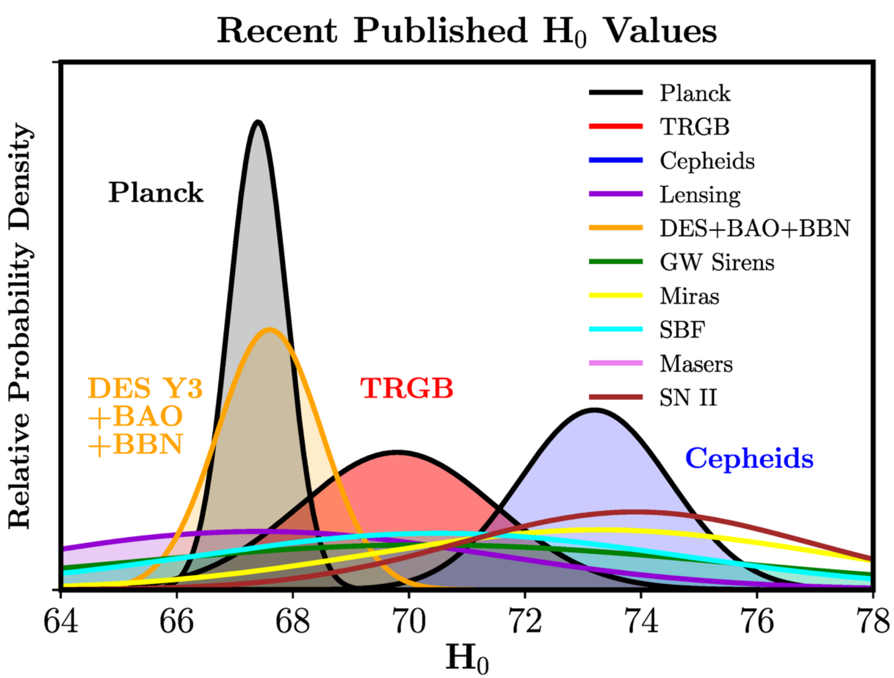

Freedman ApJ 919 (2021) 16 [2106.15656]

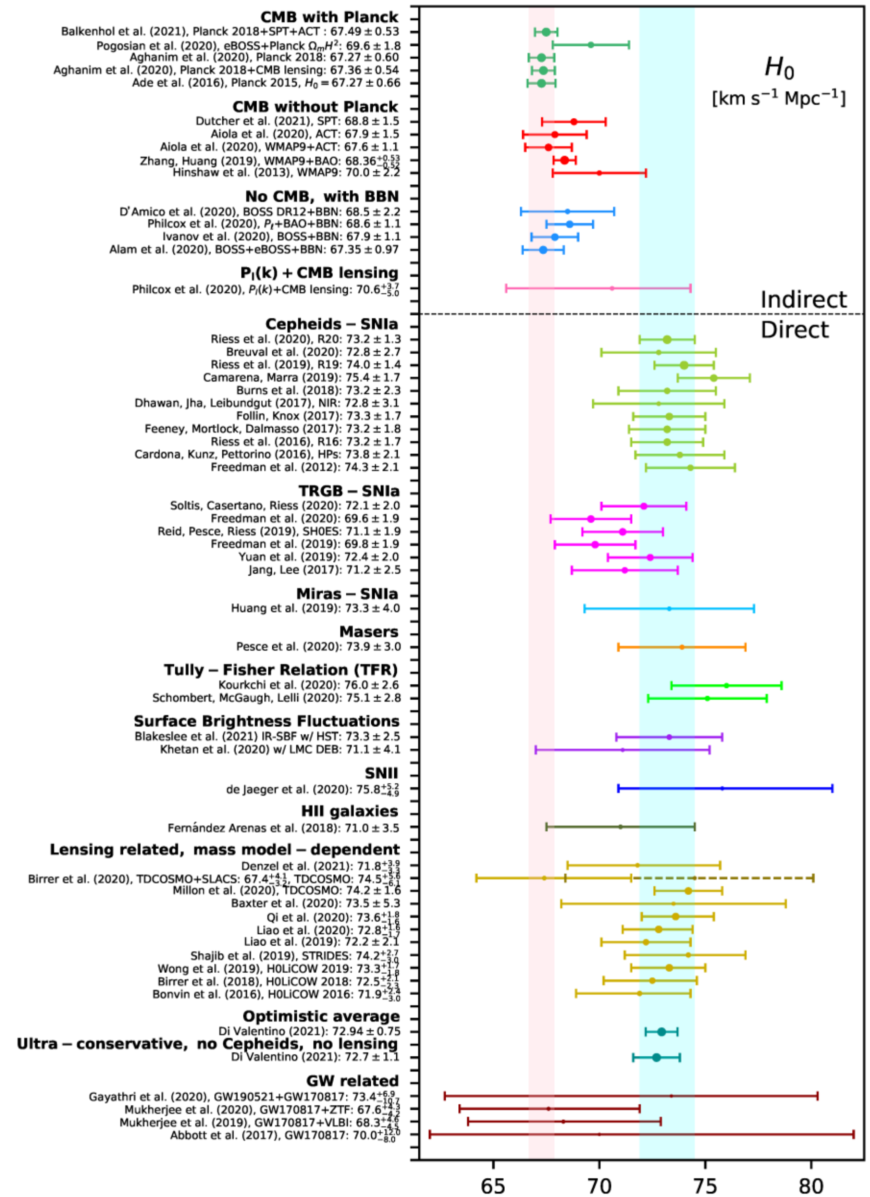

Di Valentino+ arXiv:2103.01183

Tip of the Red-Giant Branch in the Galaxy NGC 4258

The Astrophysical Journal, 835:28 (17pp), 2017 January 20 Jang & Lee

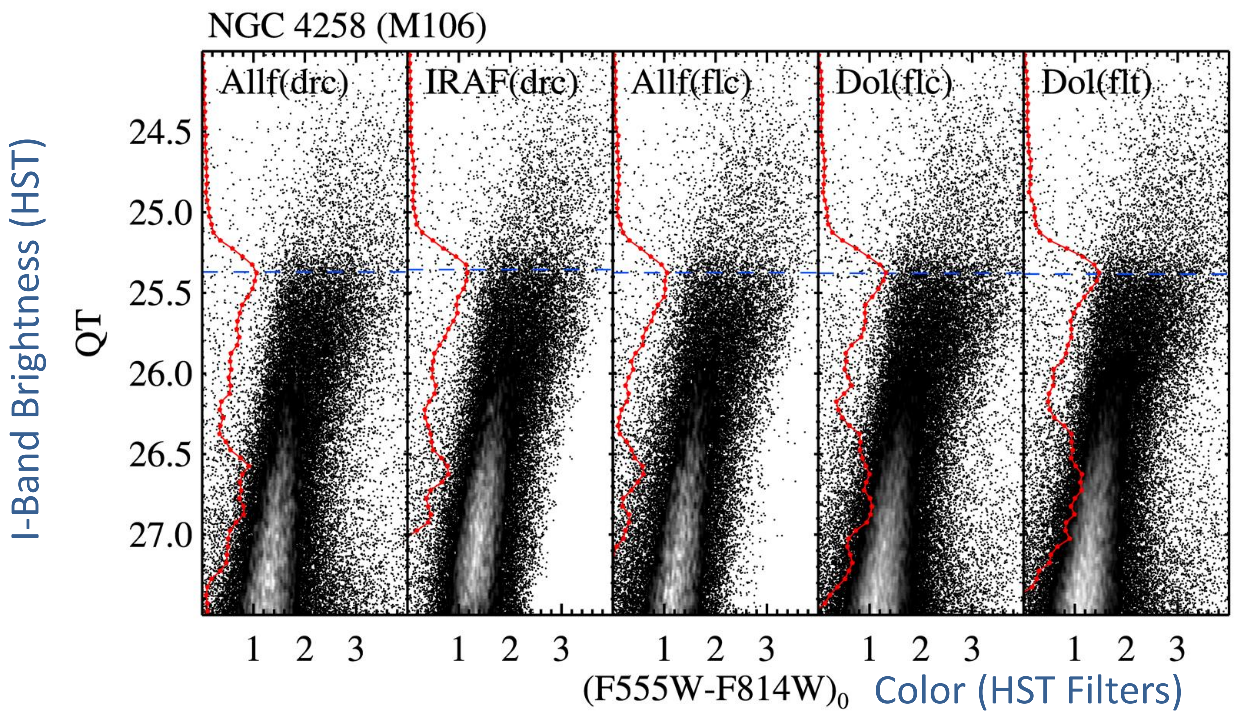

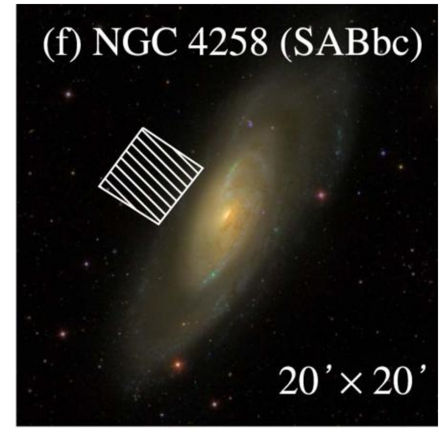

Figure 7. *QT* − (F555W − F814W)$_0$ CMDs of NGC 4258 from five different reduction methods : ALLFRAME on drc, IRAF/DAOPHOT on drc, ALLFRAME on flc, DOLPHOT on flc, and DOLPHOT on flt (from left to right). Edge detection responses are shown by the solid lines. Note that the estimated TRGB magnitudes (dashed lines) agree very well.

NGC 4258 hosts a water megamaser
→ Quasi-geometric distance determination
→ Among the best absolute TRGB calibrations
→ One rung in cosmic distance ladder

Color-Magnitude Diagram for Globular Clusters

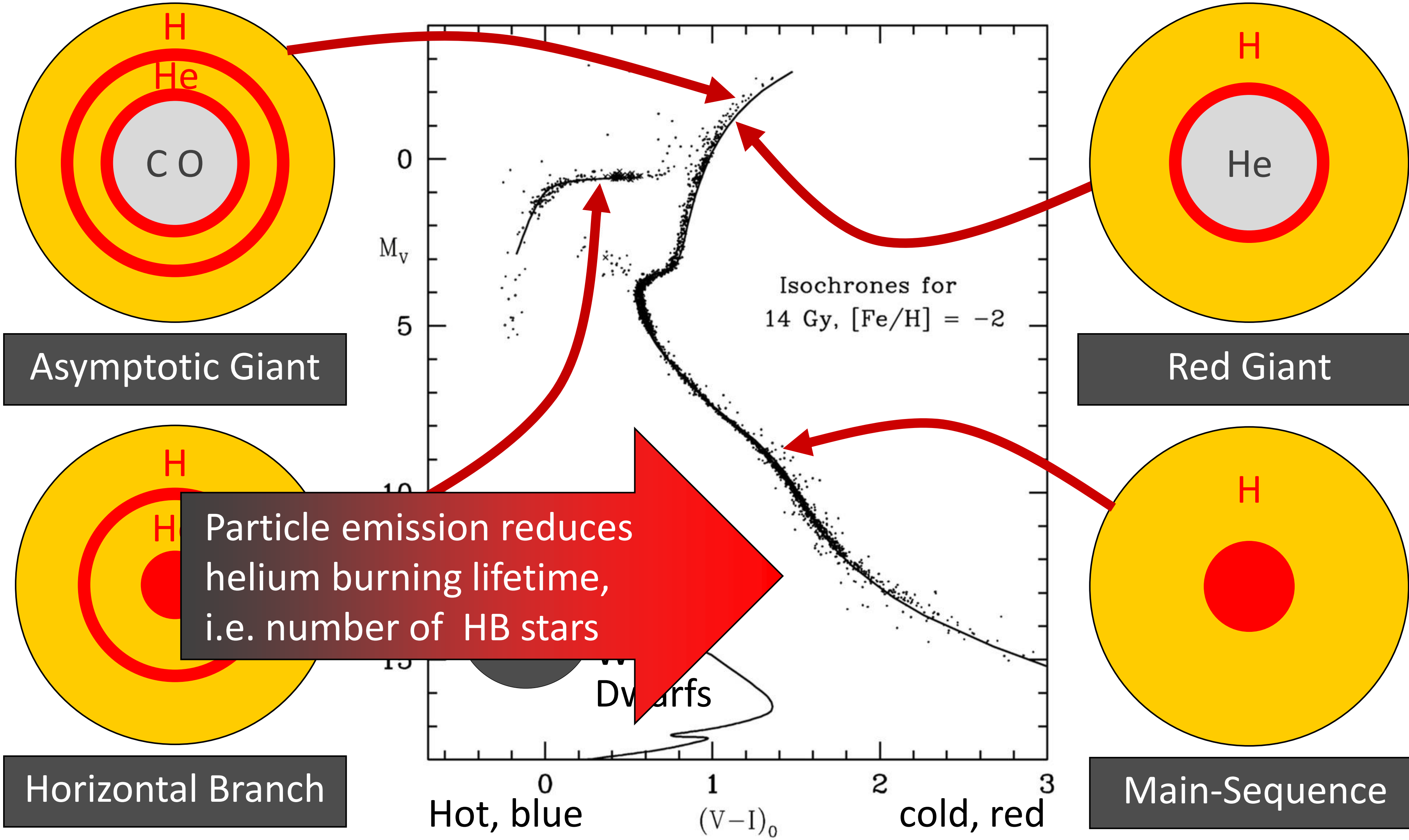

Color-magnitude diagram synthesized from several low-metallicity globular clusters and compared with theoretical isochrones (W.Harris, 2000)

Helium Burning Lifetime: R-Method

Number ratio ("R") of HB/RGB fixes He-burning lifetime
(if RGB not affected by new energy loss)

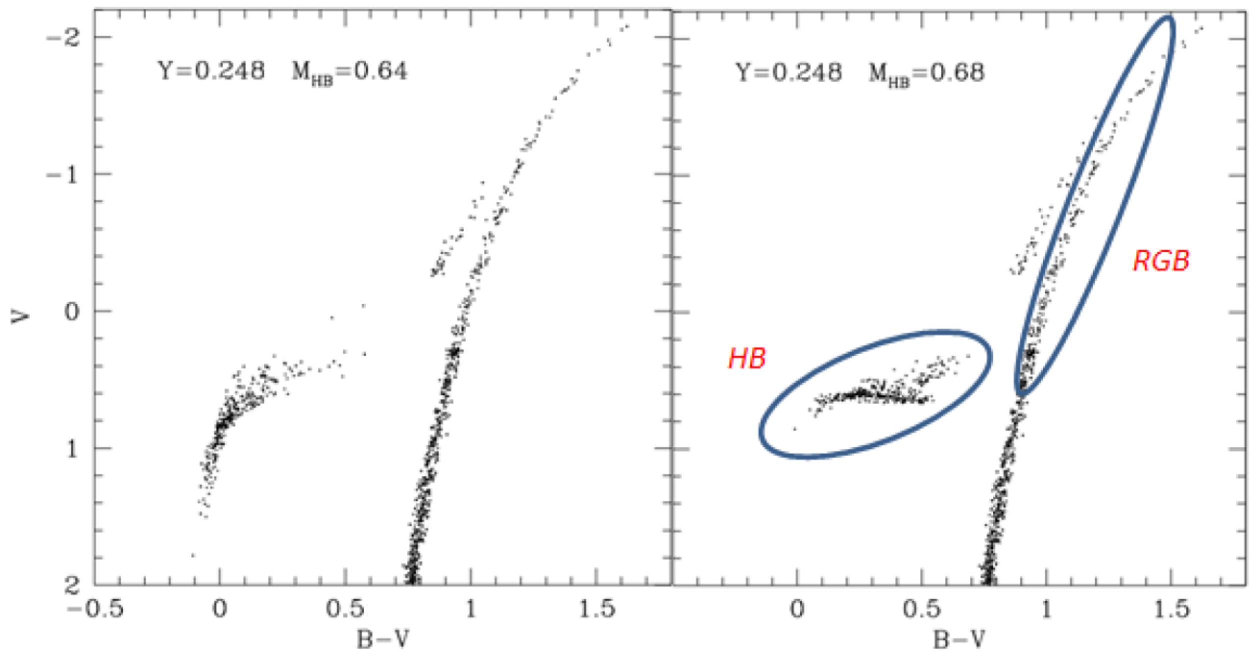

Figure 1: Example of synthetic CM diagrams. The diagram in the left panel has been obtained by assuming a stronger average mass loss rate during the RGB. As a result, the mean mass of HB stars (M_{HB}) is lower than that of the diagram in the right panel. The HB and the RGB portions used in the calculation of the R parameter are surrounded by ellipses.

Straniero, Ayala, Giannotti, Mirizzi & Domínguez,
doi:10.3204/DESY-PROC-2015-02/straniero_oscar

ALP Limits from Globular Clusters

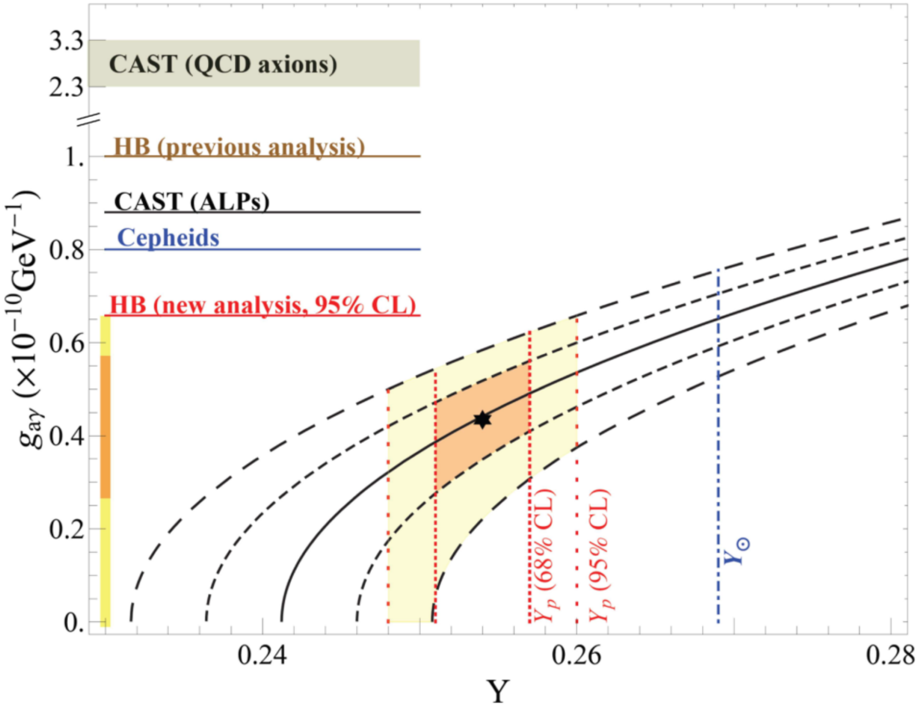

Parameter	error	Reference
$^{14}N(p,\gamma)^{15}O$	7%	[1]
$^{4}He(2\alpha,\gamma)^{12}C$	10%	[2]
$^{12}C(\alpha,\gamma)^{16}O$	20%	[6]
R	1.39 ± 0.03	[4]
Y	0.255 ± 0.002	[5],[3]

Helium abundance and energy loss rate from modern number counts HB/RGB in 39 globular clusters R = 1.39 ± 0.03

$$R_{\rm th} = 1.48 + 6.26(Y - 0.255) - 0.41 g_{10}^2$$

$g_{a\gamma} < 0.66 \times 10^{-10}\,\mathrm{GeV}^{-1}$ **(95% CL)**

Same as CAST limit within 2 digits ☺

Small “cooling hint” almost certainly systematics (as usual in astrophysics) eg nuclear reaction rates
Need more systematic exploration of systematics!

Ayala, Dominguez, Giannotti, Mirizzi & Straniero, arXiv:1406.6053
doi:10.3204/DESY-PROC-2015-02/straniero_oscar
Update including ALP masses: Lucente, Straniero, Carenza, Giannotti & Mirizzi, arXiv:2203.01336

HB vs. AGB Clump on Luminosity Function

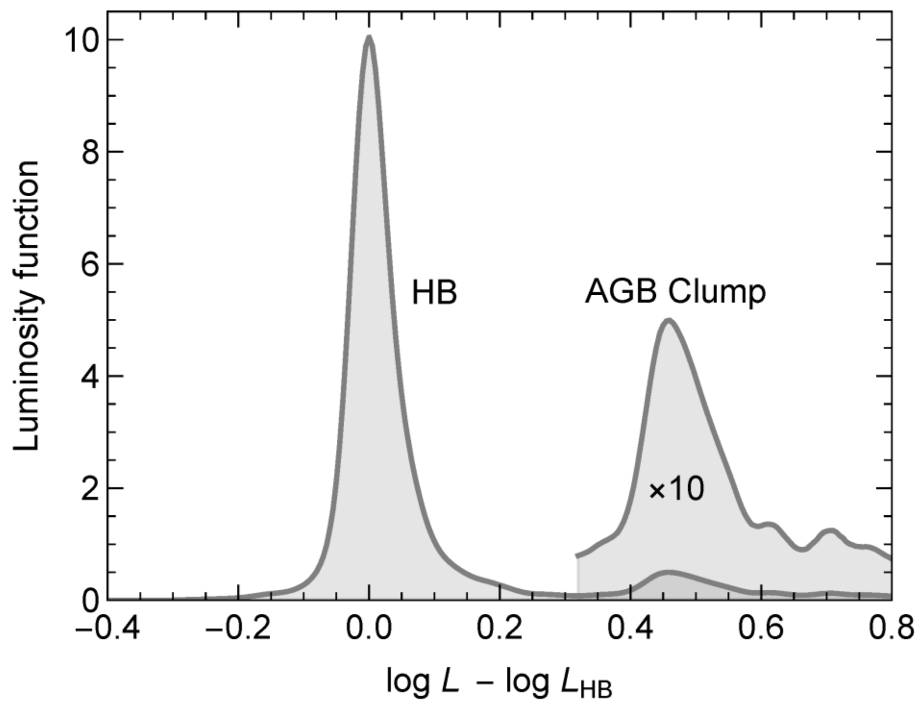

Figure 8: Empirical luminosity function, normalized to one, of the HB plus AGB stars from 14 GCs without a blue extension of the HB [212], using HST photometric data of Piotto et al. [213] and Sarajedini et al. [214]. We show a superposition of the two curves of Fig. 6 of [212], weighted with the number of stars (2414 for Sarajedini et al. and 4036 for Piotto et al.), although there is large overlap between the used clusters. Each one was aligned to its HB luminosity, defined as the maximum of the distribution. The AGB clump at $\log L - \log L_{\rm HB} = 0.455$ sticks out as a narrow peak. The separation between HB and AGB is taken at the minimum between the peaks, and the AGB itself until $\log L - \log L_{\rm HB} = 1$. A total of 725 AGB and 5725 HB stars went into the construction of this distribution, corresponding to $R_2 = 0.127$ for the clusters that went into this plot.

AGB/HB Counts in 48 Globular Clusters

				Piotto et al. (2002)			Sarajedini et al. (2007)			Sandquist (2000)		
NGC	[Fe/H]	$L1$	$L2$	n_{HB}	n_{AGB}	R_2	n_{HB}	n_{AGB}	R_2	n_{HB}	n_{AGB}	R_2
104	-0.72	0.078	0.068	358	53	0.148	591	82	0.139	368	38	0.103
362	-1.26	0.086	0.608	238	40	0.168	318	43	0.135	94	14	0.149
1261	-1.27	0.088	0.644	94	22	0.234	233	34	0.146	148	26	0.176
1851	-1.18	0.098	0.679	272	37	0.136	411	49	0.119	209	24	0.115
1904	-1.60	...	...	163	11	0.067	...	...	...	122	16	0.131
2419	-2.15	0.192	0.852	225	22	0.098	...	...	...	...	...	...
2808	-1.14	0.094	0.904	809	61	0.075	1200	104	0.087	247	22	0.089
4833	-1.85	0.287	0.538	94	10	0.106	...	...	...	...	...	...
5024	-2.10	0.158	0.602	224	18	0.080	360	44	0.122	302	39	0.129
5272	-1.50	0.150	0.613	...	...	...	323	40	0.124	562	65	0.116
5634	-1.88	...	...	130	15	0.115	...	...	...	...	...	...
5694	-1.98	...	...	222	26	0.117	...	...	...	56	14	0.250
5824	-1.91	...	...	463	63	0.136	...	...	...	...	...	...
5904	-1.29	0.150	0.681	162	21	0.130	280	52	0.186	555	94	0.169
5927	-0.49	0.043	0.062	201	12	0.060	...	...	...	134	20	0.149
6093	-1.75	0.464	0.447	162	31	0.191	341	51	0.150	170	39	0.229
6139	-1.65	...	...	282	35	0.124	...	...	...	114	24	0.211
6171	-1.02	0.100	0.513	...	...	...	56	10	0.179	117	29	0.248
6205	-1.53	0.527	0.441	192	20	0.104	390	48	0.123	90	12	0.133
6218	-1.47	0.561	0.299	...	...	...	82	11	0.134	91	12	0.132
6229	-1.18	...	...	278	34	0.122	...	...	...	92	19	0.207
6254	-1.26	0.588	0.260	...	...	...	157	18	0.115	69	13	0.188
6266	-1.18	...	...	446	40	0.090	...	...	...	114	18	0.158
6284	-1.26	...	...	127	16	0.126	...	...	...	...	...	...
6304	-0.45	0.062	0.060	99	8	0.081	...	...	...	...	...	...
6341	-2.31	0.261	0.542	...	...	...	245	33	0.135	140	20	0.143
6356	-0.40	...	...	362	25	0.069	...	...	...	...	...	...
6362	-0.59	0.122	0.621	38	6	0.158	...	...	...	...	...	...
6388	-0.55	0.057	0.836	1347	176	0.131	...	...	...	...	...	...
6402	-1.28	...	...	349	29	0.083	...	...	...	...	...	...
6441	-0.46	0.048	0.904	1380	154	0.112	...	...	...	...	...	...
6539	-0.63	...	...	114	15	0.132	...	...	...	...	...	...
6541	-1.81	0.563	0.347	...	...	...	248	41	0.165	...	...	...
6569	-0.76	...	...	166	30	0.181	...	...	...	...	...	...
6584	-1.50	0.102	0.558	55	8	0.145	...	...	...	...	...	...
6624	-0.44	0.077	0.085	121	9	0.074	188	20	0.106	126	30	0.238
6637	-0.64	0.078	0.065	135	25	0.185	244	43	0.176	127	21	0.165
6638	-0.95	...	...	101	28	0.277	...	...	...	...	...	...
6652	-0.81	0.073	0.080	61	5	0.082	83	9	0.108	75	20	0.267
6681	-1.62	0.558	0.334	100	9	0.090	...	...	...	82	8	0.098
6723	-1.10	0.127	0.704	102	11	0.108	194	22	0.113	101	15	0.149
6752	-1.54	0.378	0.578	...	...	...	173	20	0.116	225	13	0.058
6864	-1.29	...	...	363	69	0.190	...	...	...	55	12	0.218
6934	-1.47	0.097	0.678	149	18	0.121	99	17	0.172	...	...	...
6981	-1.42	0.142	0.570	61	7	0.115	188	36	0.191	45	10	0.222
7078	-2.37	0.174	0.713	376	48	0.128	537	57	0.106	153	23	0.150
7089	-1.65	0.150	0.790	167	18	0.108	702	100	0.142	...	...	...
7099	-2.27	0.462	0.261	89	6	0.067	...	...	...	202	11	0.054

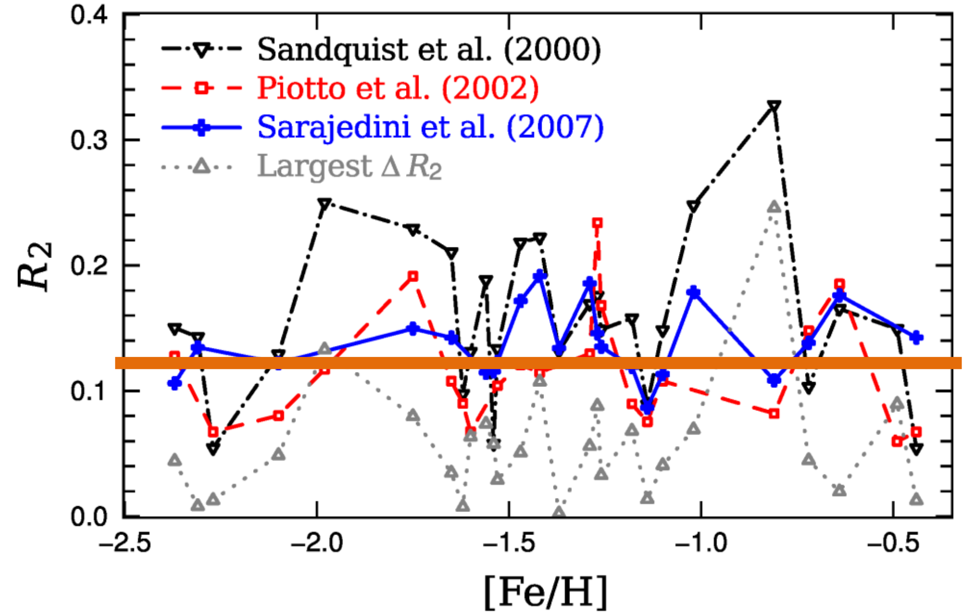

Figure 1. Comparison of R_2 for clusters shown in Table 1, limited to those with at least two different sources of photometry. The R_2 determined from the Sandquist (2000), Piotto et al. (2002), and Sarajedini et al. (2007) data are shown in black dash-dots, red dashes, and a blue solid line, respectively. The dotted grey line shows the maximum difference between R_2 determinations from different photometry.

$$R_2 = N_{AGB}/N_{HB} = 0.117 \pm 0.005$$

The treatment of mixing in core helium burning models II. Constraints from cluster star counts
Constantino, Campbell, Lattanzio & van Duijneveldt, arXiv:1512.04845

Predicting the Axion-Modified Ratios

M.J. Dolan, F.J. Hiskens & R.R. Volkas, arXiv:2207.03102

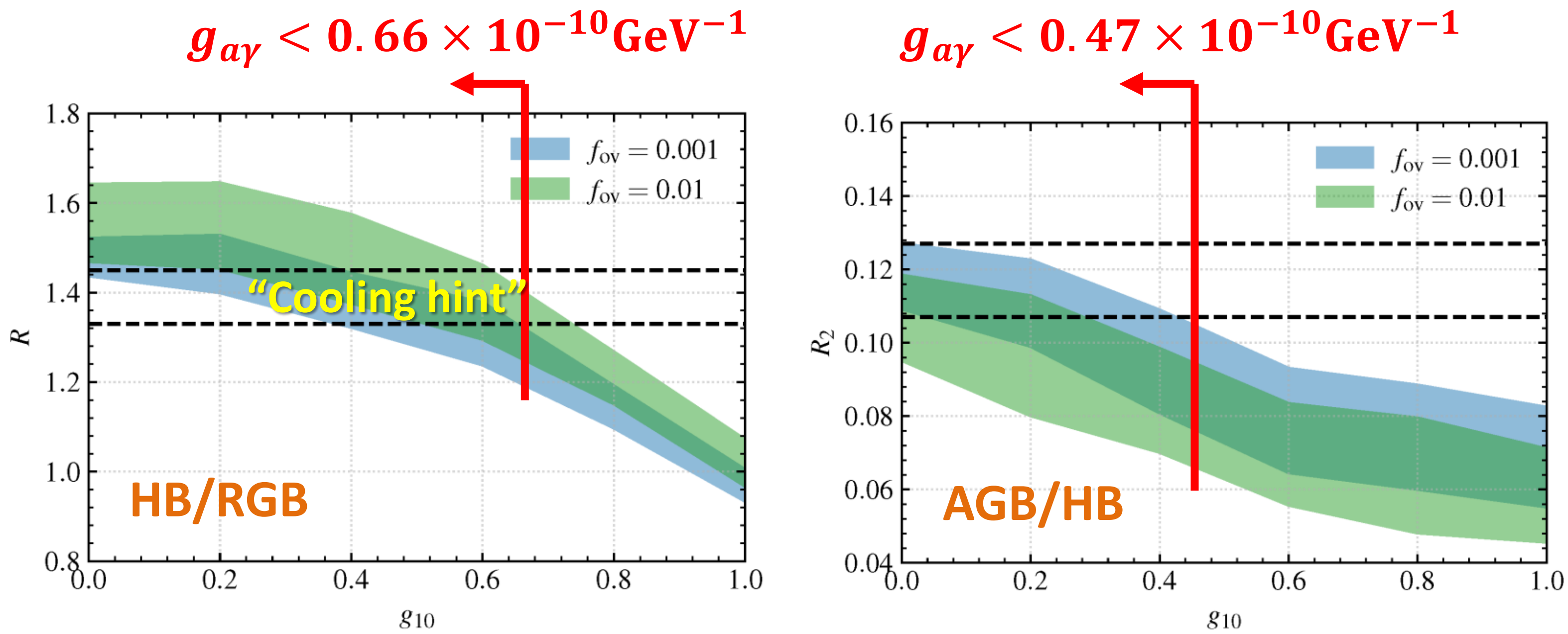

Figure 2. (Left panel): Predicted values of R as a function of g_{10} given standard convective core overshoot with $f_{\rm ov} = 0.001$ (blue) and $f_{\rm ov} = 0.01$ (green). The observed limit on R is indicated by the region between the dashed black lines (95% C.I.). (Right panel): The full range of R_2 values predicted as functions of g_{10} given standard overshoot with $f_{\rm ov} = 0.001$ (blue) and $f_{\rm ov} = 0.01$ (green). The observed limit is again shown by the dashed black lines.

Probably one should analyze GCs for all observables simultaneously using modern high-statistics (GAIA) data

White Dwarfs

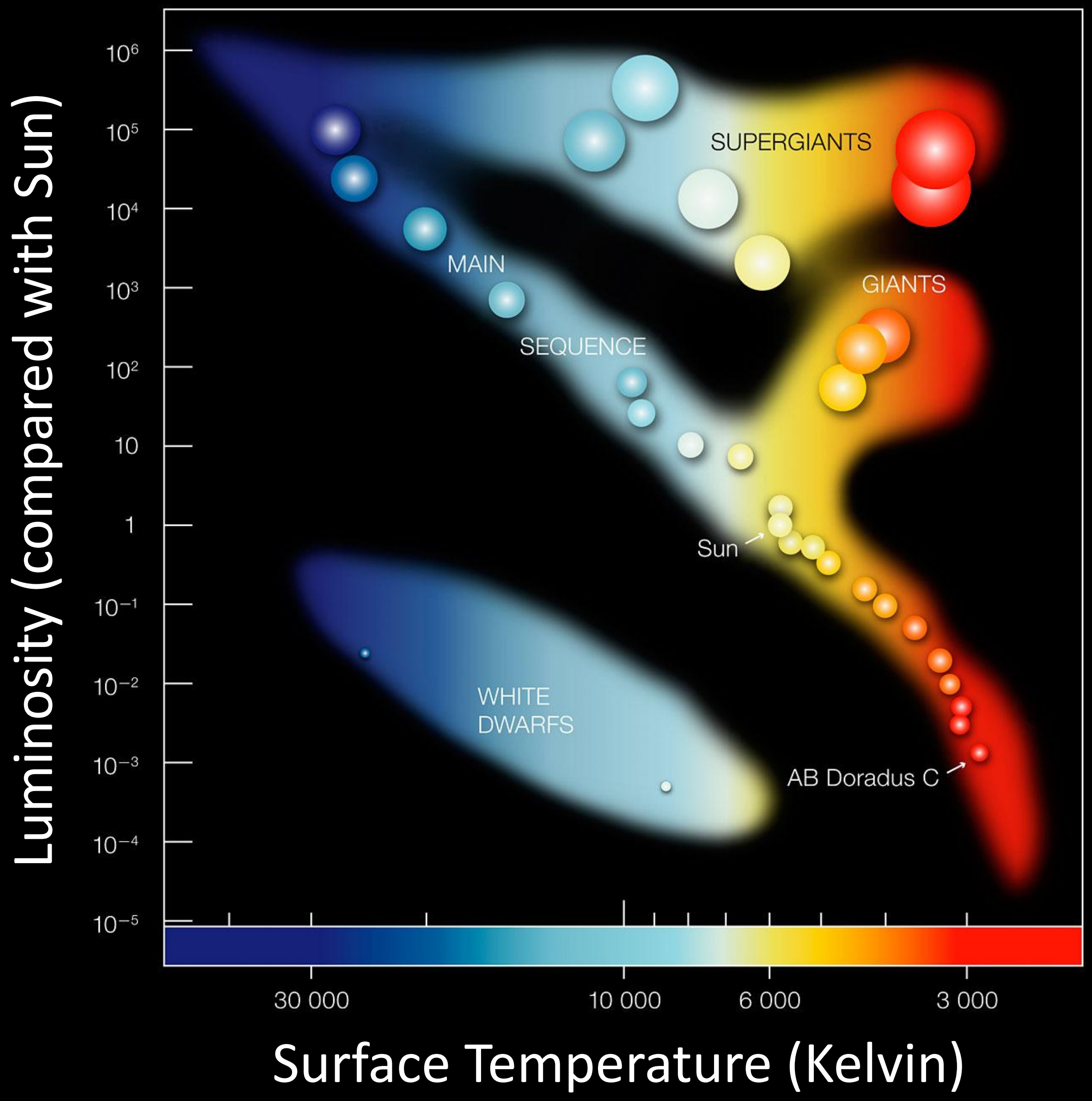

https://www.eso.org/public/images/eso0728c/

White Dwarfs

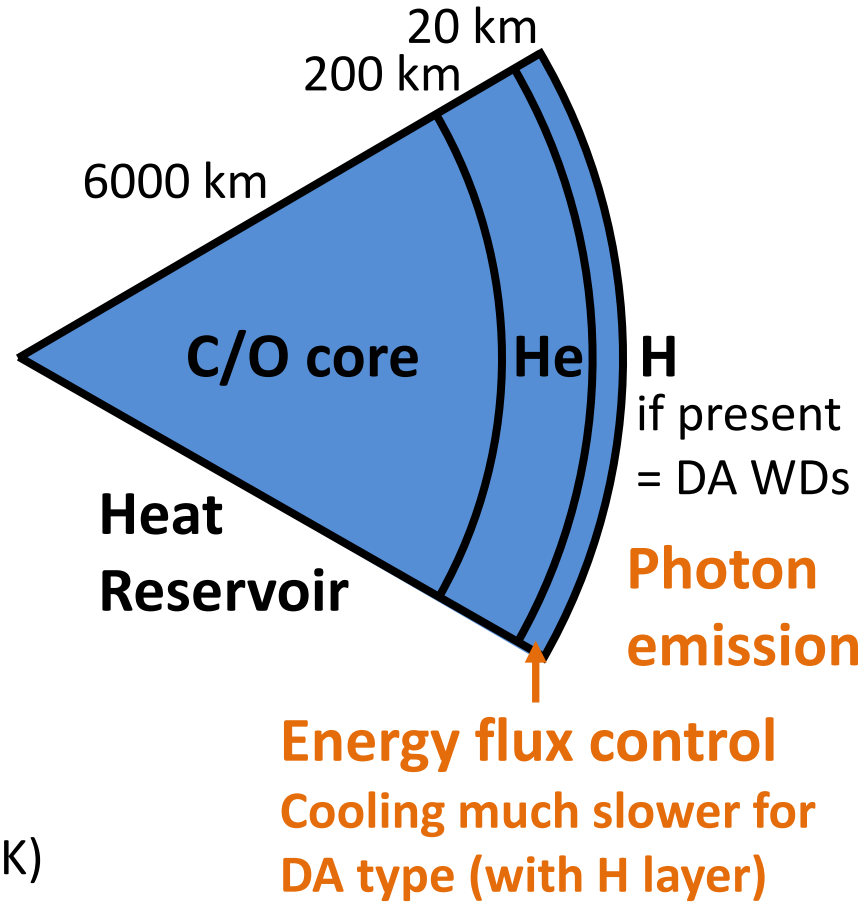

$R \simeq 6000\ \mathrm{km}$ (Size of the Earth)
$T_{\rm eff} \simeq 10{,}000\text{–}30{,}000\mathrm{K}$ (Sun 6000 K)
$L \simeq 10^{-4}\text{–}10^{-1} L_\odot$
$M \simeq 0.5\text{–}0.8 M_\odot$
$\rho \simeq 10^6 \mathrm{g/cm^3}$ (very degenerate)

Axion Bounds from WD Luminosity Function

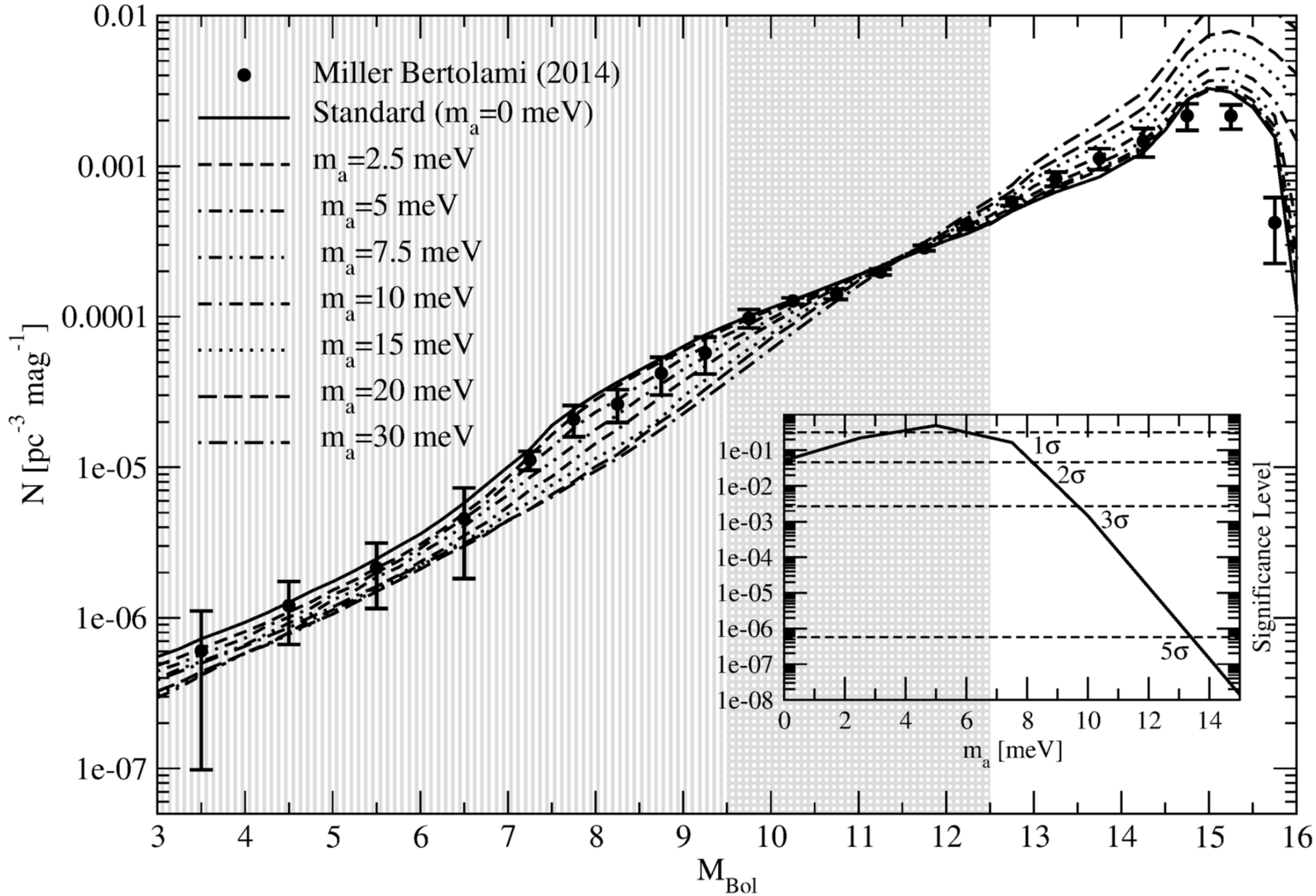

Limits on axion-electron coupling and mass limit in DFSZ model:

$g_{ae} \lesssim 3 \times 10^{-13}$ $\qquad$ $m_a \cos^2\beta \lesssim 10\ \mathrm{meV}$

Miller Bertolami, Melendez, Althaus & Isern, arXiv:1406.7712, 1410.1677

For extensions and review see: Isern, arXiv:2002.08069

Pulsating Stars

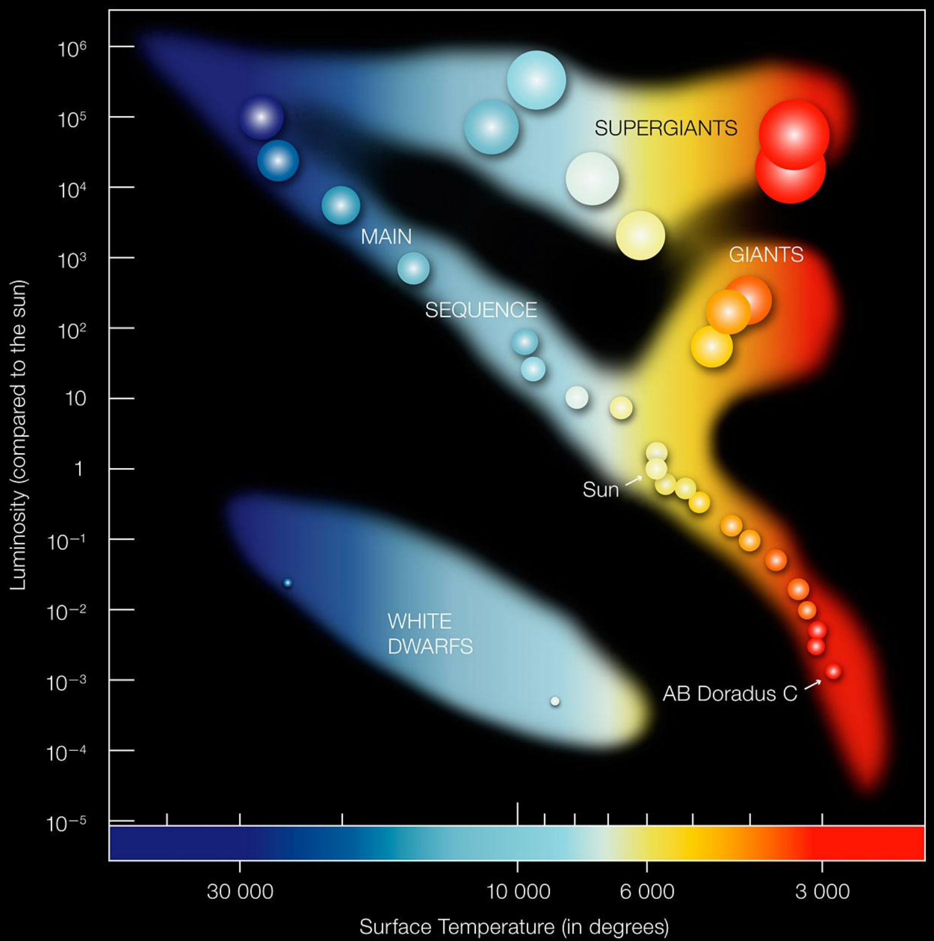

https://www.eso.org/public/images/eso0728c/

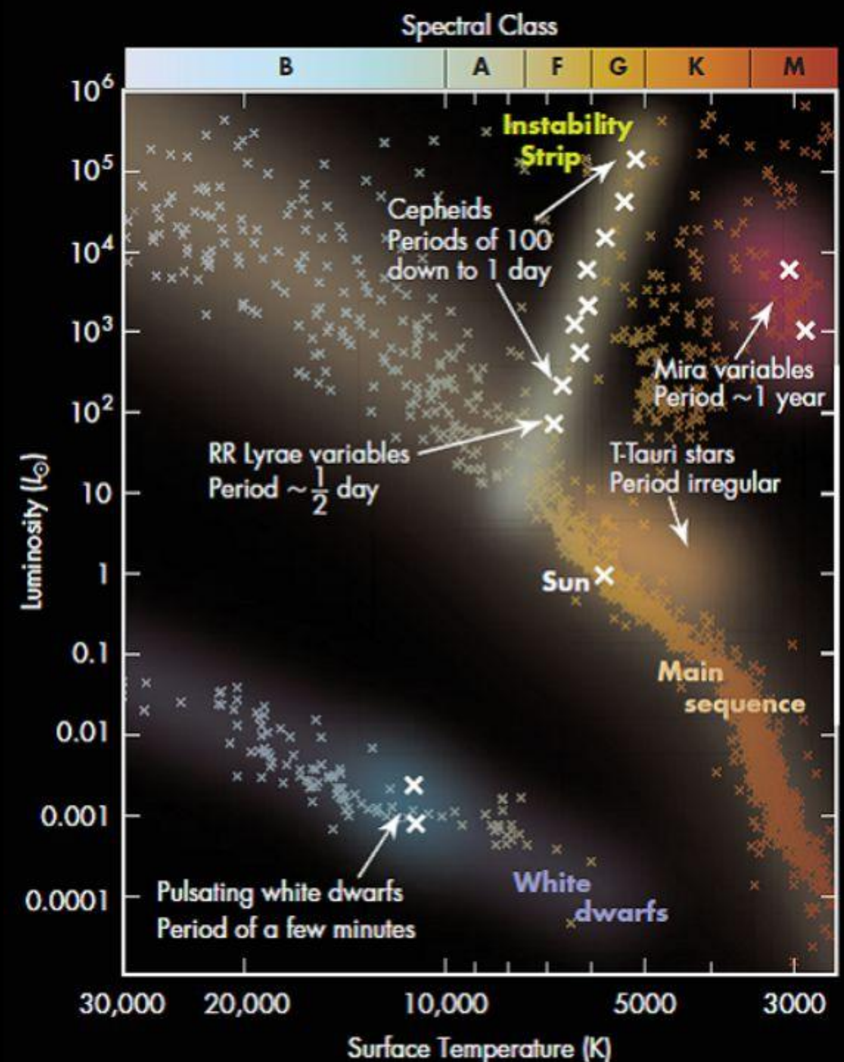

https://scienceatyourdoorstep.com/2021/01/04/what-are-variable-stars/

Non-Radial g-Modes

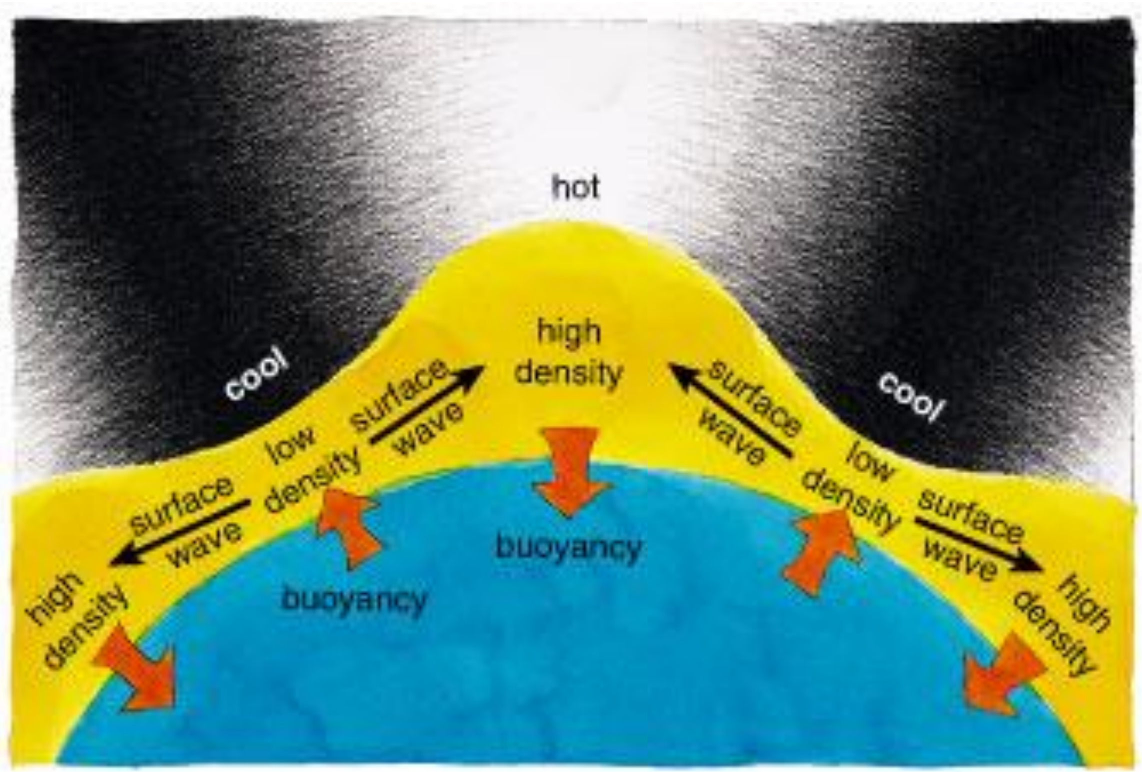

From a talk by J. Isern

- Long period waves (100 – 1000 s)
- Gravity is the restoring force

$$\frac{d \log \Pi}{dt} \propto -\frac{d \log T}{dt}$$

- Period decreases as the star cools
- Characteristic rate $10^{-15}\ s/s$
- Measures cooling speed of a single star

Pulsating White Dwarf G117–B15A

Kepler+ ApJ 254 (1982) 676

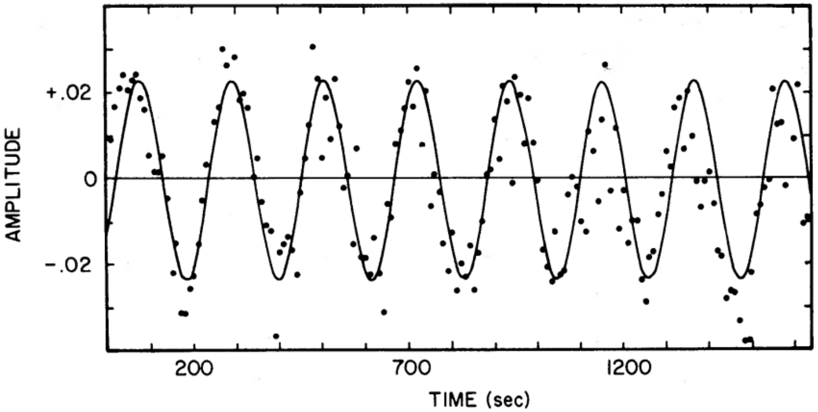

FIG. 1.—A portion of the light curve of G117−B15A in unfiltered light during run 2075. The light curve has been normalized so that the time-averaged brightness of G117−B15A is equal to 1.00, and then 1.00 has been subtracted from the light curve. The solid line is a sine curve with a period of 215.19 s and a semiamplitude of 0.022 mag.

$D = 57.5 \pm 0.1$ pc
$T = 12{,}400$ K
$M = 0.69\, M_\odot$
Period 215.2 s

Kepler+ ApJ 906 (2021) 7

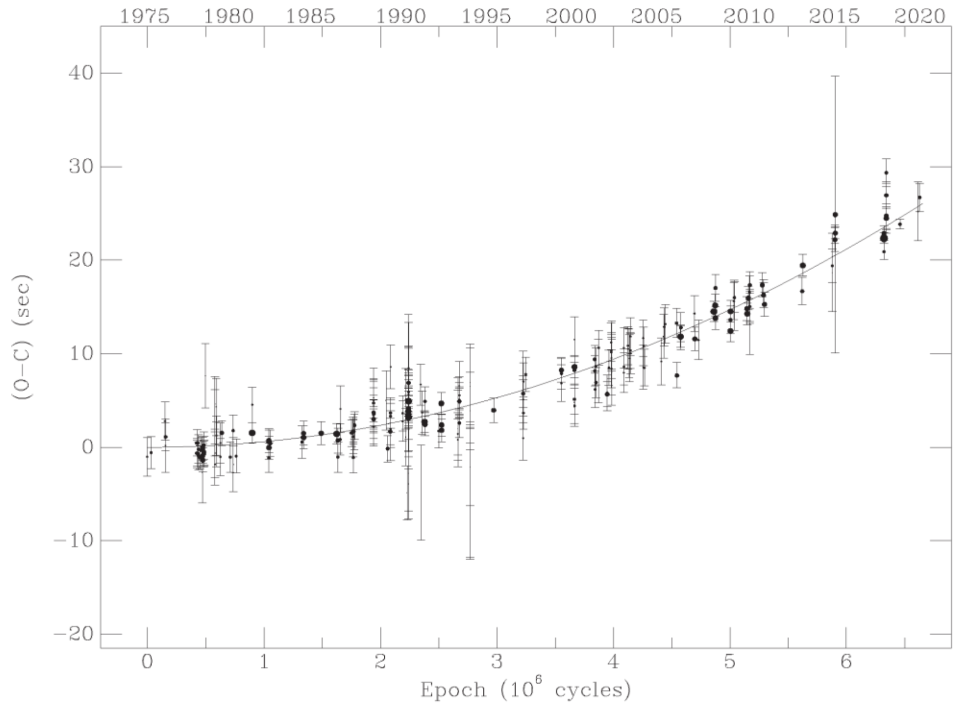

Figure 1. ($O - C$): observed minus calculated times of maxima for the 215 s pulsation of G 117-B15A. The size of each point is proportional to its weight, i.e., inversely proportional to the uncertainty in the time of maxima squared. We show $\pm 1\sigma$ error bars for each point, and the line shows our best-fit parabola to the data. The fact that the line does not overlap these error bars is a demonstration that they are underestimated. Note that as the period of pulsation is 215.1973882 s, the observed total change in phase is only 50 deg.

"Most stable optical clock", slipped by 26 s (of 215.2 s period) in 45 years

$$\dot{P}/P = (5.12 \pm 0.82) \times 10^{-15}\ \mathrm{s/s}$$

G117–B15A Period Decrease: Hint for Axion Cooling?

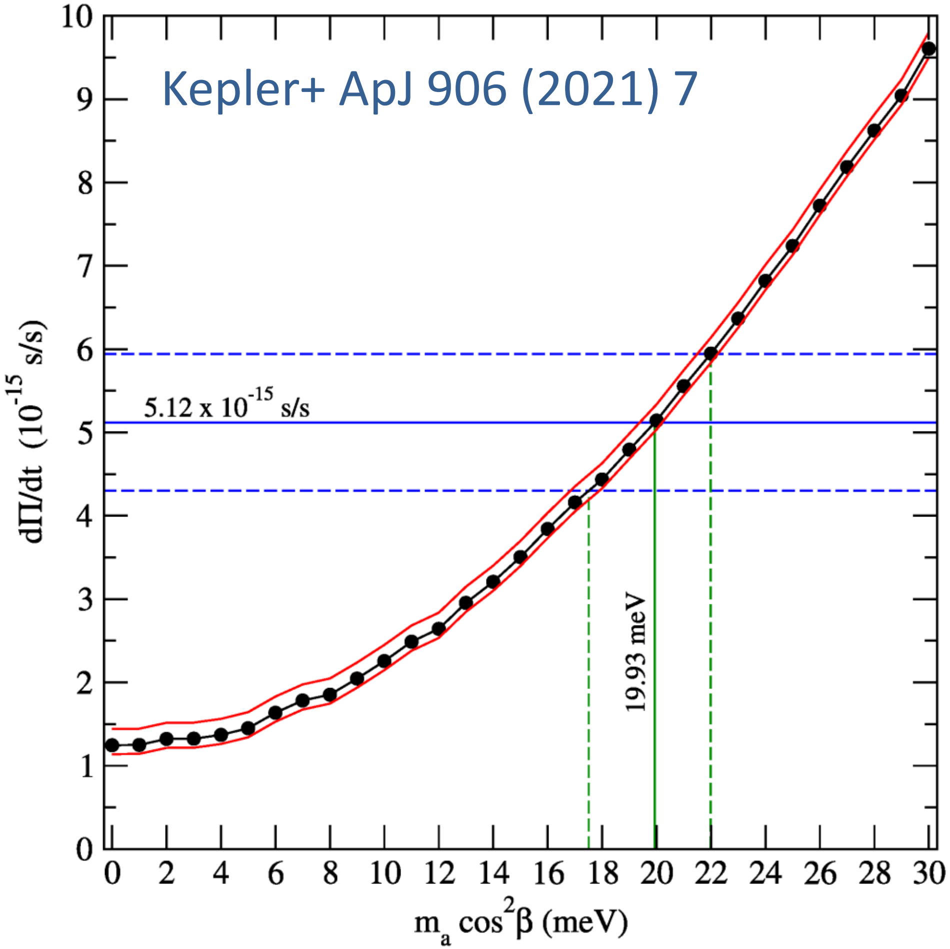

Figure 2. The rate of period change for the mode with $\ell = 1$ and $k = 2$, corresponding to a period of ~215 s in terms of the axion mass (black circles). Dashed lines represent the uncertainties in the value in the observed $\dot{P}$ and the axion mass, while the red curves represent the internal uncertainties in $\dot{P}$ due to modeling.

$$\dot{P}/P = (5.12 \pm 0.82) \times 10^{-15}\ \mathrm{s/s}$$

Emission of axions & friends with direct electron coupling

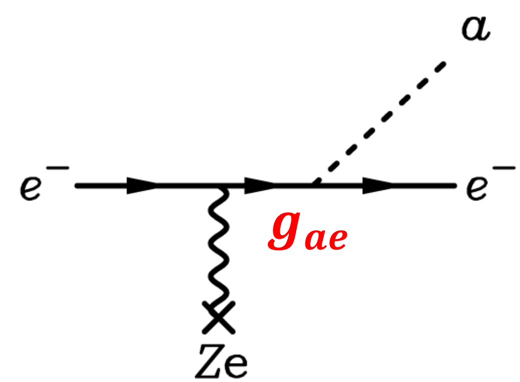

Bremsstrahlung emission by degenerate electrons

Case of DFSZ Axion

$$g_{ae} = 0.28 \times 10^{-13}\ \frac{m_a \cos^2\beta}{\mathrm{meV}}$$

Nominal cooling signal

$$g_{ae} = (5.7 \pm 0.6) \times 10^{-13}$$

White-Dwarf Bounds on Axion-Electron Coupling

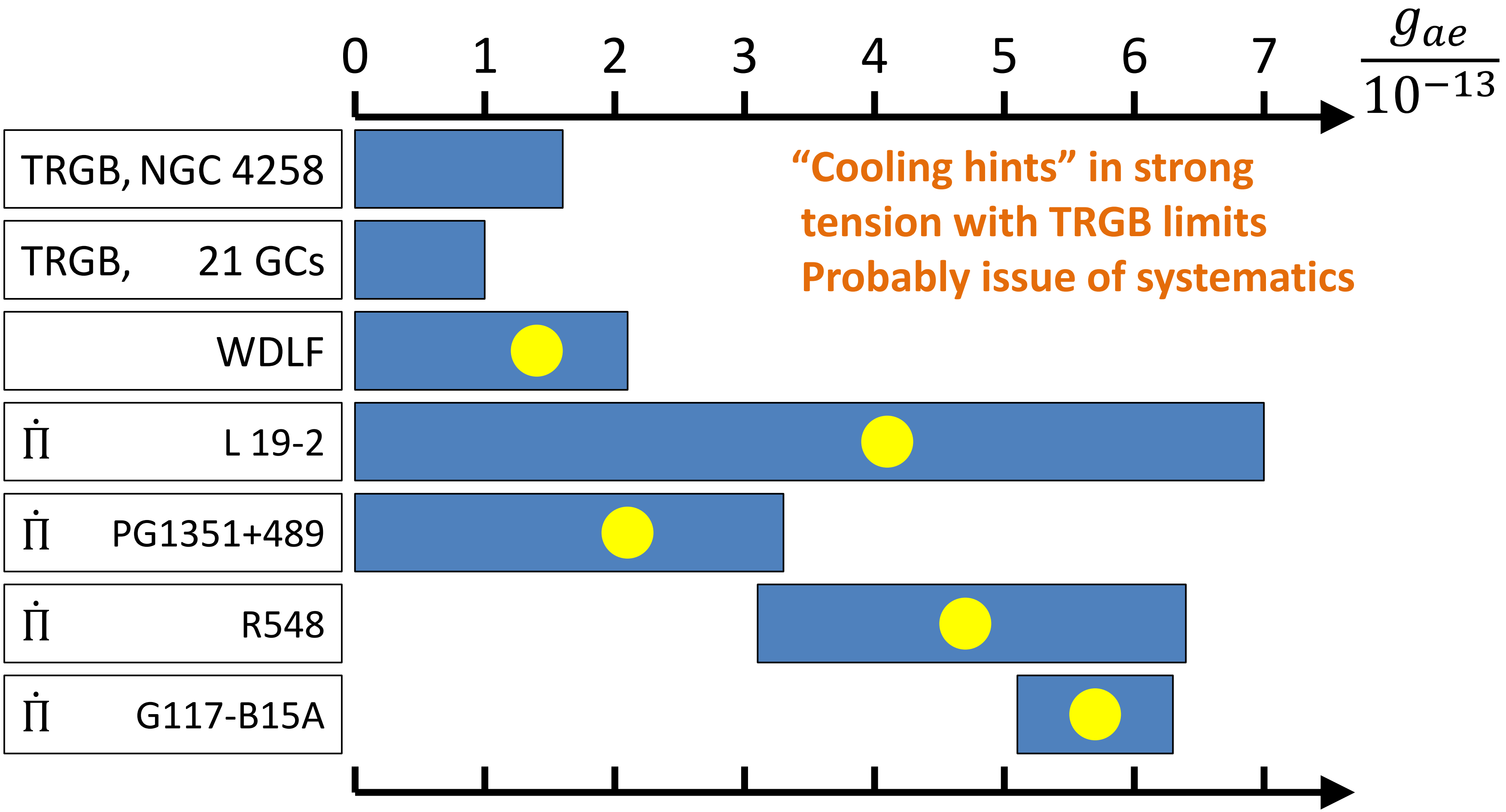

White Dwarfs as Physics Laboratories: Lights and Shadows, arXiv:2202.02052
J. Isern, S. Torres & A. Rebassa-Mansergas
Stellar Evolution Confronts Axion Models, arXiv:2109.10368
L. Di Luzio, M. Fedele, M. Giannotti, F. Mescia & E. Nardi

Neutron Star Cooling

Neutron Star Cooling

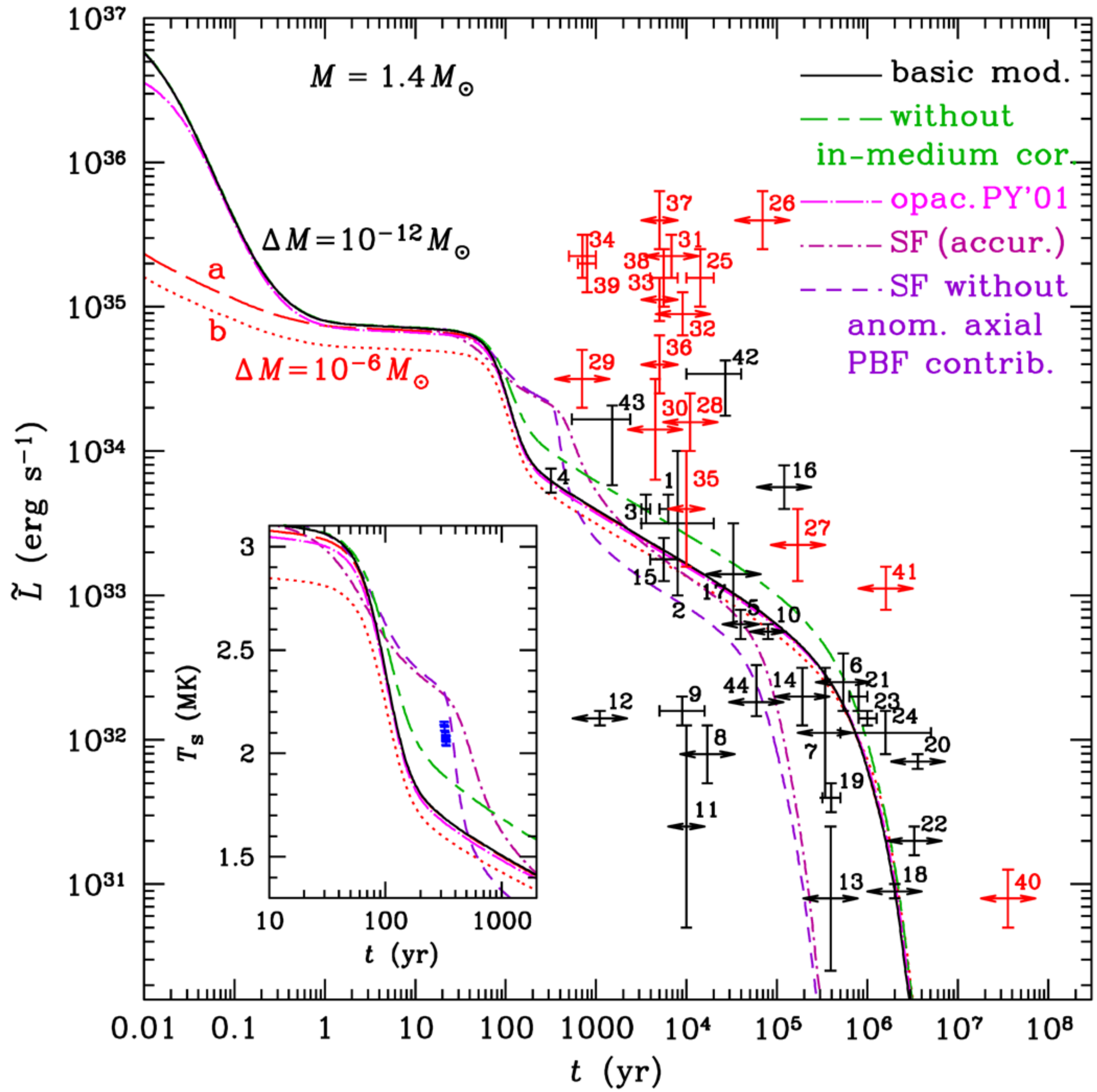

Potekhin & Chabrier: Magnetic neutron star cooling and microphysics [1711.07662]

Cooling Simulations of Five Neutron Stars

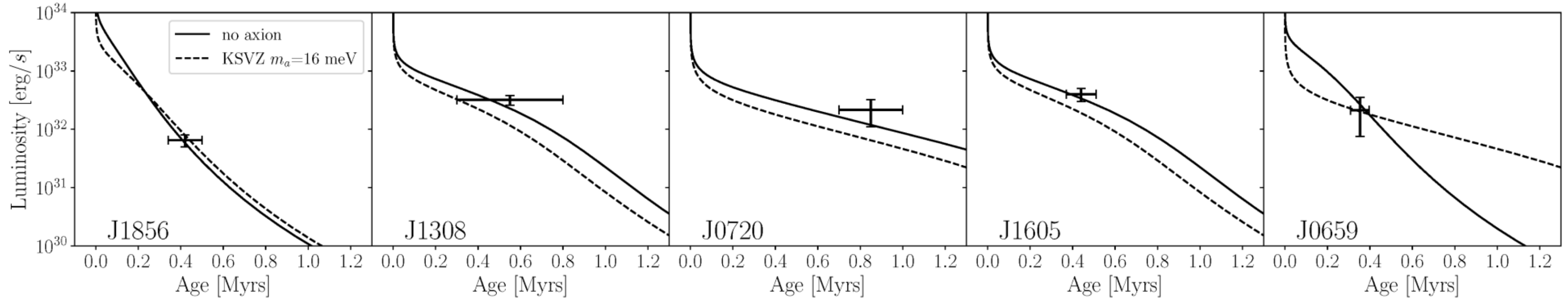

Figure 1. The luminosity and age data for each of the NSs considered in this work (see Tab. I). We show the best-fit cooling curves computed in this work for each of these NSs under the null hypothesis and with the axion mass fixed to $m_a = 16$ meV, which is our 95% upper limit on the QCD axion mass in the context of the KSVZ model.

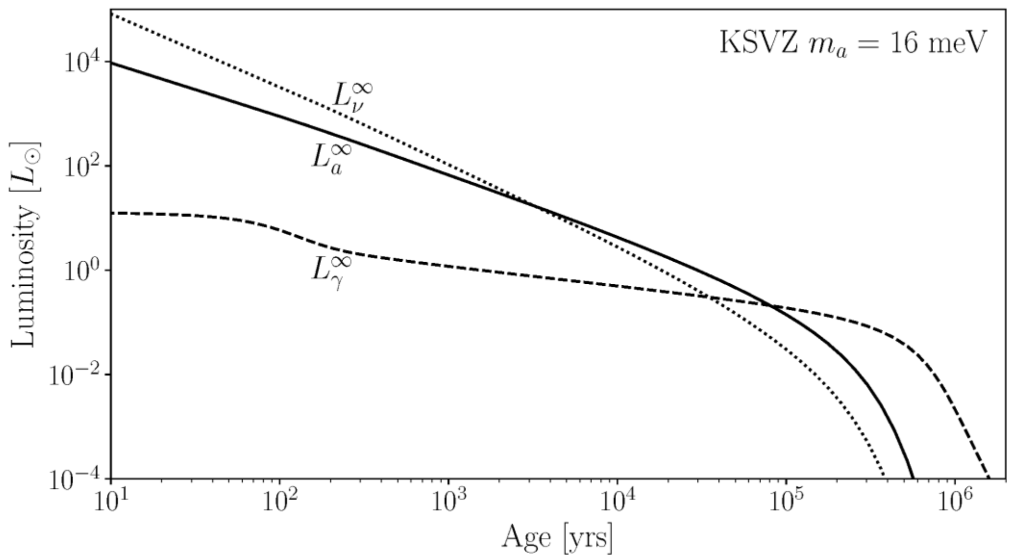

Cooling of J1605 with KSVZ axions, BSk22 EOS, SBF-0-0 superfluidity model, $M_{\rm NS} = 1.0\ M_\odot$

Upper Limit on the QCD Axion Mass from Isolated Neutron Star Cooling

Buschmann, Dessert, Foster, Long & Safdi, 2111.09892

Neutron-Star Cooling Bounds

Caputo & Raffelt, arXiv:2401.13728

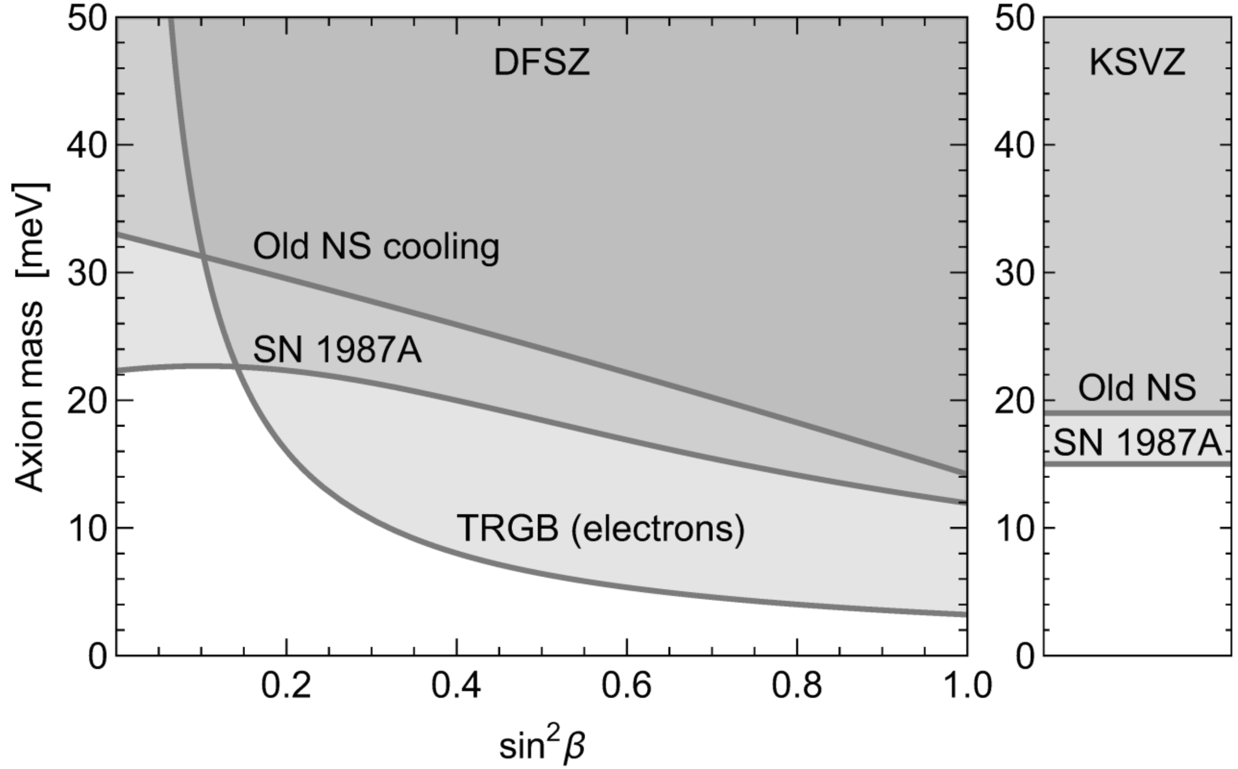

DFSZ Axions

$$\mathcal{L}_{af} = C_f\, \overline{\Psi}_f \gamma^\mu \gamma_5 \Psi_f \frac{\partial_\mu a}{2 f_a}$$

$$C_n = -0.160 \pm 0.025 + 0.414 \cos^2\beta$$

$$C_p = -0.182 \pm 0.025 - 0.435 \cos^2\beta$$

$$C_e = \tfrac{1}{3} \cos^2\beta$$

Upper Limit on the QCD Axion Mass from Isolated Neutron Star Cooling
Buschmann, Dessert, Foster, Long & Safdi, arXiv:2111.09892

Superradiance

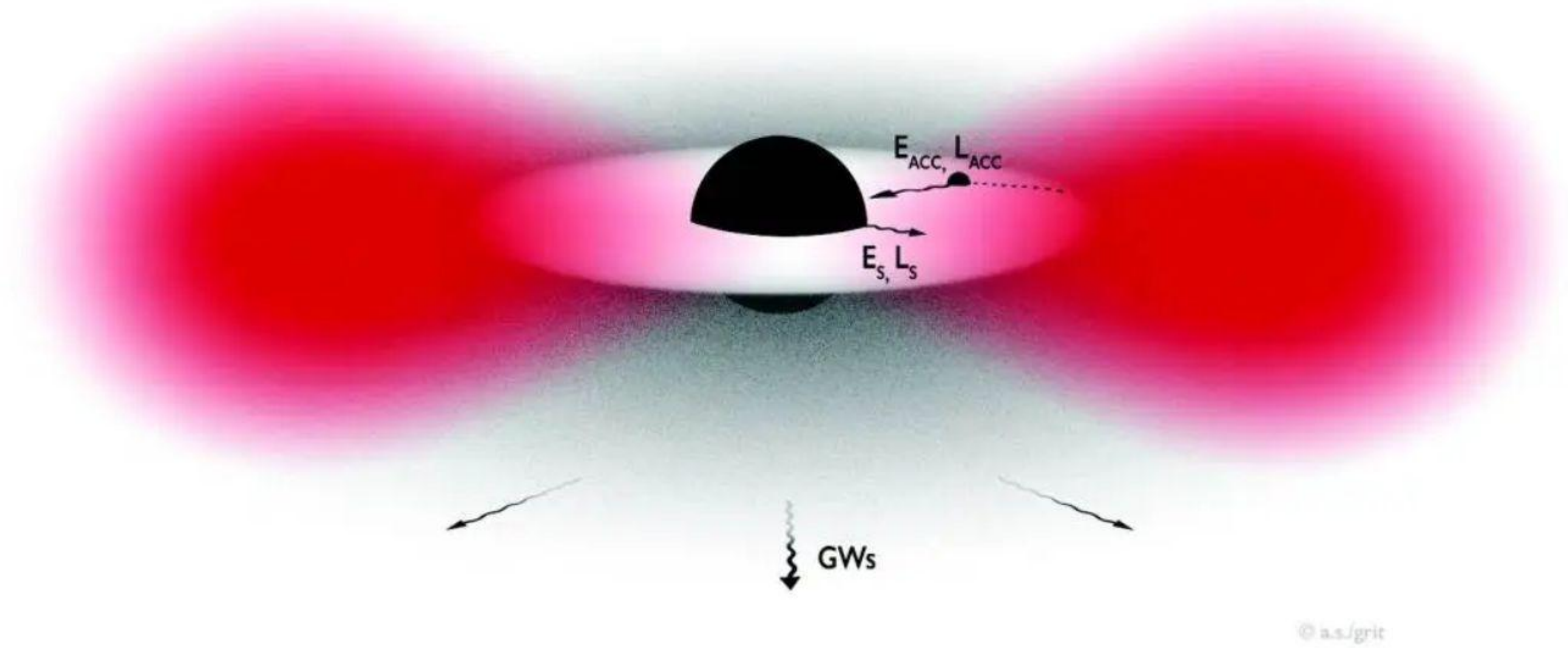

Superradiance: New Frontiers in Black Hole Physics (2020 edition)

R. Brito, V. Cardoso & P. Pani, 1501.06570v8 (8 Jan 2021)

Rotational Superradiance

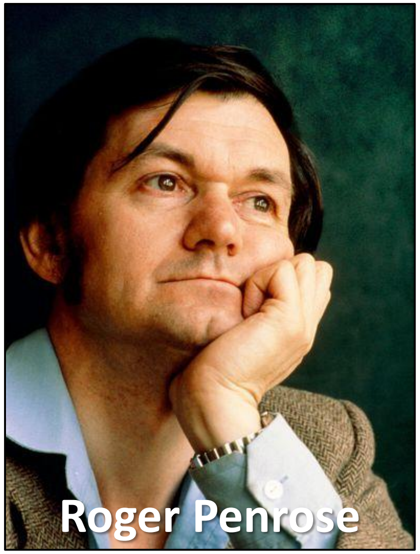

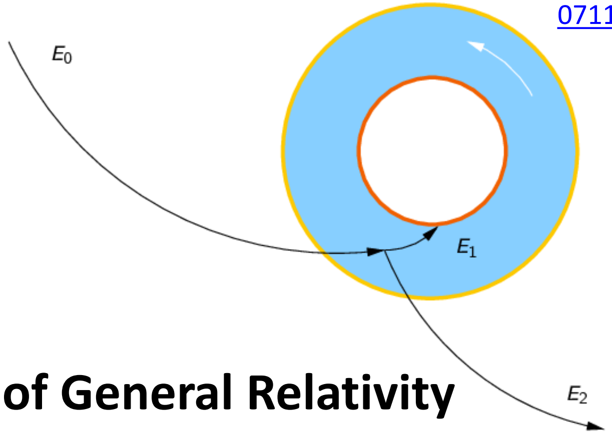

[0711.4416](0711.4416)

Gravitational Collapse: The Role of General Relativity
Riv. Nuovo Cim., Num. Spez. 1 (1969) 257
Reprinted in Gen. Rel. Grav. 34 (2002) 1141

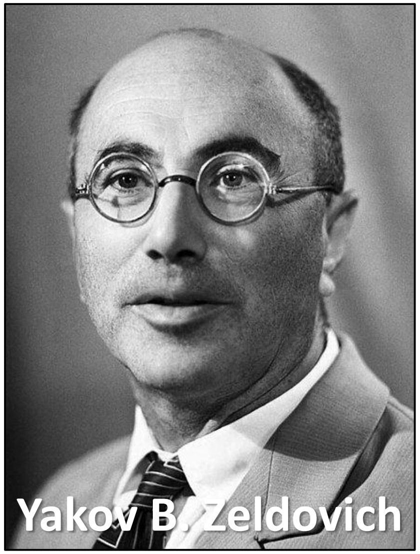

Generation of Waves by a Rotating Body
JETP Lett. 14 (1971) 180

Amplification of Cylindrical Electromagnetic Waves Reflected from a Rotating Body
Zh. Eksp. Teor. Fiz. 62 (1972) 2076

Superradiance

Extraction of rotational energy from spinning object by low-frequency modes $\omega < \Omega$ of an external bosonic field

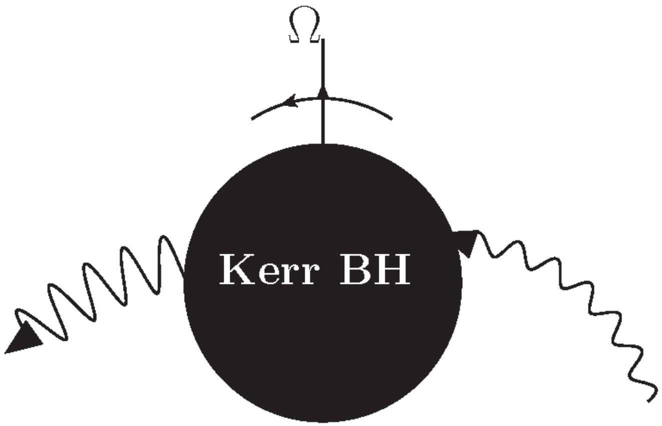

$m\Omega > \omega$

- **Bosons with mass get gravitationally bound**
- **Superradiant run-away mode** $\phi = Y_{lm}(\theta, \phi)\psi_{lmn}(r)e^{\Gamma t}$
- **"Bosonic atom"**
- **Transitions → Gravitational waves**

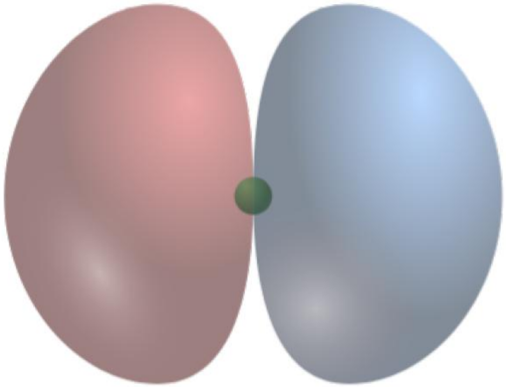

Superradiance: New Frontiers in Black Hole Physics (2020 edition)

R. Brito, V. Cardoso & P. Pani, [1501.06570v8] (8 Jan 2021)

Signatures

- **Constraints on light particles from BH spin**

  Exploring the string axiverse with precision black hole physics
  Arvanitaki & Dubovsky, [1004.3558]
  Discovering the QCD axion with black holes and gravitational waves, Arvanitaki, Baryakhtar & Huang, [1411.2263]

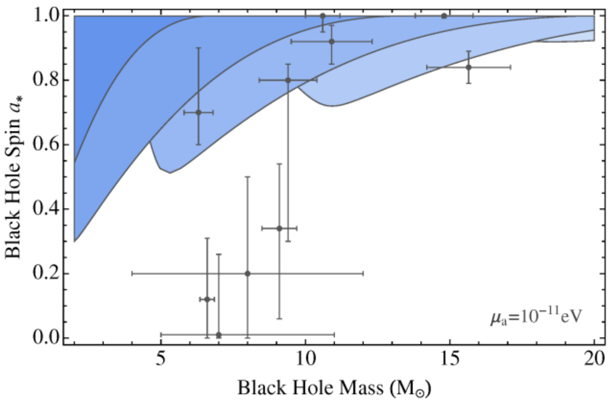

- **Gravitational waves from "atomic transitions"**

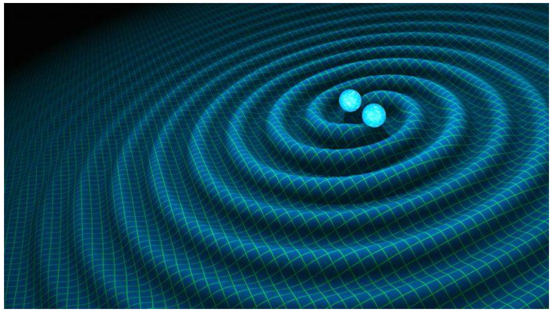

- **Effects on binaries**

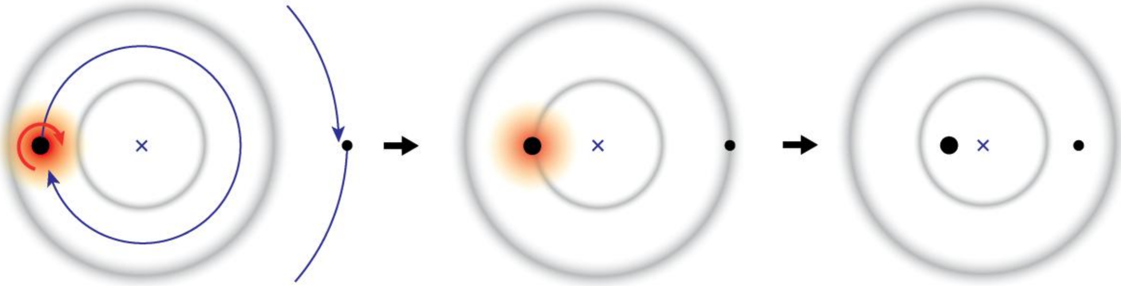

Probing Ultralight Bosons with Binary Black Holes
Baumann, Chia & Porto, [1804.03208]

Impact on Black Hole Spins

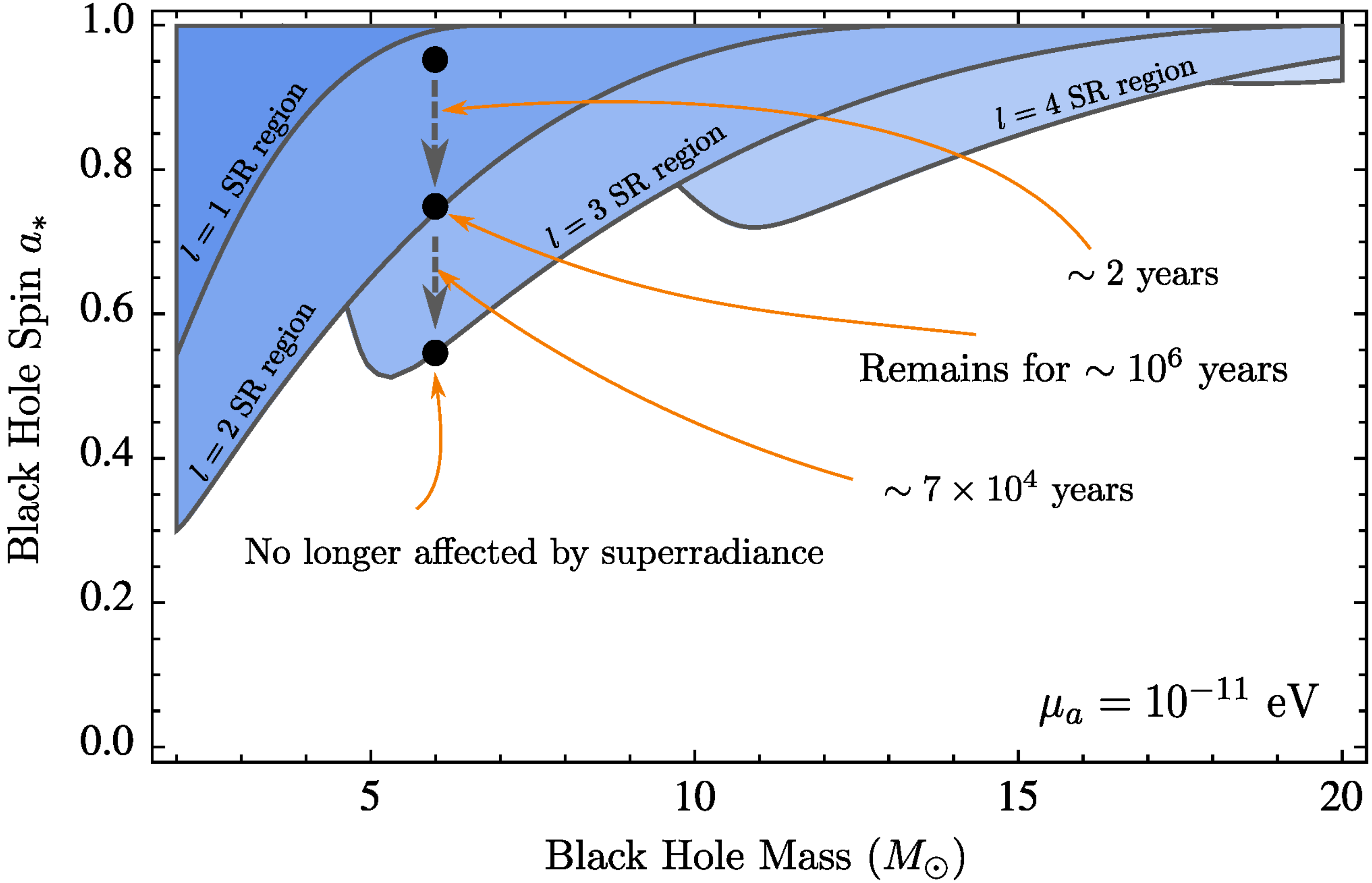

Discovering the QCD axion with black holes and gravitational waves

Arvanitaki, Baryakhtar & Huang, [1411.2263](1411.2263)

Constraints from Black Hole Spins

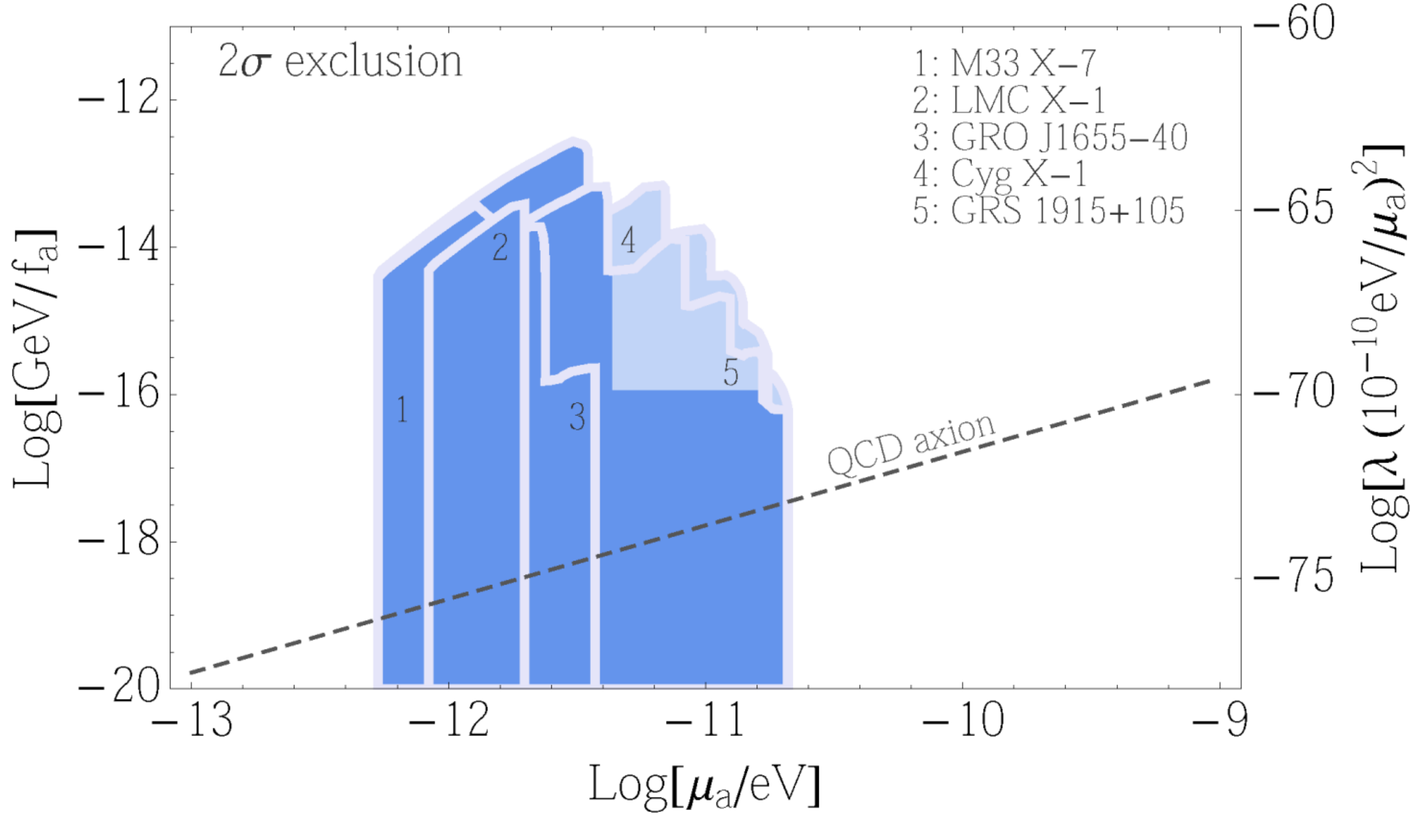

#	Object	Mass ($M_\odot$)	Spin	Age (yrs)	Period (days)	$M_{\rm comp.\,star}$ ($M_\odot$)	$\dot{M}/\dot{M}_E$
1	M33 X-7	15.65 ± 1.45	$0.84^{+.10}_{-.10}$[51]	3×10^6 [52]	3.4530 [53]	$\gtrsim 20$ [53]	$\gtrsim 0.1$[53]
2	LMC X-1	10.91 ± 1.4	$0.92^{+.06}_{-.18}$ [54]	5×10^6 [52]	3.9092 [55]	31.79±3.48 [55]	0.16 [55]
3	GRO J1655-40	6.3 ± 0.5	$0.72^{+.16}_{-.24}$ [51]	3.4×10^8 [56]	2.622 [56]	2.3 - 4 [56]	$\lesssim 0.25$ [57]
4	Cyg X-1	14.8 ± 1.0	> 0.99 [58]	4.8×10^6[59]	5.599829 [52]	17.8 [52]	0.02[52]
5	GRS1915+105	10.1 ± 0.6	> 0.95 [51, 60]	4×10^9 [61]	33.85 [62]	0.47 ± 0.27 [62]	$\gtrsim 1$ [62].

Arvanitaki, Baryakhtar & Huang, 1411.2263

Gravitational Wave Signals

- Transitions between levels

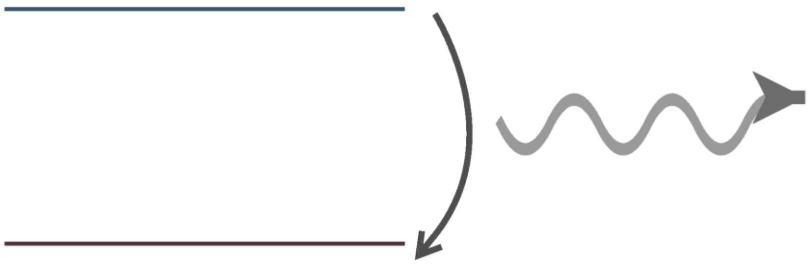

- Annihilations to gravitons

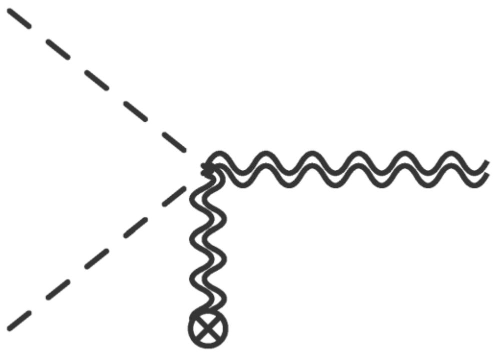

Arvanitaki, Baryakhtar, Dimopoulos, Dubovsky & Lasenby, arXiv:1604.03958

Direct Constraints on the Ultralight Boson Mass from Searches of Continuous Gravitational Waves

C. Palomba,[1] S. D'Antonio,[2] P. Astone,[1] S. Frasca,[3,1] G. Intini,[3,1] I. La Rosa,[4] P. Leaci,[3,1] S. Mastrogiovanni,[5] A. L. Miller,[3,1,6] F. Muciaccia,[3] O. J. Piccinni,[3,1] L. Rei,[7] and F. Simula[1]

Superradiance limits from LIGO O2 all-sky search for periodic GWs

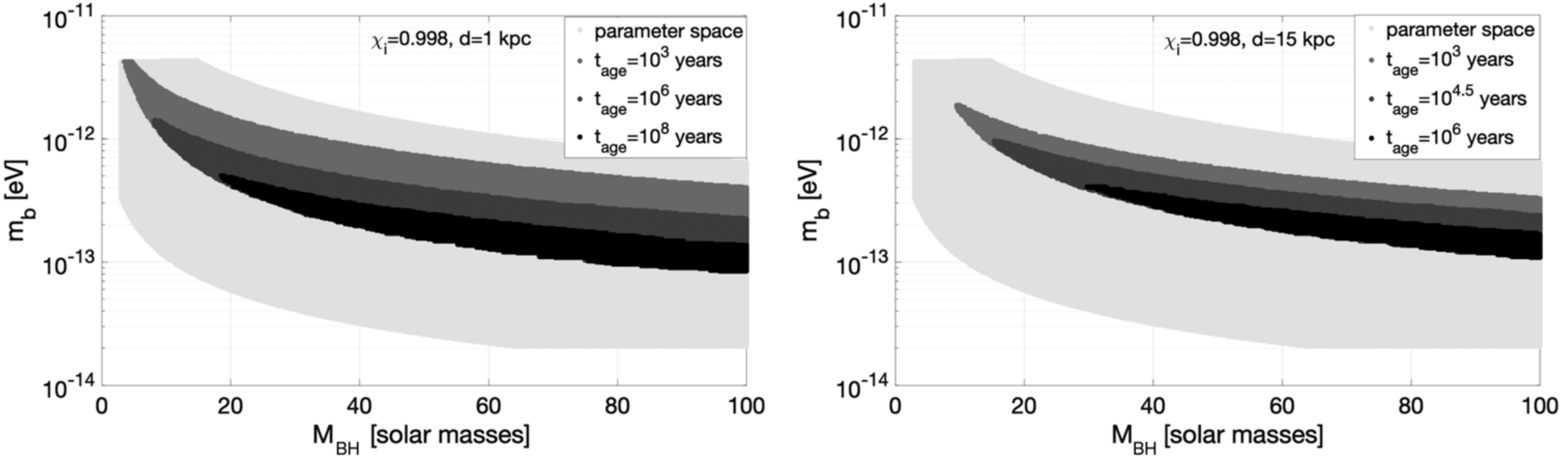

FIG. 2. 95% C.L. exclusion regions in the plane $m_b - M_{\rm BH}$ assuming a maximum distance $d = 1$ kpc (left plot) and $d = 15$ kpc (right plot), a black hole initial adimensional spin $\chi_i = 0.998$, and three possible values for $t_{\rm age}$: 10^3, 10^6, 10^8 yr (left plot) and 10^3, $10^{4.5}$, 10^6 yr (right plot). The larger light gray area is the accessible parameter space. As expected, the extension of the excluded region decreases for increasing $t_{\rm age}$ (corresponding to darker color).

See also:
Search for ultralight bosons in Cygnus X-1 with Advanced LIGO, arXiv:1909.11267

Superradiance in Neutron Stars

- Crucial issue is absorption of bosons within neutron star
- Not enough absorption for axions in nuclear matter?

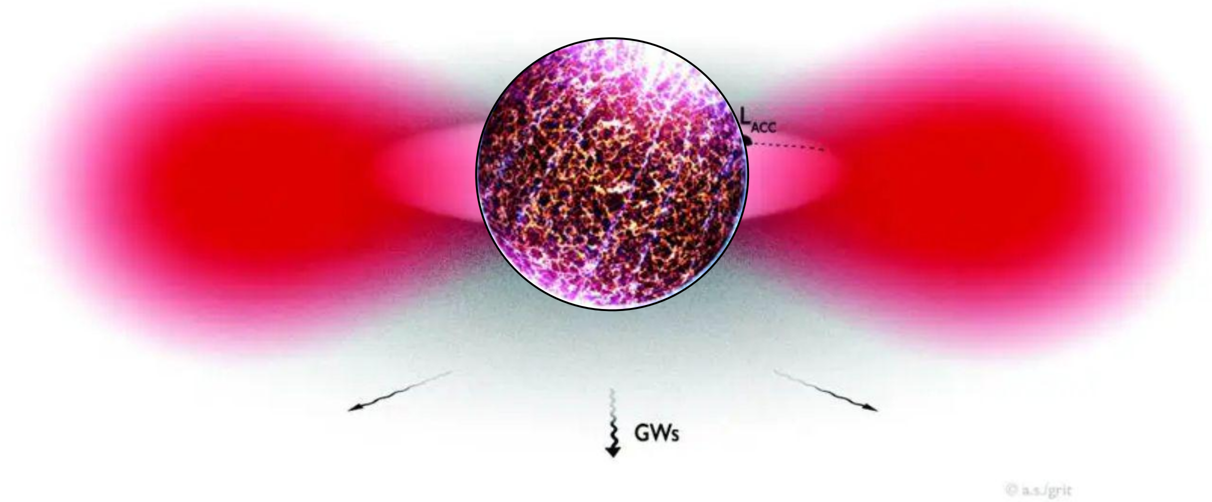

Superradiance in rotating stars and pulsar-timing constraints on dark photons
V.Cardoso, P.Pani & T.-T.Yu, [1704.06151]

Axion superradiance in rotating neutron stars
F.V.Day & J.I.McDonald, [1904.08341]

Superradiance in stars: non-equilibrium approach to damping of fields in stellar media
F.Chadha-Day, B.Garbrecht & J.I.McDonald, [2207.07662]

Peccei-Quinn Scale vs. Axion Mass

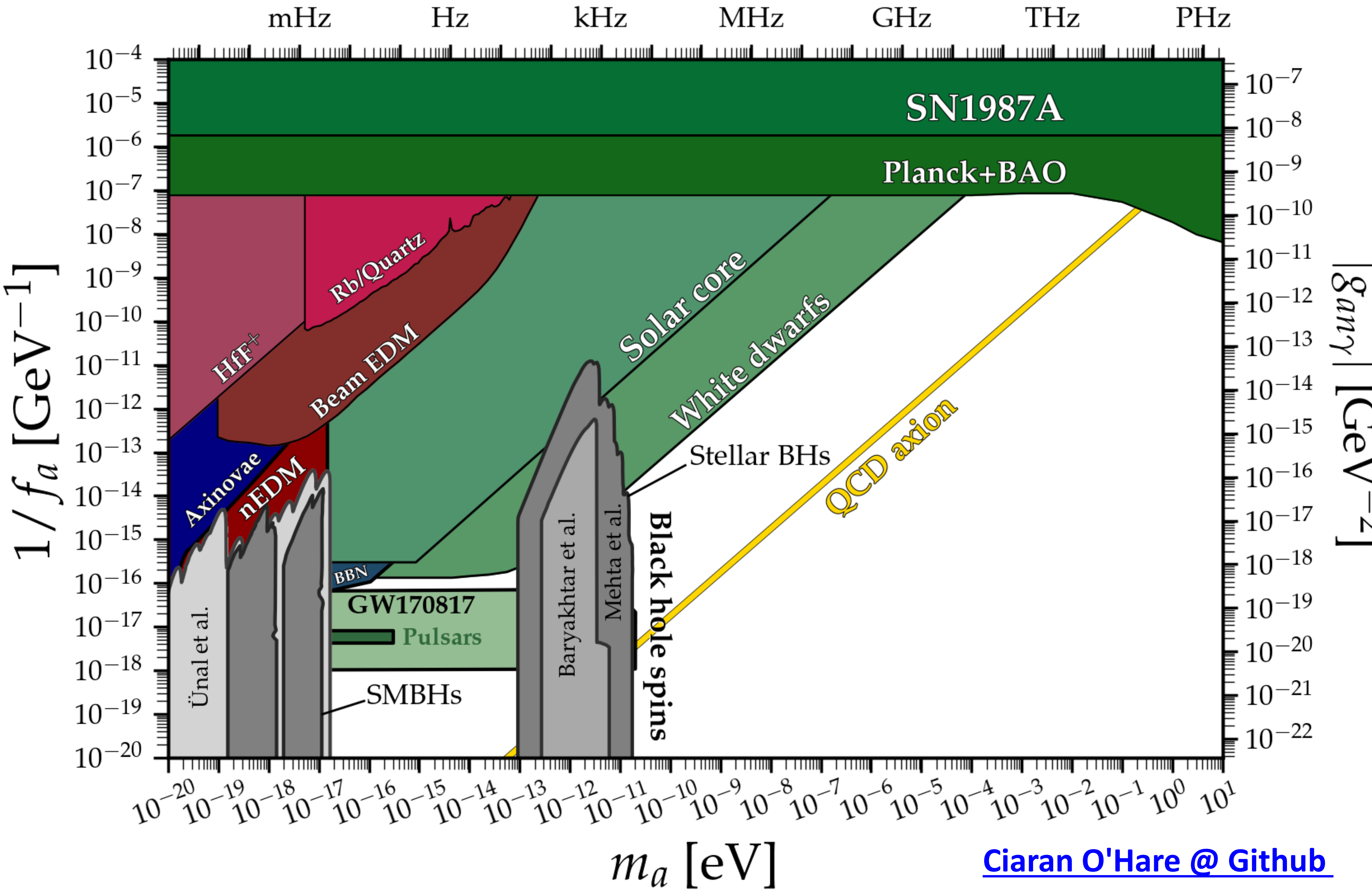

[Ciaran O'Hare @ Github](#)

Axions and Stellar Structure

Coupled systems are coupled:
Stars destabilize axions, axions destabilize stars

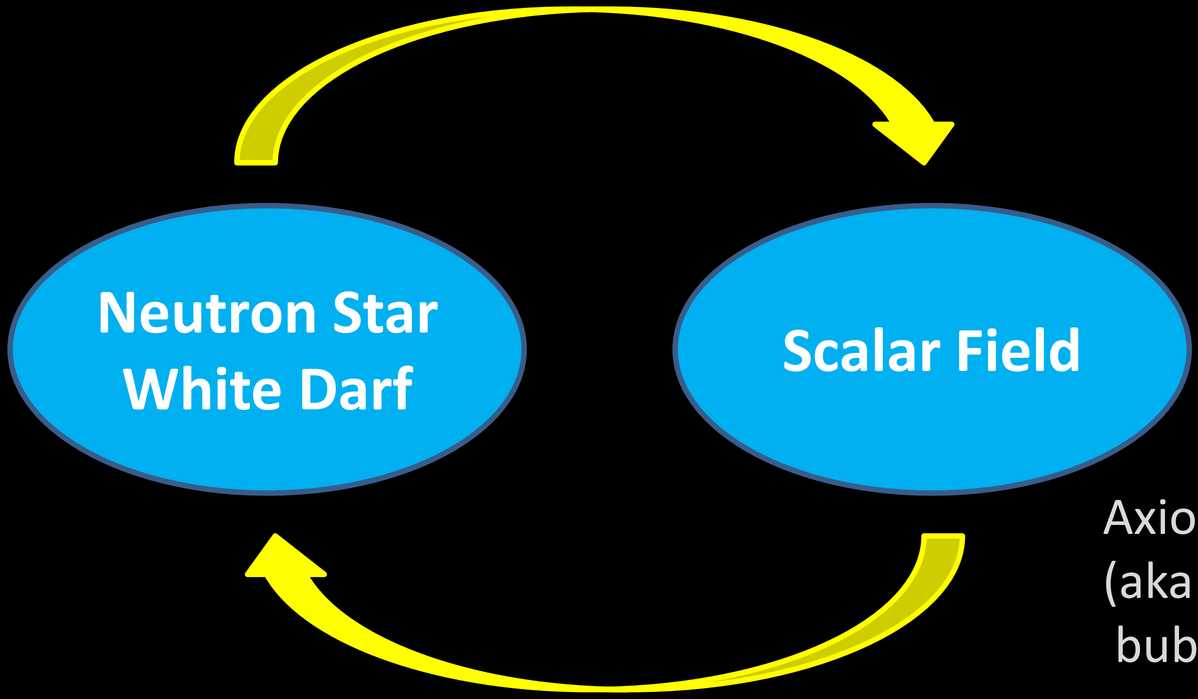

Axion condensation
(aka axion sourcing,
bubble formation)

Adapted from Andi Weiler

Axion Potential in Vacuum

Non-perturbative effects generate $\Lambda_{\rm QCD}$

UV $\quad \dfrac{g_s^2}{32\pi^2}\dfrac{\phi}{f_a}\, G\tilde{G}$

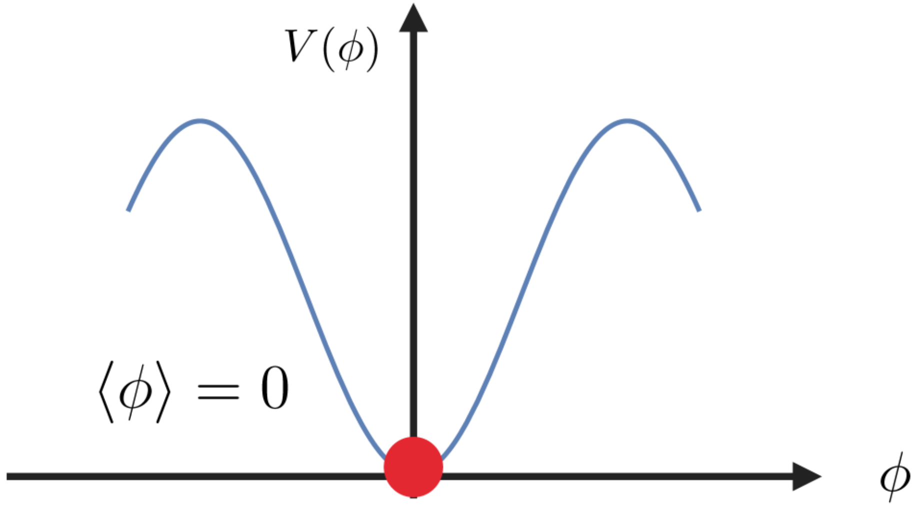

IR $\quad V(\phi) = -m_\pi^2 f_\pi^2 \sqrt{1 - \dfrac{4 m_u m_d}{(m_u + m_d)^2}\sin^2\left(\dfrac{\phi}{2f_a}\right)}$

$$\simeq -\underbrace{\frac{m_\pi^2 f_\pi^2}{4}}_{m_a^2 f_a^2}\left[\cos\left(\frac{\phi}{f_a}\right) - 1\right]$$

$2\pi f_a$ periodic potential

Axion Potential in Dense Medium

Nuclear chiral perturbation theory with QCD axion

$$\mathcal{L}_{\text{chiral}} = \text{Tr}\left[U\, M_q e^{i\phi/f_a} + \text{h.c.}\ \right] \bar{N}N + \cdots$$

Leads to non-derivative nucleon couplings

$$\mathcal{L} \supset -\left[m_N + \sigma_{\pi N}\left(\cos\frac{\phi}{f_a} - 1\right)\right]\bar{N}N \qquad \sigma_{\pi N} \simeq 50\ \text{MeV}$$

For nonvanishing nucleon density $n_N = \langle \bar{N}N \rangle$ an axion potential

$$V(\phi) = -\frac{m_\pi^2 f_\pi^2}{4}\left(1 - \underbrace{\frac{4\sigma_{\pi N} n_N}{m_\pi^2 f_\pi^2}}\right)\left(\cos\frac{\phi}{f_a} - 1\right)$$

$\mathcal{O}(1)$ at nuclear density

Hook & Huang 1708.08464, Balkin+ 2105.13354

Light QCD Axions at Finite Density

$$V(\phi) = -\frac{m_\pi^2 f_\pi^2}{4}\left(\epsilon - \frac{4\sigma_{\pi N} n_N}{m_\pi^2 f_\pi^2}\right)\left(\cos\frac{\phi}{f_a} - 1\right)$$

Axions with smaller mass

$$n < n_c = \epsilon \, \underbrace{\frac{m_\pi^2 f_\pi^2}{4\sigma_{\pi N}}}_{(2.1\ \mathrm{fm})^{-3}}$$

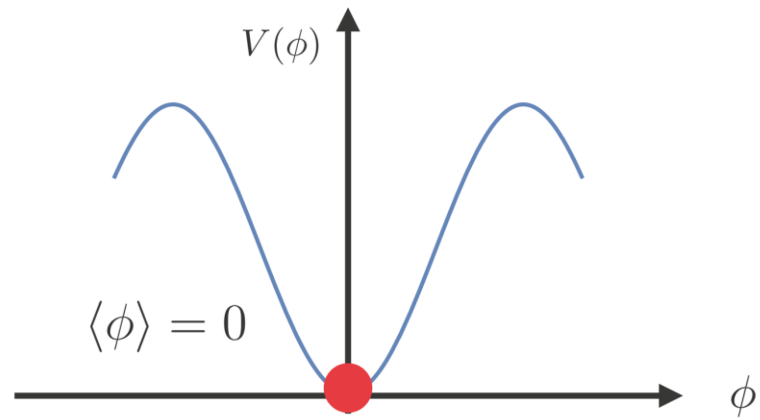

New minima appear at large density

$$n > n_c = \epsilon \, \frac{m_\pi^2 f_\pi^2}{4\sigma_{\pi N}}$$

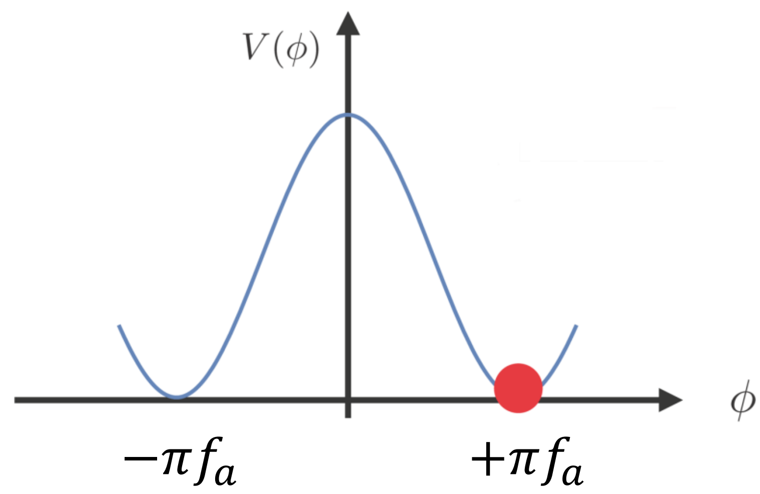

Hook & Huang 1708.08464, Balkin+ 2105.13354

Axion Profile of a Neutron Star

$\phi = \theta f$

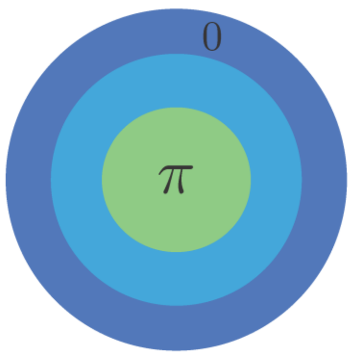

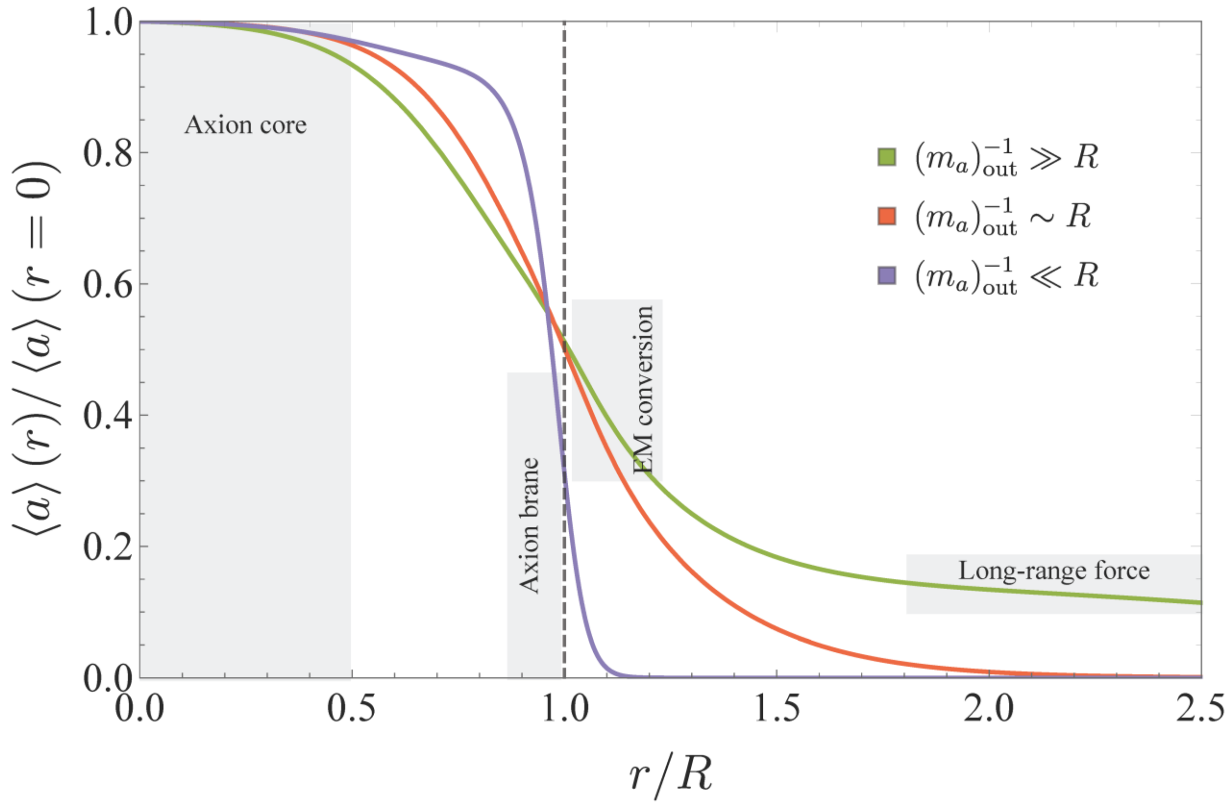

Nucleon mass shifted

$m_N \to m_N - \sigma_{\pi N}$

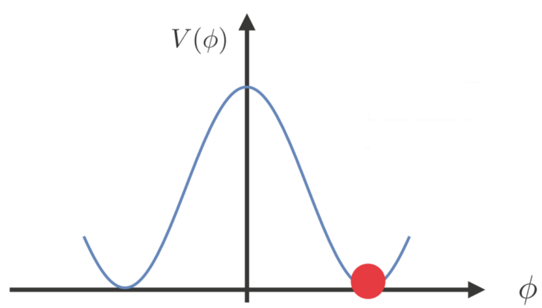

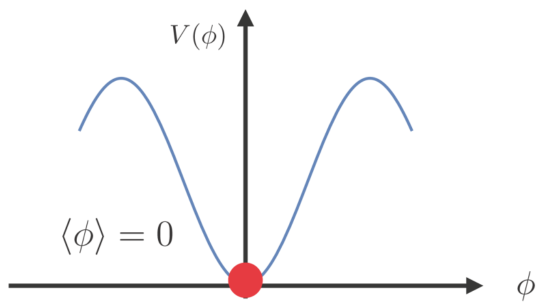

Hook & Huang [1708.08464](1708.08464)
Balkin+ [2105.13354](2105.13354)

Binary Neutron Star Merger GW 170817

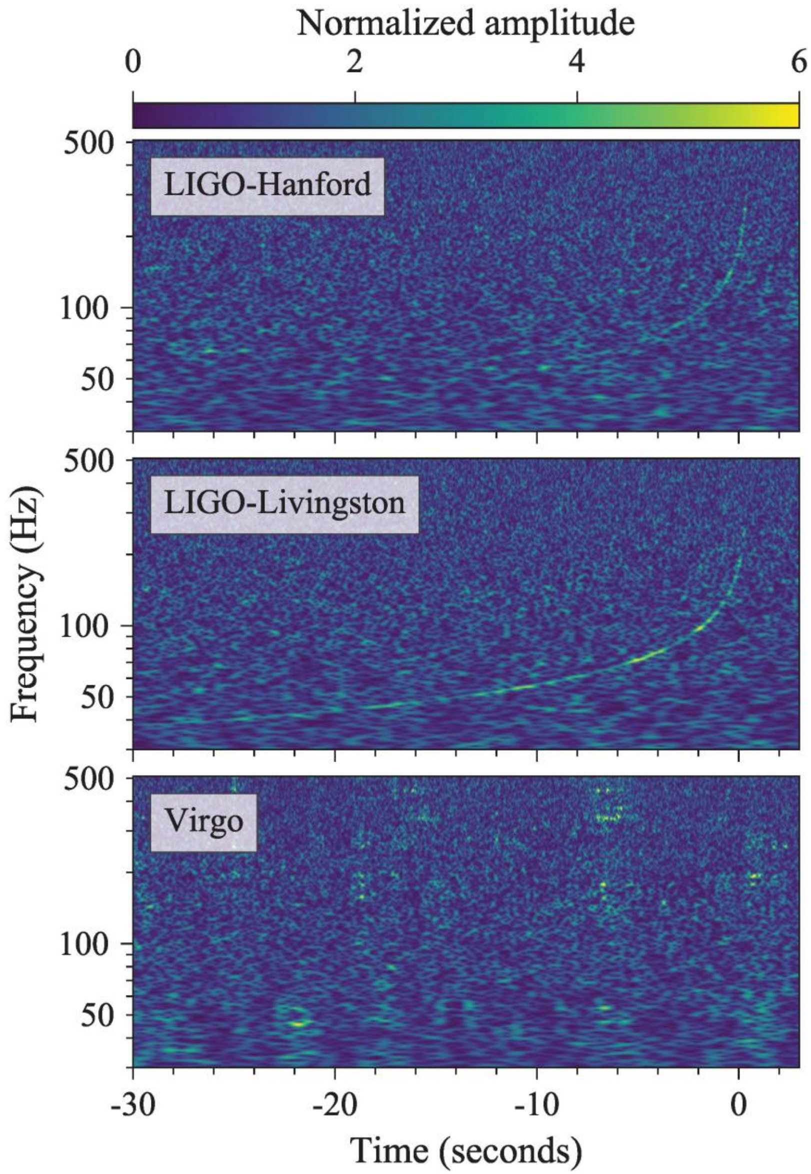

LIGO & Virgo, [1710.05832](https://arxiv.org/abs/1710.05832)

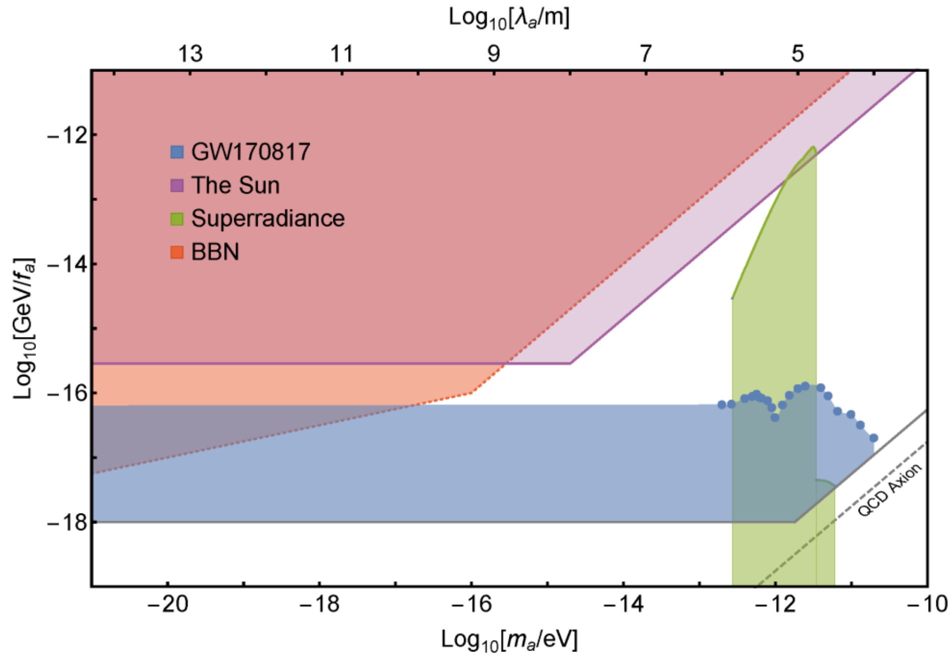

First Constraints on Nuclear Coupling of Axionlike Particles from the Binary Neutron Star Gravitational Wave Event GW 170817

J.Zhang+, [2105.13963](https://arxiv.org/abs/2105.13963)

Changed Equation of State (EoS)

Energy/nucleon

Pressure

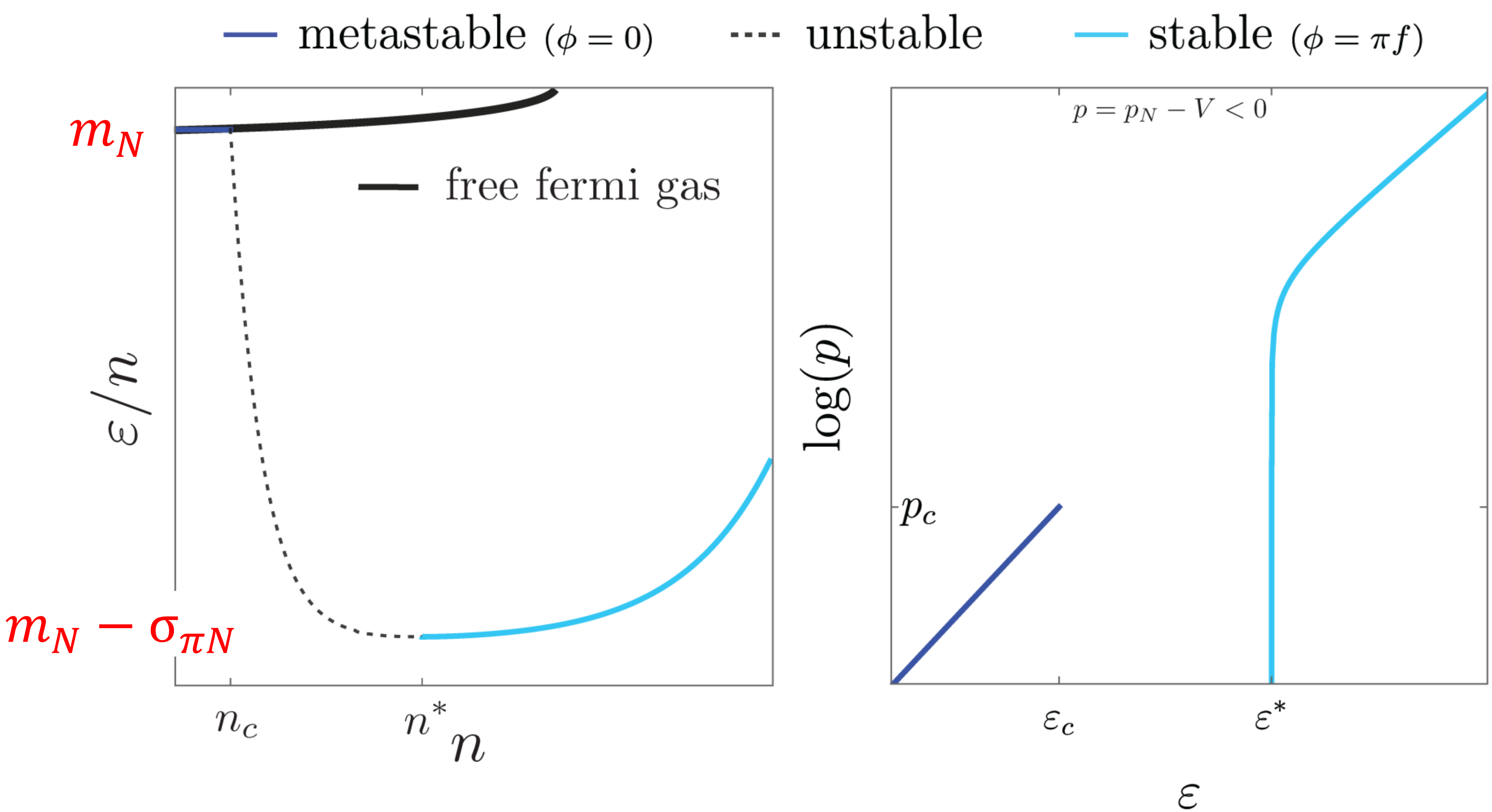

White-Dwarf Mass-Radius Relation

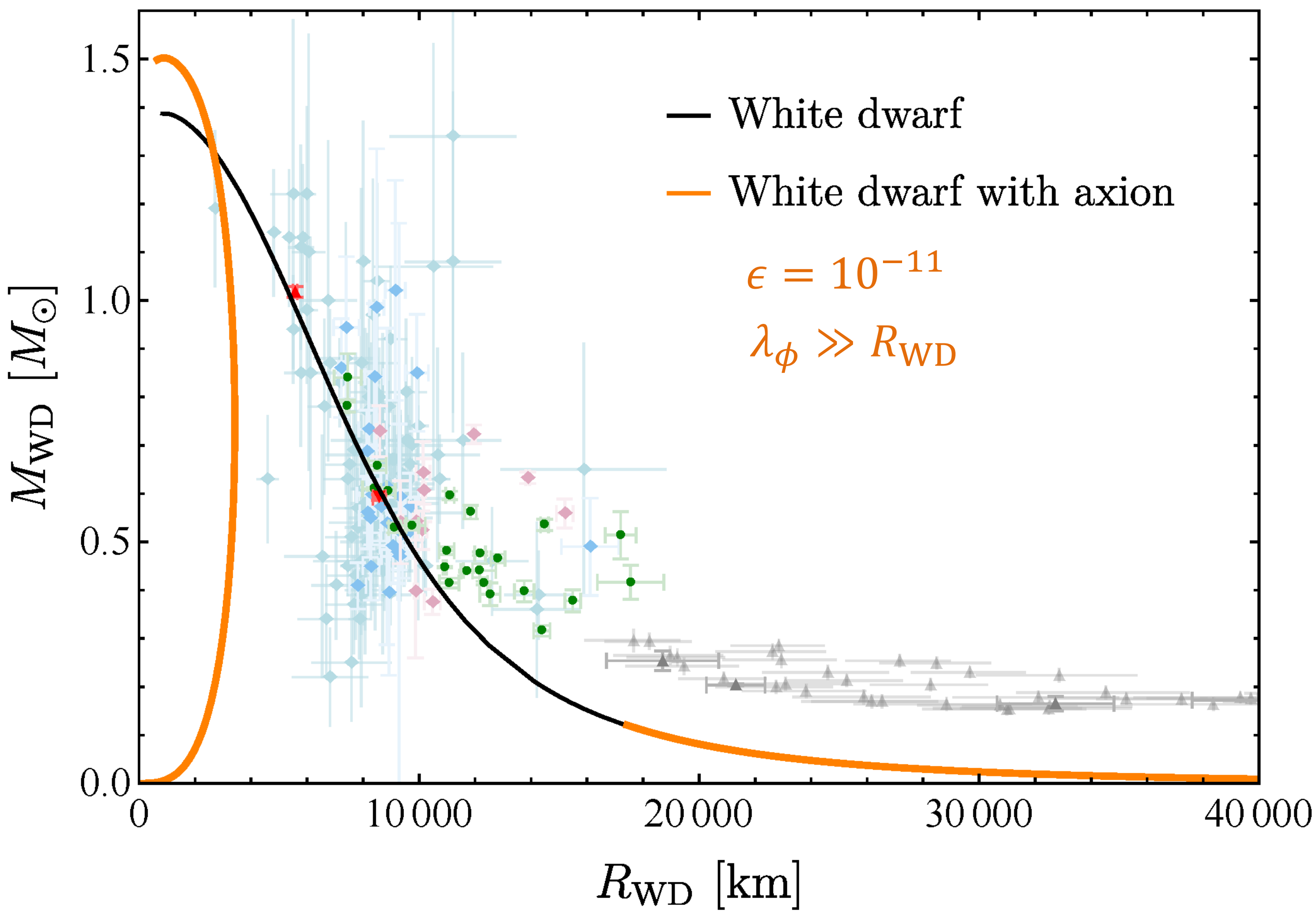

R. Balkin, J. Serra, K. Springmann, S. Stelzl & A. Weiler, 2211.02661

Axion Bounds from Stellar Structure

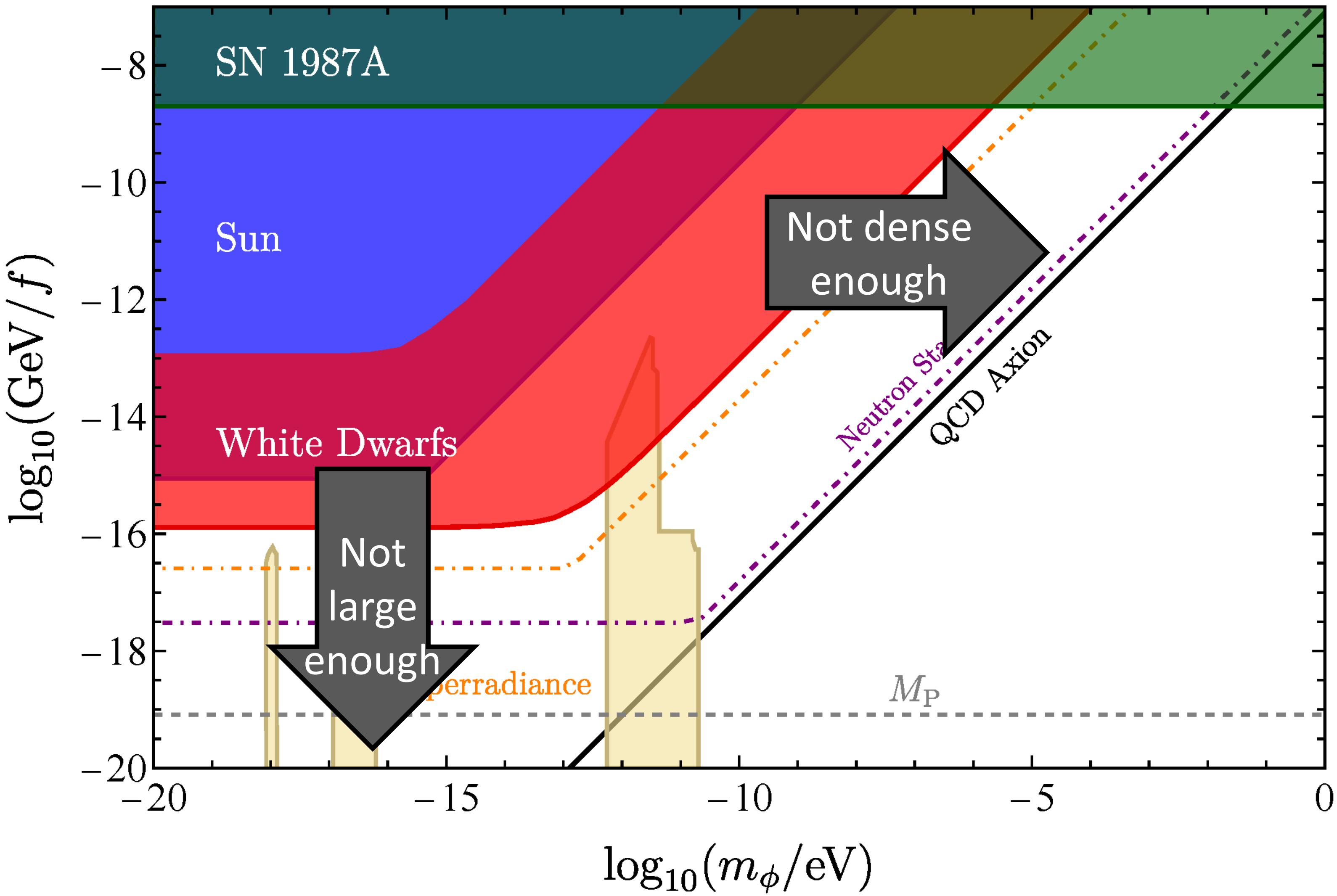

R. Balkin, J. Serra, K. Springmann, S. Stelzl & A. Weiler, [2211.02661](https://arxiv.org/abs/2211.02661)

Peccei-Quinn Scale vs. Axion Mass

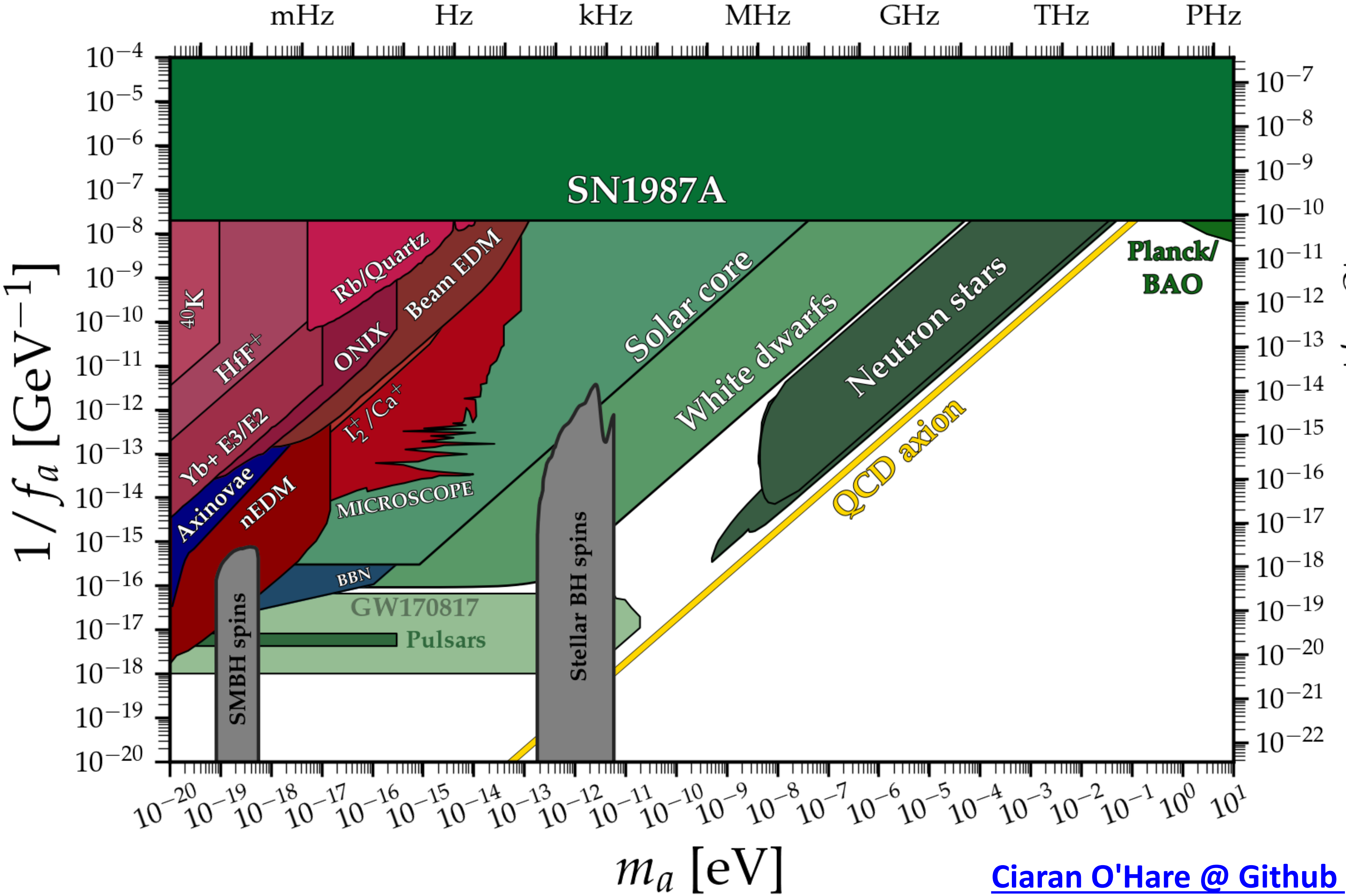

Ciaran O'Hare @ Github